

APPLICATIONS OF DYNAMICAL SYSTEMS TO INDUSTRIAL  
MICROBIOLOGY

APPLICATIONS OF DYNAMICAL SYSTEMS TO  
INDUSTRIAL MICROBIOLOGY

By TYLER MEADOWS, B.Sc., M.Sc.

*A Thesis Submitted to the School of Graduate Studies in the Partial  
Fulfillment of the Requirements for the Degree Doctor of Philosophy*

McMaster University © Copyright by Tyler Meadows September  
10, 2019

McMaster University

Doctor of Philosophy (2019)

Hamilton, Ontario (Math and Stats)

TITLE: Applications of dynamical systems to industrial microbiology

AUTHOR: Tyler Meadows (McMaster University)

SUPERVISOR: Dr. Gail S. K. Wolkowicz

NUMBER OF PAGES: xvi, 139

# Abstract

The use of microorganisms in industrial processes has become very common. In this thesis, we analyze three models of such systems that have applications in green technology. The first is a simplified model of anaerobic digestion, originally introduced as a qualitative simplification of the anaerobic digestion model no 1 (ADM1). While ADM1 is very complicated, the simplified model is composed of only five ordinary differential equations. We show that this model can be reduced to a two-dimensional system that is equivalent to the basic chemostat model with explicit species death rate and non-monotone response function. We show that this chemostat model has no periodic solutions and completely characterize the possible dynamics of the two dimensional system and then the full five-dimensional system. In the second model, we consider the self-cycling fermentation process with two limiting essential resources with impulses that occur when both resources fall below a prescribed threshold. We show that the successful operation of the self-cycling fermentor is initial-condition dependent and that success is equivalent to the convergence of solutions to a periodic solution. We show numerically that there is an optimal choice for the emptying/refilling fraction and that the optimal choice is not always  $1/2$ , the standard choice in the engineering literature. In the third model, we consider the self-cycling fermentation process with an arbitrary number of nutrients with impulses that occur when one specified nutrient concentration falls below a prescribed threshold. We show that successful operation of the self-cycling fermentor is equivalent to the convergence of solutions to a periodic solution. We derive conditions for the existence of this periodic solution and initial-condition-dependent conditions for convergence to this solution.

# *Acknowledgements*

I want to thank all of the graduate students in the Math and Stats department that have been a part of this journey. Special thanks go to my friends and office mates over the years, Diogo Pocas, Karsten Hempel, Spencer Hunt, Dora Rosati, Irena Papst, Ramsha Khan, Pritpal ‘Pip’ Matharu, Niky Hristov, Alexandr Chernyavsky, Szymon Sobieszek and Lee van Brussel. The AIMS lab was sometimes a distracting place to be, but the community at McMaster made the degree much easier.

I would like to thank several faculty members for their continued support and interest over the years. Thank you to the professors that regularly attended the AIMS seminars, Dr. Nicholas Kevlahan, Dr. Bartosz Protas, Dr. Dmitry Pelinovski, and the late Dr. Walter Craig. Thank you for taking time out of studying fluids every once in a while to learn a little about biology in the AIMS Seminars.

Without funding from the department of Mathematics and Statistics at McMaster, NSERC funding through Dr. Wolkowicz, and OGS over the past 4 years, I would not have been able to do any of the research in this thesis. I am very grateful for the financial support, and hope that what I have accomplished is worthy of the investment.

Thank you to my committee, Dr. Stan Alama and Dr. Ben Bolker, for being available to answer questions when I had them. Although no PDEs made their way into this thesis, they have made their way into much of my other work, and I wouldn’t be able to do anything with them if it weren’t for Dr. Alama. Thanks to Dr. Bolker for encouraging me to keep the biology in mind and not get too lost

in the math; this advice early in my PhD has kept a lot of my work grounded in reality.

Thank you to Dr. Wolkowicz for the constant support and direction, but for also challenging me to find my own way. I'm very grateful that you didn't just hand me a project on day one, but let me explore ideas in mathematical biology until I found something that I liked, and that you agreed would work. I will particularly miss our weekly meetings, which often went well over the hour we had scheduled. Your help was instrumental in me completing my PhD on time and in helping to shape me into the mathematician I am today.

Finally, I want to thank my fiancée, Jennifer Leonard, for being okay with me being a student for the last 6 years and for agreeing to come with me on the next part of this journey. You're the best, and I don't know how to thank you for everything you do.

# Contents

<b>Abstract</b>	<b>iii</b>
<b>Acknowledgements</b>	<b>iv</b>
<b>Declaration of Authorship</b>	<b>xiv</b>
<b>1 Introduction</b>	<b>1</b>
<b>2 Global analysis of a simplified model of anaerobic digestion and a new result for the chemostat</b>	<b>8</b>
2.1 Introduction . . . . .	9
2.2 The Model . . . . .	13
2.3 Global Analysis of Growth in the Chemostat . . . . .	17
2.4 Global Analysis of the Full System (2.1) . . . . .	23
2.5 Bifurcation Analysis of Full System (2.1) . . . . .	24
2.6 Stochastic Simulations of the Full System (2.1) . . . . .	29
2.7 Conclusion . . . . .	37
2.A Proofs . . . . .	40
<b>3 Growth on two essential nutrients in a self-cycling fermenter</b>	<b>53</b>
3.1 Introduction . . . . .	54

3.2	Model Formulation . . . . .	57
3.3	Dynamics of System (3.3) . . . . .	59
3.4	Analysis of the Full System (3.1) . . . . .	61
3.4.1	Existence of Periodic Orbits . . . . .	69
3.4.2	Global Stability of Periodic Orbits . . . . .	72
3.5	Maximizing the Output . . . . .	85
3.6	Discussion . . . . .	89
<b>4</b>	<b>Growth on multiple essential limiting nutrients in a self-cycling fermentor</b>	<b>98</b>
4.1	Introduction . . . . .	99
4.2	The Model . . . . .	102
4.3	The Periodic Solution . . . . .	109
4.3.1	Stability of the Periodic Solution . . . . .	118
4.4	Conclusions . . . . .	126
<b>5</b>	<b>Conclusions</b>	<b>132</b>

# List of Figures

2.1	The anaerobic digestion process. (1) Acidogenic microorganisms break down simple substrates into VFAs and ammonia. (2) Methanogenic microorganisms break down VFAs into biogas such as methane. This process is inhibited by ammonia. . . . .	11
2.2	Phase portraits of system (2.8) with the level sets of $V(S, X)$ . The dashed lines are the nullclines for $X$ and the dashed curve is the nullcline for $S$ . The equilibria $\mathcal{E}_0$ , $\mathcal{E}_1$ , and $\mathcal{E}_2$ are indicated by circles, and the point $(\sigma_2, X_{\sigma_1}^*)$ is indicated by a diamond. The grey curves are the level sets of $V(S, X)$ . The bold curve is the level set of $V(S, X)$ that passes through the point $(\sigma_2, X_{\sigma_1}^*)$ . These figures were produced using Maple [12]. . . . .	22
2.3	Plots of each prototype in 3-dimensions: (a) $\mu_{2,I}(S_2, S_3)$ , (b) $\mu_{2,II}(S_2, S_3)$ , (c) $\mu_{2,III}(S_2, S_3)$ . (d) shows all three prototypes on the same axes for comparison. Parameters values used are given in Table 2.1. . . . .	25
2.4	Bifurcation diagrams with bifurcation parameter $D$ in (a), (c), (e) and $S^{(0)}$ in (b),(d), (f) and response function $\mu_2(S_2, S_3) = \mu_{2,I}(S_2, S_3)$ in (a) and (b), and $\mu_2(S_2, S_3) = \mu_{2,II}(S_2, S_3)$ in (c) and (d) and $\mu_2(S_2, S_3) = \mu_{2,III}(S_2, S_3)$ in (e) and (f). . . . .	28

2.5	Bifurcation diagrams with bifurcation parameter $S^{(0)}$ illustrating two saddle node bifurcations. (a) $\mu_2(S_2, S_3) = \mu_{2,I}(S_2, S_3)$ . (b) $\mu_2(S_2, S_3) = \mu_{2,III}(S_2, S_3)$ . The diagrams with $\mu_{2,II}(S_2, S_3)$ do not exhibit this behaviour. . . . .	28
2.6	Sample paths of system (2.1) for the methanogens, $X_2(t)$ , using the environmental fluctuation based method in Figures 2.6(a) and 2.6(b), and using the mutation based method in Figures 2.6(c) and 2.6(d). On the left, the initial conditions are given in (2.14) and are in the basin of attraction of $E_0$ for the deterministic system. On the right, the initial conditions are given in (2.13) and are in the basin of attraction of $E_1$ for the deterministic system. The darker curve in each graph is the solution of the deterministic system and the lighter curves show the results of different stochastic runs. . . . .	32
2.7	Sample paths of system (2.1) for the methanogens, $X_2(t)$ , using Gillespie's SSA in Figures 2.7(a) and 2.7(b), and using the tau-leaping method in Figures 2.7(c) and 2.7(d). On the left, the initial conditions are given in (2.14) and are in the basin of attraction of $E_0$ for the deterministic system. On the right, the initial conditions are given in (2.13) and are in the basin of attraction of $E_1$ for the deterministic system. The darker curve in each graph is the solution of the deterministic system and the lighter curves show the results of different stochastic runs. . . . .	33

- 3.1  $u_0 = (s_1^0, s_2^0)$ , indicated by  $\triangle$ , is the initial condition.  $u^{\text{in}} = (s_1^{\text{in}}, s_2^{\text{in}})$ , indicated by  $\nabla$ , is the input concentration.  $u_k^\pm = (s_1(t_k^\pm), s_2(t_k^\pm))$ ,  $k = 1, 2, \dots$ , satisfy  $u_k^+ = (1 - r)u_k^- + ru^{\text{in}}$ , where  $u^{\text{in}} = (s_1^{\text{in}}, s_2^{\text{in}})$ . Each connected piece of the solution has slope  $R_{21}$ .  $\hat{u} = (\bar{s}_1, \widehat{s}_2) = (\bar{s}_1, s_2^{\text{in}} - R_{21}(s_1^{\text{in}} - \bar{s}_1))$  and  $\hat{u}^+ = (\bar{s}_1^+, \widehat{s}_2^+) = ((1 - r)\bar{s}_1 + rs_1^{\text{in}}, s_2^{\text{in}} - (1 - r)R_{21}(s_1^{\text{in}} - \bar{s}_1))$ . The set  $\Omega_1$  lies above and to the right of  $\Gamma^-$  and between the two lines with slope  $R_{21}$ , through  $(0, \bar{s}_2)$  and  $(\bar{s}_1, 0)$ , respectively. . . . . 62
- 3.2 No periodic solution exists, and the  $x$ -component of every solution tends to 0 as  $t \rightarrow \infty$ . In the simulation, the response functions are  $f_i(s_i) = \frac{m_i s_i}{a_i + s_i}$ ,  $i = 1, 2$ , with  $(m_1, m_2, a_1, a_2) = (2, 2, 1.4, 1.2)$ . The parameters are  $(Y_1, Y_2, D) = (2, 0.7, 0.5)$  and  $(\bar{s}_1, \bar{s}_2, s_1^{\text{in}}, s_2^{\text{in}}, r) = (0.7, 0.6, 1, 1, 0.4)$ . The initial condition is  $u_0 = (s_1(0), s_2(0), x(0)) = (0.1, 0.7, 0.3)$ . After a finite number of impulses, the orbit converges before reaching the threshold for an impulse, indicated by  $\square$ . The value of  $\mu(r) \approx -0.08 < 0$ . . . . . 70
- 3.3 If  $x(0) \leq X(s_1(0), s_2(0))$ , then only finitely many impulses occur. The orbit converges, indicated by  $\square$ , after a finite number of impulses, and the  $x$ -component of the solution tends to 0 as  $t \rightarrow \infty$ . The parameters are the values given in Example 3.4.13, and the initial condition is  $(s_1(0), s_2(0), x(0)) = (0.23, 0.6, 0.5)$ . . . . . 82
- 3.4 If  $L$  lies in  $\Omega_{1A}$  and  $x(0) > X(s_1(0), s_2(0))$ , then the solution converges to the periodic orbit. The parameters are the values given in Example 3.4.13, and the initial condition is  $(s_1(0), s_2(0), x(0)) = (0.23, 0.6, 0.53)$ . . . . . 83

3.5	If $u_0 \in \Omega_\lambda \setminus \Omega_{1A}$ and $\Omega_\lambda \cup \Omega_{1A}$ is connected, when $X(s_1^0, s_2^0) \leq 0$ , the fermentation is still always successful for all $x(0) > 0$ . The parameters are the values given in Example 3.4.17. The initial condition is $(s_1(0), s_2(0), x(0)) = (0.6, 0.7, 0.01)$ . . . . .	84
3.6	(A) $T(r)$ is the minimal period of the periodic orbit, $r \in (r_*, 1)$ . The dashed line is $r = r_*$ . As $r \rightarrow r_*$ or $r \rightarrow 1$ , $T(r) \rightarrow \infty$ . (B) The maximum of $Q(r)$ is attained at $r \approx 0.6416$ , indicated by the dotted line. In the simulation, the response functions are $f_i(s_i) = \frac{m_i s_i}{a_i + s_i}$ , $i = 1, 2$ , with parameters given in Example 3.4.17. . . . .	89
4.1	For any $\mathbf{s}^0$ , $V_i(\mathbf{s}^0)$ is the length of the perpendicular line segment connecting $\mathbf{s}^0$ to the solution segment through $\mathbf{s}^{\text{in}}$ in the $s_1$ - $s_i$ plane. For each $i$ , $\bar{V}_i$ is the distance from $\partial\Omega_1$ to $\mathbf{s}^{\text{in}}$ in the $s_1$ - $s_i$ plane. . . . .	111
4.2	The dynamics of Example 4.3.6 illustrated by projecting orbits onto $s_1$ - $s_3$ space, with the line through $\mathbf{s}^{\text{in}}$ shown in dotted red on the left. Solutions of $s_3$ and $x$ as functions of time are shown on the right. As predicted by Lemma 4.3.3, only finitely many impulses occur and $x(t) \rightarrow 0$ as $t \rightarrow \infty$ . . . . .	113
4.3	The dynamics of Example 4.3.10, in which $\mu(r) < 0$ , illustrated by projecting orbits onto $s_1$ - $s_3$ space, with the line through $\mathbf{s}^{\text{in}}$ shown in dotted red on the left. Solutions of $s_3$ and $x$ as functions of time are shown on the right. As predicted by Proposition 4.3.9, only finitely many impulses occur and $x(t) \rightarrow 0$ as $t \rightarrow \infty$ . . . . .	117

4.4 The dynamics of Example 4.3.15 illustrated by projecting orbits onto  $s_1$ - $s_2$  space, with the line through  $\mathbf{s}^{\text{in}}$  shown in dotted red on the left. Solutions of  $s_2$  and  $x$  as functions of time are shown on the right. On the top,  $x^0 < X(\mathbf{s}^0)$  and so  $x(t) \rightarrow 0$  as  $t \rightarrow \infty$  after at most  $N_0 = 4$  impulses. On the bottom  $x^0 > X(\mathbf{s}^0)$  and so solutions converge to the periodic solution. . . . . 125

# List of Tables

2.1	The parameter values used in the following bifurcation diagrams are the ones used in [4], except $m_{II}, m_{III}, r$ , and $a$ , which were chosen so that the response functions $\mu_{2,II}$ and $\mu_{2,III}$ closely resemble $\mu_{2,I}$ . The parameter $D$ is the bifurcation parameter in Figures 2.4(a), 2.4(c) and 2.4(e), and $S^{(0)}$ is the bifurcation parameter in Figures 2.4(b), 2.4(d) and 2.4(f). . . . .	27
2.2	Equilibria for system (2.1) with parameters given in Table 2.1, with $\mu_2(S_2, S_3) = \mu_{2,III}(S_2, S_3)$ . . . . .	30

# Declaration of Authorship

I, Tyler Meadows, declare that this thesis titled, “Applications of dynamical systems to industrial microbiology” and the work presented in it are my own. I confirm that:

- Chapter 1: Introduction
  - This chapter is completely my own work
- Chapter 2: Global Analysis of a simplified model of anaerobic digestion and a new result for the chemostat
  - The content of this chapter is copyright of the SIAM Journal of Applied Mathematics and appears here with their permission. It originally appeared as T. Meadows, M. Weeder mann, and G. S. K. Wolkowicz. Global analysis of a simplified model of anaerobic digestion and a new result for the chemostat. *SIAM J. Appl. Math.*, 79(2):668–669, 2019
  - This chapter is the work of myself, Dr. Gail S. K. Wolkowicz, and Dr. Marion Weeder mann.
  - I am the primary author of this publication, the bulk of the research contained in this chapter was conducted by myself and Dr. Gail S. K. Wolkwoicz.

- Chapter 3: Growth on two limiting essential resources in a self-cycling fermentor
  - The content of this chapter is copyright of the Journal of Mathematical Biosciences and Engineering and appears here with their permission. It originally appeared as T.-H. Hsu, T. Meadows, L. Wang, and G. S. K. Wolkowicz. Growth on two limiting essential nutrients in a self-cycling fermentor. *Math. BioSci. Eng.*, 16:78–100, 2019
  - This chapter is the work of myself, Dr. Ting-Hao Hsu, Dr. Gail S. K. Wolkowicz, and Dr. Lin Wang.
  - Ting-Hao and I were the primary authors on this publication. We worked together to complete the mathematical analysis, and worked with Dr. Gail S. K. Gail to write the paper. The original idea and some preliminary work in this publication were done by Dr. Lin Wang and Dr. Gail S. K. Wolkowicz. The figures were produced by Dr. Ting-Hao Hsu.
  
- Chapter 4: Growth on multiple essential limiting nutrients in a self-cycling fermentor
  - This chapter has been submitted to *Nonlinear Analysis: Real World Applications*.
  - This chapter is completely my own work.
  - The original idea for this chapter stemmed from a few conversations

with Dr. Gail S. K. Wolkowicz about directions to explore further in the previous chapter.

- Chapter 5: Discussion and Conclusions

- This chapter is completely my own work.

- It should go without saying that Gail's influence is all over this thesis, whether from helping with ideas for proofs, giving me directions to explore, letting me know when my descriptions are too vague, or editing my sometimes horrible grammar.

# Chapter 1

## Introduction

While the use of microorganisms in industrial processes is not new, the mathematical modelling of these industrial processes is, with the first serious models appearing in the 1960s. There are two main philosophies for modelling these complex systems. On the one hand, we can try to capture as many of the specific interactions occurring in the system as possible. Such models can end up as very detailed descriptions of the true situation, and can give accurate quantitative predictions for a given set of initial conditions if the functions are known and the parameters can be measured. However, they are often large and complicated, only qualitative properties of the functions are usually known and many (if not most) of the parameters are not measurable. For example, the anaerobic digestion model No. 1 (ADM1) [3] is a system of 32 differential equations and 8 algebraic equations that describe 7 different microbial species, the nutrients that are consumed, and certain products produced by the microorganisms. The size and complexity of these models often limits our ability to do rigorous mathematical analysis and hence make predictions concerning the full spectrum of dynamics of the system

or even understand the mechanisms responsible for certain outcomes. Numerical simulations are possible, but functions, parameters, and initial conditions must be specified. After creating a detailed model of the system, we can try to reduce the model to include what we suspect are the most important aspects. In the case of anaerobic digestion, this approach was taken in, for example, [4] and [18]. The goal in this case is to obtain a model that is simple enough for mathematical analysis but is still a good approximation of the actual system being modelled.

Another approach is to start with a basic model and use it as a foundation to build from. This way, modellers can ensure that they understand the fundamental mechanisms before testing more complex ideas. These models tend to be simple enough for rigorous mathematical analysis, since they typically focus on only one or two important interactions. The ability to conduct mathematical analysis can lead to important insights that would not be possible through numerical simulation alone. One very successful model in microbiology is the basic model of species competition in the chemostat [15].

The chemostat is a laboratory apparatus, originally developed by Novick and Szilard [14] to study bacterial growth in the laboratory. Ecologists have since used chemostats as a lab-scale model of a lake ecosystem. The basic setup involves a small tank that is filled with a solution containing a community of microorganisms and an abundance of all the nutrients the microorganisms need to grow and survive, except for one nutrient that is present in limiting quantities. A fresh supply of nutrients is fed into the tank at a constant rate, while excess liquid is removed at the same rate in order to keep the volume constant. Chemostats are operated under ideal conditions. The input nutrient concentration and dilution rates are

held constant, and the medium in the tank is stirred in order to keep the content of the vessel homogeneous. Under these conditions, a system of autonomous ordinary differential equations can be used to predict the concentration of limiting nutrients,  $s(t)$ , and the biomass,  $x_i(t)$ ,  $i = 1, 2, \dots, n$ , at time  $t$ , of populations competing for the limiting nutrient. The basic model of the chemostat model is given by

$$s'(t) = D(s^{\text{in}} - s(t)) - \sum_{i=1}^n \frac{1}{y_i} \mu_i(s(t)) x_i(t), \quad (1.1)$$

$$x'_i(t) = -Dx_i(t) + \mu(s(t))x_i(t) - k_i x_i(t), \quad i = 1, \dots, n, \quad (1.2)$$

where  $D$  is the flow rate of the incoming nutrient solution;  $s^{\text{in}}$  is the concentration of the incoming limiting nutrient;  $\mu_i : \mathbb{R}_+ \rightarrow \mathbb{R}_+$  is the nutrient-dependent growth rate of the microbial population,  $x_i$ , often called a *response function*;  $y_i$  is a species dependent conversion factor called a *yield coefficient*; and  $k_i$  is each species' decay rate, or maintenance coefficient. The simplicity of this mathematical model allowed for detailed mathematical analysis. In particular, the analysis of this model led to the prediction that the relative values of the minimum concentration of the limiting nutrient required to sustain growth of each species of the microbial community (called the *break-even concentration*) was the key factor in determining the outcome of microbial competition in the chemostat. When species-specific death rates were ignored, the analysis of the model in the case of Monod response functions was done in [9], in the case of general monotone response functions restricted to a globally attracting simplex in [1], and for general monotone and non-monotone response functions with general initial conditions in [5]. When death rates were included, the analysis in the case of Monod response functions was done in [7] and for general monotone response functions and some

non-monotone response functions in [20]. This competitive-exclusion principle was verified experimentally in 1980 by Hansen and Hubbell [6].

The model of the basic chemostat has been used as the foundation for many other models of microbial systems. In [10], the chemostat model was modified to consider the case that the medium in the tank is not perfectly well-stirred, a situation that is likely to occur in large bioreactors or lakes. The unstirred chemostat model in [10] was then used to develop a model of microbial growth in the large intestine [2]. In [8], the chemostat model was modified to include periodically varying nutrient input concentrations, meant to describe seasonally varying nutrient input in lakes. Even highly complicated models, such as ADM1, often use the chemostat model as a foundation.

The goal of this thesis is to investigate several models that can be seen as either modifications of the chemostat model or as simplifications of more detailed models. By rigorously analyzing these models, we hope to contribute to the understanding of microbial dynamics and how microbial populations can be used in industrial processes.

In Chapter 2, we study a qualitative simplification of ADM1, which is used to describe the industrial anaerobic digestion process used for biogas production. Biogas is an important (and relatively easy to produce) biofuel that can be used in place of natural gas and other fossil fuels to produce energy. In contrast to ADM1's 32 differential equations, the simplified model (proposed by Bornhöft *et al.* [4]) has only 5 state variables. While the authors claim that the simplified model has the same qualitative long-term dynamics as ADM1, we show that

this cannot be the case and that the simplified model is missing a key secondary biogas-producing equilibrium that was shown to potentially be the optimal biogas-producing equilibrium in [18]. We show that, at its core, the simplified model is equivalent to a variant of the basic model of growth in the chemostat in which the response function is non-monotone (i.e., the nutrient is inhibitory at both low and high concentrations) and the species decay rate is not neglected. The dynamics of this model had not been completely analyzed in the case when the parameters predict existence of two interior equilibria with bistability involving one of the interior equilibria and the washout steady state. We show that no periodic orbits are possible in this case, and that all solutions converge to an equilibrium point, completing the analysis of this system. Despite our objections on the validity of the model proposed in [4], we conduct some stochastic simulations of the system, and demonstrate that if stochasticity causes the microorganism population to die out, then it does so shortly after start up. Once the system is near equilibrium, the dynamics appear robust to stochastic perturbations. This chapter appeared in SIAM Journal of Applied Math as [13].

In Chapter 3 we investigate the growth of a microorganism on two essential, limiting nutrients in a self-cycling fermentor (also called a sequential batch reactor), which is a variant on the chemostat model in which nutrient is not continuously fed into the system, but input as a discrete event when a prescribed condition (called an impulse condition or decanting condition) is met. By assuming that the emptying/refilling time is much shorter than the growth dynamics (i.e., instantaneous), we can model the self-cycling fermentation process using a system of impulsive differential equations.

Impulsive differential equations are a form of discontinuous dynamical system in which the flow of a continuous dynamical system is intermittently mapped elsewhere in phase space. To describe a system of impulsive differential equations, we require the differential equations that govern the flow between mappings, a condition to define when the mappings occur (called an impulse condition) and the mappings on phase-space that occur when the impulse condition is met (called impulses or an impulse map). Each piece of information is important to the dynamics, and the problems encountered can be much more complex than those encountered in ordinary differential equations. Nevertheless, the questions we ask are often the same, for example: ‘What are the long term dynamics of the system?’ and ‘How do the long term dynamics depend on parameters or initial conditions?’ Many of the tools used to answer these questions are also similar to those used in continuous dynamical systems, such as Lyapunov’s second method, which makes regular appearances throughout this thesis.

For the model studied in Chapter 3, we derive conditions for the existence of a periodic solution to the system of equations that corresponds to the survival of the microorganism. We further derive initial-condition-dependent criteria for solutions to converge to this periodic orbit and show that, when these criteria are not satisfied, the microorganism eventually dies out. With the application of wastewater treatment in mind, we numerically find an optimal fraction of liquid to add and remove at impulses to maximize the throughput of the fermentor. This chapter appears in *Mathematical Biosciences and Engineering* as [11].

Chapter 4 is an extension of the results of Chapter 3. In this model, we consider an arbitrary number of limiting essential nutrients in a self cycling fermentor. In

contrast to Chapter 3, the response functions considered are general monotone-increasing functions that vanish if any nutrient concentration vanishes. This class of functions includes the response functions used in Chapter 3 as an example. We also consider different impulse conditions, with impulses occurring only when the tracked nutrient reaches a threshold value. Again, we find conditions for the existence of a periodic solution and determine initial-condition-dependent criteria for other solutions to converge to the periodic solution.

In Chapter 5, we summarize the results of the thesis and discuss how they fit into the landscape of current research.

# Chapter 2

## Global analysis of a simplified model of anaerobic digestion and a new result for the chemostat

### Abstract

A. Bornhöft, R. Hanke-Rauschenbach, and K. Sundmacher, [*Nonlinear Dyn.*, 73 (2013), pp. 535–549] introduced a qualitative simplification to the ADM1 model for anaerobic digestion. We obtain global results for this model by first analyzing the limiting system, a model of single species growth in the chemostat in which the response function is non-monotone and the species decay rate is included. Using a Lyapunov function argument and the theory of asymptotically autonomous systems, we prove that even in the parameter regime where there is bistability, no periodic orbits exist and every solution converges to one of the equilibrium points. We then describe two

algorithms for stochastically perturbing the parameters of the model. Simulations done with these two algorithms are compared with simulations done using the Gillespie and tau-leaping algorithms. They illustrate the severe impact environmental factors may have on anaerobic digestion in the transient phase.

## 2.1 Introduction

Anaerobic digestion is a biochemical process where microorganisms or multicellular organisms break down organic material in the absence of oxygen. Anaerobic digestion is an important part of many industrial practices, including the treatment of wastewater and the production of biogas. The role of anaerobic digestion in such applications has been an active area of recent research [1, 2, 3, 4, 10, 12, 14, 15, 19, 21]. This paper focuses on a particular model of anaerobic digestion in biogas production.

The foundation of previous work on the mathematical analysis of the production of biogas is the *Anaerobic Digestion Model 1* (ADM1) [1] introduced in 2002. If implemented as a system of differential equations, this model has 32 state variables, including seven different species of microorganisms. Understandably, anything other than numerical analysis has not been feasible.

In an effort to formally analyze the system, several groups [4, 10, 12, 24] have studied various subsystems of ADM1. Recently, Weederemann et al. [24, 25] combined two previous models [10, 12] to get a reasonably complete picture using only

eight state variables. Due to the inclusion of two pathways to biogas production in [24] and because the model captures the ADM1's sensitivity to the accumulation of acetic acid, [24] illustrates some of the complexity of ADM1, which must exhibit the same or an even richer dynamics than the model in [24].

Bornhöft et al. [4] introduced a model with five state variables based on their observations from a numerical steady-state analysis of the ADM1 model, and conjectured that their model undergoes the same bifurcations as the ADM1 model with the substrate inlet concentration as bifurcation parameter. The model in [4] is the first simplified model to consider the effects of ammonia. It is demonstrated that the proposed model is able to capture the same effects of ammonia on anaerobic digestion that are displayed by the ADM1 model. However, the analysis in this paper shows that the model does not possess all of the dynamics of ADM1, even if a broader class of growth functions is considered than the ones that were initially proposed. The model is missing some of the dynamics shown in [24], namely the possible bistability between two equilibria that both correspond to biogas production, a behaviour of the full ADM1 model that is also noted in [4].

The model in [4] considers two stages of anaerobic digestion, acidogenesis and methanogenesis. In the first stage, simple substrates are broken down by acidogenic microorganisms. The microorganisms use the energy from the simple substrates to grow, and produce volatile fatty acids (VFAs) and ammonia as byproducts. The VFAs and ammonia have opposing effects on the pH of the system; an increase in the concentration of VFAs will decrease the pH, while an increase in the concentration of ammonia will increase the pH. In the second stage, methanogenic microorganisms convert the VFAs to biogas. The methanogenic microorganisms

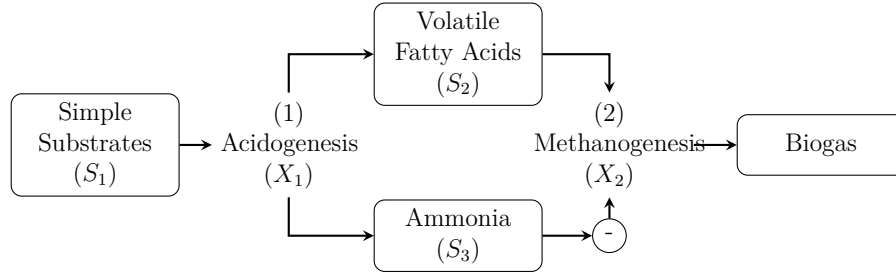


FIGURE 2.1: The anaerobic digestion process. (1) Acidogenic microorganisms break down simple substrates into VFAs and ammonia. (2) Methanogenic microorganisms break down VFAs into biogas such as methane. This process is inhibited by ammonia.

are very sensitive to the environment, and can only tolerate a relatively narrow pH range. Furthermore, ammonia is toxic to the methanogenic microorganisms in large quantities and will restrict their growth. The flow chart in Figure 2.1 summarizes the process.

In this paper we provide a formal mathematical analysis of the model proposed in [4], allowing a more general class of response functions. In Section 2.2, we describe the model and assumptions, and give properties of the solutions of the system. If the substrate input concentration is too low, the system converges to a state where no microorganisms are present. We show that if the substrate input concentration is high enough to allow the acidogenic microbial population to survive, the system reduces to a limiting system that is a two-dimensional basic model of growth in the chemostat that includes the decay rates and allows for any non-monotone response function.

In Section 2.3, we study the dynamics of this limiting system. We obtain a new global result in the case that the parameters allow bistability by proving that no nontrivial periodic orbits exist.

In Section 2.4 we use the theory of asymptotically autonomous systems and the results for the limiting system from Section 2.3 to provide a complete global analysis of the anaerobic digestion model in [4] for a more general class of response functions.

In Section 2.5, we propose two alternative prototype functions to model the growth of the methanogenic archaea and capture the inhibition by ammonia. These prototypes complement the one used in [4], which has the property that there is no growth in the absence of ammonia. The prototypes we introduce allow growth in the absence of ammonia, but are either unimodal or decreasing in ammonia. We provide bifurcation diagrams for all three prototypes, and compare how they influence the outcome.

In Section 2.6 we further investigate the model when the parameters are selected so that there are two stable steady states. In industrial applications of processes such as anaerobic digestion, operators must be aware of how physical and environmental processes, and changes in the biology of the species can affect the long term health of the reactor. One way to address these challenges is to include the effects of stochasticity in simulations of the model. Stochasticity can be a result of random births and deaths, or of fluctuations in the model parameters, possibly due to mutations or changes in the environment. Models of chemostats that include stochasticity have been considered in the literature (e.g., [6, 13]), but our approach differs from the ones presented in those papers. We consider stochasticity in the case where there are fluctuations in the parameters, and compare the results to two well known methods for simulating stochasticity in the case where there are random births and deaths. Our studies give new insight into why seemingly identical

reactor setups can lead to very different reactor performances. In Section 2.7, we summarize our results and discuss their implications for biogas production using anaerobic digestion.

## 2.2 The Model

Let  $X_1$ ,  $X_2$ ,  $S_1$ ,  $S_2$  and  $S_3$  denote the concentrations of the acidogenic microorganisms, methanogenic microorganisms, simple substrates, acetic acid and ammonia, respectively. The model is described by the system

$$\dot{S}_1 = (S^{(0)} - S_1)D - y_1\mu_1(S_1)X_1, \quad (2.1a)$$

$$\dot{X}_1 = -D_1X_1 + \mu_1(S_1)X_1, \quad (2.1b)$$

$$\dot{S}_2 = -DS_2 + y_2\mu_1(S_1)X_1 - y_3\mu_2(S_2, S_3)X_2, \quad (2.1c)$$

$$\dot{S}_3 = -DS_3 + y_4\mu_1(S_1)X_1, \quad (2.1d)$$

$$\dot{X}_2 = -D_2X_2 + \mu_2(S_2, S_3)X_2, \quad (2.1e)$$

where  $D$  is the dilution rate,  $S^{(0)}$  is the input concentration of simple substrates,  $D_i = D + k_i$ , where  $k_i \geq 0$  are the respective decay rates of  $X_i$ , and  $y_i$  are yield constants.

Let  $\mathbb{R}_+$  and  $\mathbb{R}_+^2$  denote the set of non-negative real numbers and the non-negative plane, respectively. We make the following assumptions concerning  $\mu_1$  and  $\mu_2$ :

(H1)  $\mu_1(S_1) \in C^1([0, \infty))$ , and  $\mu_1'(S_1) > 0$  for all  $S_1 > 0$ .

(H2)  $\mu_1(0) = 0, \mu_1(S_1) > 0$  for all  $S_1 > 0$ .

(H3)  $\mu_2(S_2, S_3) \in C^1(\mathbb{R}_+^2)$ , and  $\mu_2(S_2, S_3) > 0$  if  $S_2 > 0$  and  $S_3 > 0$ .

(H4)  $\lim_{S_3 \rightarrow \infty} \mu_2(S_2, S_3) = 0$  for all  $S_2 \geq 0$ .

(H5)  $\lim_{S_2 \rightarrow \infty} \mu_2(S_2, S_3) = 0$  for all  $S_3 \geq 0$ .

(H6)  $\mu_2(0, S_3) = 0$  for all  $S_3 \geq 0$  and  $\mu_2(S_2, 0) \geq 0$  for all  $S_2 > 0$

(H7) There exists  $\Gamma(S_3) \in C(\mathbb{R}_+)$  such that for  $S_2 < \Gamma(S_3)$ ,  $\partial_{S_2}\mu_2(S_2, S_3) > 0$  and for  $S_2 > \Gamma(S_3)$ ,  $\partial_{S_2}\mu_2(S_2, S_3) < 0$ .

Unlike in [4], we do not assume that both  $X_i$  have identical decay rates. (H1) and (H2) are satisfied by any of the Holling type I, II or III growth functions, which are standard to chemostat models. (H3), (H4), and (H5) capture the inhibitory nature of  $S_2$  and  $S_3$ , guaranteeing that large quantities of either  $S_2$  or  $S_3$  will be detrimental to the growth of  $X_2$ . (H6) ensures that an absence of acetic acid will result in no growth of the methanogenic microorganisms, while an absence of ammonia does not necessarily have this effect. We would like to note that the prototype describing the growth of methanogens proposed in [4] has the property that  $\lim_{S_3 \rightarrow 0} \mu_2(S_2, S_3) = 0$  for all  $S_2 \geq 0$ . We decided to relax this condition. (H7) intends to capture the nature of the inhibition mechanisms outlined in [4], whereby small concentrations of  $S_2$  are limiting on the growth of  $X_2$ , while large concentrations of  $S_2$  will increase the pH and hence be inhibitory. The curve  $\Gamma(S_3)$  is intended to describe how ammonia will decrease the pH to counteract the increase in pH caused by an increase in acetic acid. We make no further assumptions about how  $\mu_2(S_2, S_3)$  changes with  $S_3$ . In many cases, including

ADM1,  $\mu_2(S_2, S_3)$  will have a unimodal shape for fixed  $S_2$ , but we do not want to rule out the possibility of other profiles that may be useful.

Here, we introduce some notation. The *break-even concentration* of  $S_1$ ,  $\lambda_1$ , is the unique positive extended real number that solves

$$\mu_1(\lambda_1) = D_1. \quad (2.2)$$

If no such number exists, we take  $\lambda_1 = +\infty$ . When  $S_1 = \lambda_1$  and  $X_2 = 0$ , the equilibrium concentrations of  $S_2$  and  $S_3$ ,  $\lambda_2$  and  $\lambda_3$ , respectively, are given by

$$\lambda_2 = \frac{y_2}{y_1}(S^{(0)} - \lambda_1) \quad (2.3)$$

$$\lambda_3 = \frac{y_4}{y_1}(S^{(0)} - \lambda_1). \quad (2.4)$$

The *break-even concentrations* of  $S_2$ ,  $\sigma_1$  and  $\sigma_2$ , are the extended real numbers  $\sigma_2 \geq \sigma_1$  that solve

$$\mu_2(\sigma_i, \lambda_3) = D_2. \quad (2.5)$$

If no such numbers exist, which is the case when  $\mu_2(\Gamma(S_3), S_3) < D_2$ , then we write  $\sigma_1 = \sigma_2 = +\infty$ .

System (2.1) has a total of four possible equilibria,

$$E = (S^{(0)}, 0, 0, 0, 0) \quad (2.6a)$$

$$E_0 = (\lambda_1, X_1^*, \lambda_2, \lambda_3, 0) \quad (2.6b)$$

$$E_1 = (\lambda_1, X_1^*, \sigma_1, \lambda_3, X_{2,\sigma_1}^*) \quad (2.6c)$$

$$E_2 = (\lambda_1, X_1^*, \sigma_2, \lambda_3, X_{2,\sigma_2}^*), \quad (2.6d)$$

where

$$X_1^* = \frac{D(S^{(0)} - \lambda_1)}{y_1 D_1} \quad \text{and} \quad X_{2,\sigma_i}^* = \frac{D(\lambda_2 - \sigma_i)}{y_3 D_2}.$$

These equilibria are only biologically meaningful if each of the components is non-negative.  $E_1$  and  $E_2$ , when they exist, are called interior equilibria, since they lie in the interior of the positive cone  $\mathbb{R}_+^5$ .  $E$  and  $E_0$  are called boundary equilibria, since they lie on the boundary of the positive cone  $\mathbb{R}_+^5$ .

The following propositions give well-posedness results for system (2.1), provide conditions for the washout of the microorganisms in the reactor when the substrate input concentration is too low, and introduce the limiting system when the input concentration is high enough so that the acidogens survive. The proofs are given in Section 2.A.

**Proposition 2.2.1.** *Assume that  $X_i(0) \geq 0$  and  $S_i(0) \geq 0$ .*

- i) If  $X_1(0) = 0$ , then solutions converge to  $E$  as  $t \rightarrow \infty$ .*
- ii) If  $X_1(0) > 0$  and  $X_2(0) = 0$ , then  $X_1(t) > 0$  and  $S_i(t) > 0$  for all  $t > 0$  while  $X_2(t) = 0$  for all  $t \geq 0$ .*

iii) If  $X_1(0) > 0$  and  $X_2(0) > 0$ , then  $X_i(t) > 0$  and  $S_i(t) > 0$  are positive for all  $t > 0$ .

iv) All solutions are bounded for  $t \geq 0$ .

**Proposition 2.2.2.** *If  $\lambda_1 \geq S^{(0)}$ , then  $E$  is a globally asymptotically stable equilibrium of (2.1).*

**Proposition 2.2.3.** *If  $\lambda_1 < S^{(0)}$ , then (2.1) is a quasi-autonomous system with limiting system*

$$\dot{S}_2 = -DS_2 + \lambda_2 D - y_3 \mu_2(S_2, \lambda_3) X_2, \quad (2.7a)$$

$$\dot{X}_2 = -D_2 X_2 + \mu_2(S_2, \lambda_3) X_2. \quad (2.7b)$$

By Theorem 1.4 in [22], it will be enough to study the dynamics of this limiting system.

## 2.3 Global Analysis of Growth in the Chemostat

After the change of variables

$$X(t) = y_3 X_2(t), \quad S(t) = S_2(t), \quad \mu(S(t)) = \mu_2(S_2(t), \lambda_3), \quad S^0 = \lambda_2,$$

system (2.7) becomes a model of the chemostat:

$$\dot{S}(t) = -(S(t) - S^0)D - \mu(S(t))X(t) \quad (2.8a)$$

$$\dot{X}(t) = -D_2X(t) + \mu(S(t))X(t). \quad (2.8b)$$

Recall that  $\mu_2(S(t), \lambda_3)$  satisfies (H3) and (H4), and hence  $\mu(S(t))$  is a non-monotone response function with break-even concentrations  $0 < \sigma_1 < \sigma_2$ , the extended real numbers that solve  $\mu(\sigma_i) = D_2$ .

We define the equilibria of (2.8) that correspond to  $E_0, E_1$ , and  $E_2$ , respectively, for system (2.1) defined in (2.6b)-(2.6d):

$$\mathcal{E}_0 = (S^0, 0), \quad \mathcal{E}_1 = (\sigma_1, X_{\sigma_1}^*), \quad \mathcal{E}_2 = (\sigma_2, X_{\sigma_2}^*).$$

where  $X_{\sigma_i}^* = \frac{D(S^0 - \sigma_i)}{D_2}$ ,  $i = 1, 2$ .

Models of the chemostat have been well studied (e.g., see [20, 11] and the references therein). Model (2.8) is a model of growth of a single species in the chemostat with non-monotone response function that includes the species decay rate, i.e.  $D_2 = D + \epsilon$  where  $\epsilon > 0$  is the species decay rate.

In Wolkowicz and Lu [26], model (2.8) extended to the  $n$  species case was analyzed. The results of that paper, if applied to the single species growth model, completely determine the dynamics of (11) when  $\mu(S(t))$  is any monotone increasing function or it is non-monotone and  $\sigma_1 < S^0 \leq \sigma_2$ . However, the case that  $\mu(S(t))$  is a non-monotone response function and  $\sigma_1 < \sigma_2 < S^0$ , remained open.

Here, we provide a proof in this case and thus complete the global analysis of system (2.8). In particular, we prove that there are no periodic orbits, and hence although the outcome is initial condition dependent, either the species dies out or it approaches an equilibrium.

In the following theorem, we summarize what is known for the dynamics of (2.8), and provide a proof in the case that had remained open.

**Theorem 2.3.1.** *Consider model (2.8). Assume  $\mu(S)$  is continuously differentiable,  $\mu(0) = 0$ ,  $\mu(S) \geq 0$  for all  $S > 0$ , and there exist positive numbers  $\sigma_1 \leq \sigma_2$  (possibly infinite) such that  $\mu(S) < D_2$  if  $0 < S < \sigma_1$ ,  $\mu(S) > D_2$  if  $\sigma_1 < S < \sigma_2$ , and  $\mu(S) < D_2$  if  $S > \sigma_2$ . Let  $S(0) \geq 0$  and  $X(0) > 0$ .*

- i) If  $S^0 \leq \sigma_1 \leq \sigma_2$ , then  $\mathcal{E}_0$  is globally asymptotically stable.*
- ii) If  $\sigma_1 < S^0 \leq \sigma_2$ , then  $\mathcal{E}_1$  is globally asymptotically stable.*
- iii) If  $\sigma_1 = \sigma_2 < S^0$ , then  $\mathcal{E}_0$  is locally asymptotically stable and attracts all solutions except the solutions in the stable manifold of  $\mathcal{E}_1 = \mathcal{E}_2$ .*
- iv) If  $\sigma_1 < \sigma_2 < S^0$ , then  $\mathcal{E}_1$  and  $\mathcal{E}_0$  are locally asymptotically stable and  $\mathcal{E}_2$  is a saddle. Furthermore, any orbit that is not in the stable manifold of  $\mathcal{E}_2$  converges to either  $\mathcal{E}_1$  or  $\mathcal{E}_2$ .*

*Proof.* *i)-ii)* See [26].

*iii)* This result follows from standard phase plane analysis. When  $\sigma_1 = \sigma_2$ ,  $\mathcal{E}_1$  and  $\mathcal{E}_2$  coalesce and are unstable. All orbits converge to  $\mathcal{E}_0$  except those in the stable manifold of the degenerate saddle  $\mathcal{E}_1 = \mathcal{E}_2$ .

*iv)* If  $\sigma_1 < \sigma_2 < S^0$ , then  $\mathcal{E}_0$ ,  $\mathcal{E}_1$ , and  $\mathcal{E}_2$  all lie in  $\mathbb{R}_+^2$ . From standard local stability analysis, it follows that  $\mathcal{E}_0$  and  $\mathcal{E}_1$  are both locally asymptotically stable and  $\mathcal{E}_2$  is a saddle.

Next we show that no nontrivial periodic solutions are possible. We proceed using proof by contradiction. Suppose that there exists a nontrivial periodic solution,  $\Phi$ . By Proposition 2.2.1 all solutions are bounded and the first quadrant is invariant. By the Poincaré-Bendixson Theorem and standard phase-plane analysis,  $\Phi$  must surround  $\mathcal{E}_1$ , and must lie in the set

$$\mathcal{G} = \{(S, X) : 0 < S < \sigma_2, X > 0\}.$$

Define the Lyapunov function,

$$V(S, X) = \int_{\sigma_1}^S \frac{(\mu(\xi) - D_2)(S^0 - \sigma_1)}{D_2(S^0 - \xi)} d\xi + \left[ X - X_{\sigma_1}^* - X_{\sigma_1}^* \ln \left( \frac{X}{X_{\sigma_1}^*} \right) \right], \quad (2.9)$$

as in [26]. See Figure 2.2 for phase portraits of system (2.8) with typical level sets of the Lyapunov function. Note that (2.9) is a valid Lyapunov function for  $\mathcal{E}_1$  in  $\mathcal{G}$ , and

$$\dot{V}(S, X) = X(\mu(S) - D_2) \left( 1 - \frac{\mu(S)(S^0 - \sigma_1)}{D_2(S^0 - S)} \right),$$

is non-positive, for all  $S \in [0, \sigma_2]$  and  $X \geq 0$ , i.e., for all  $S$  in the closure of  $\mathcal{G}$ . By examining

$$\nabla V(S, X) = \left( \frac{(\mu(S) - D_2)(S^0 - \sigma_1)}{D_2(S^0 - S)}, 1 - \frac{X_{\sigma_1}^*}{X} \right) = \mathbf{0},$$

we see that  $\mathcal{E}_1$  and  $(\sigma_2, X_{\sigma_1}^*)$  are the only critical points of  $V(S, X)$  with  $S \leq \sigma_2$ .  $(\sigma_2, X_{\sigma_1}^*)$  is directly above  $\mathcal{E}_2$  in phase space, since by definition  $X_{\sigma_1}^* > X_{\sigma_2}^*$ . Notice that  $\partial^2 V(S, X)/\partial X^2 = X_{\sigma_1}^*/X^2 > 0$  for all  $X > 0$ ,  $\partial V(S, X)/\partial S < 0$  for  $0 < S < \sigma_1$ ,  $\partial V(S, X)/\partial S > 0$  for  $\sigma_1 < S < \sigma_2$ , and  $\partial V(S, X)/\partial S < 0$  for  $\sigma_2 < S < S^0$ . It follows that  $\mathcal{E}_1$  is a local minimum of  $V(S, X)$ , and  $(\sigma_2, X_{\sigma_1}^*)$  is a saddle point of  $V(S, X)$ . The level set  $V(S, X) = V(\sigma_2, X_{\sigma_1}^*)$  is given by

$$V(\sigma_2, X_{\sigma_1}^*) = \int_{\sigma_1}^{\sigma_2} \frac{(\mu(\xi) - D_2)(S^0 - \sigma_1)}{D_2(S^0 - \xi)} d\xi.$$

For  $S \leq \sigma_2$ , it is a closed curve surrounding  $\mathcal{E}_1$  and it passes through the point  $(\sigma_2, X_{\sigma_1}^*)$  (see the bold level set in Figure 2.2). The set

$$\mathcal{U} = \{(S, X) \in \mathbb{R}_+^2 : 0 \leq S \leq \sigma_2, V(S, X) \leq V(\sigma_2, X_{\sigma_1}^*)\}$$

is a positively invariant set where  $\dot{V}(S(t), X(t)) \leq 0$ . For the periodic orbit,  $\Phi$ , to surround  $\mathcal{E}_1$ , it must enter  $\mathcal{U}$ . Since  $\mathcal{U}$  is a positively invariant set, it follows that  $\Phi$  is contained entirely in  $\mathcal{U}$ . By the minor variation of LaSalle's invariance principle [26], any trajectory in  $\mathcal{U}$  converges to the largest invariant set in  $\mathcal{U} \cap \{(S, X) : \dot{V}(S, X) = 0\}$ . The only such invariant set is  $\mathcal{E}_1$ , and therefore  $\Phi = \mathcal{E}_1$  is an equilibrium point, a contradiction.

Now, from standard phase plane analysis and the Poincaré-Bendixson Theorem, it follows that all orbits converge to one of the three equilibria as  $t$  tends to infinity. The one-dimensional stable manifold of  $\mathcal{E}_2$  acts as a separatrix, defining the basins of attraction for  $\mathcal{E}_1$  and  $\mathcal{E}_0$ . □

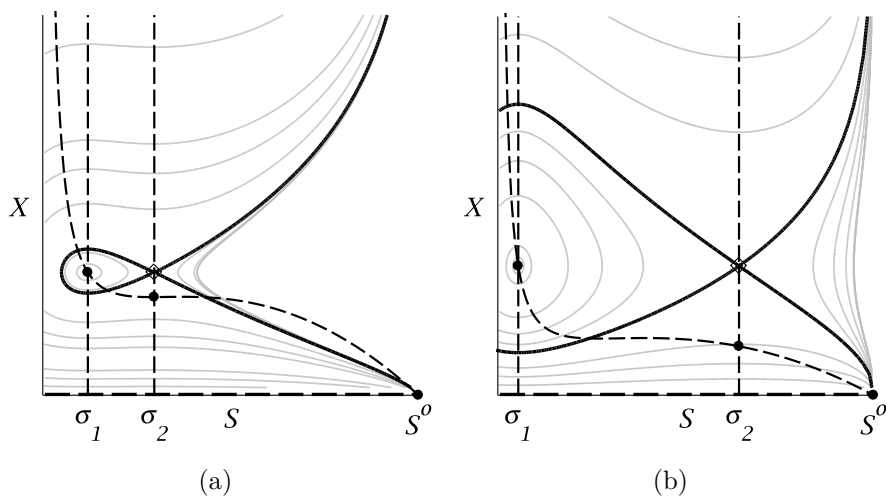


FIGURE 2.2: Phase portraits of system (2.8) with the level sets of  $V(S, X)$ . The dashed lines are the nullclines for  $X$  and the dashed curve is the nullcline for  $S$ . The equilibria  $\mathcal{E}_0$ ,  $\mathcal{E}_1$ , and  $\mathcal{E}_2$  are indicated by circles, and the point  $(\sigma_2, X_{\sigma_1}^*)$  is indicated by a diamond. The grey curves are the level sets of  $V(S, X)$ . The bold curve is the level set of  $V(S, X)$  that passes through the point  $(\sigma_2, X_{\sigma_1}^*)$ . These figures were produced using Maple [16].

## 2.4 Global Analysis of the Full System (2.1)

**Theorem 2.4.1.** *Consider model (2.1).*

- i) If  $\lambda_1 \geq S_1^{(0)}$ , then  $E$  is globally asymptotically stable.*
- ii) If  $\lambda_1 < S_1^{(0)}$  and  $\lambda_2 \leq \sigma_1 \leq \sigma_2$ , then  $E_0$  is a globally asymptotically stable equilibrium.*
- iii) If  $\lambda_1 < S_1^{(0)}$  and  $\sigma_1 < \lambda_2 \leq \sigma_2$ , then  $E_1$  is a globally asymptotically stable equilibrium.*
- iv) If  $\lambda_1 < S_1^{(0)}$  and  $\sigma_1 < \sigma_2 < \lambda_2$ , then  $E_0$  and  $E_1$  are locally asymptotically stable, and  $E_2$  is a saddle. Furthermore any orbit that does not lie on the stable manifold of  $E_2$  converges to one of  $E_0$  or  $E_1$ .*

*Proof.* *i)* was proved in Proposition 2.2.2.

*ii) - iv)* Since each of the  $E_i$ ,  $i = 0, 1, 2$  for model (2.1) corresponds to  $\mathcal{E}_i$  for system (2.8), the results follow from the results for the limiting system given in Theorem 2.3.1, followed by an application of the theory for asymptotically autonomous systems, either by using Theorem 1.4 in [22], or by a direct proof using the Butler-McGehee Lemma (as stated in Lemma 5.2 in [5] and applied there). □

## 2.5 Bifurcation Analysis of Full System (2.1)

As a result of the analysis of the previous two sections, the only possible bifurcations that can occur in (2.1) are transcritical bifurcations and saddle-node bifurcations.

In [4], a prototype growth function was introduced to capture the inhibition caused by ammonia. This prototype

$$\mu_{2,I}(S_2, S_3) = \frac{m_I S_2 S_3}{(K + S_2)(S_3 + k_1 S_2)(1 + k_2 S_3)}, \quad (2.10)$$

has the property that when there is no ammonia, which is toxic to the methanogenic microorganisms, the methanogenic microorganisms are unable to grow. We introduce two additional prototype functions

$$\mu_{2,II}(S_2, S_3) = \frac{m_{II} S_2}{K + k_1(S_2 - S_3)^2 + r S_2 S_3}, \quad (2.11a)$$

$$\mu_{2,III}(S_2, S_3) = \frac{m_{III} S_2(1 + S_3)}{(K + k_1 S_2 + r S_2^2)(a + S_3^2)}, \quad (2.11b)$$

that satisfy (H3)-(H7). Both  $\mu_{2,II}(S_2, S_3)$  and  $\mu_{2,III}(S_2, S_3)$  satisfy the additional property,  $\mu_{2,I}(S_2, 0) \geq 0$  with equality only when  $S_2 = 0$  or in the limit as  $S_2 \rightarrow \infty$ . For the parameters given in Table 2.1,  $\mu_{2,II}(S_2, S_3)$  is strictly decreasing in  $S_3$  and can be thought of as the opposite extreme of  $\mu_{2,I}(S_2, S_3)$ . It describes the scenario where ammonia is strictly inhibitory and the methanogenic microorganisms do best without any ammonia present. With a different set of parameters this response function can be unimodal in  $S_3$ . The third prototype,  $\mu_{2,III}(S_2, S_3)$  covers the middle ground between  $\mu_{2,I}(S_2, S_3)$  and  $\mu_{2,II}(S_2, S_3)$ ; it is unimodal in  $S_3$ , like

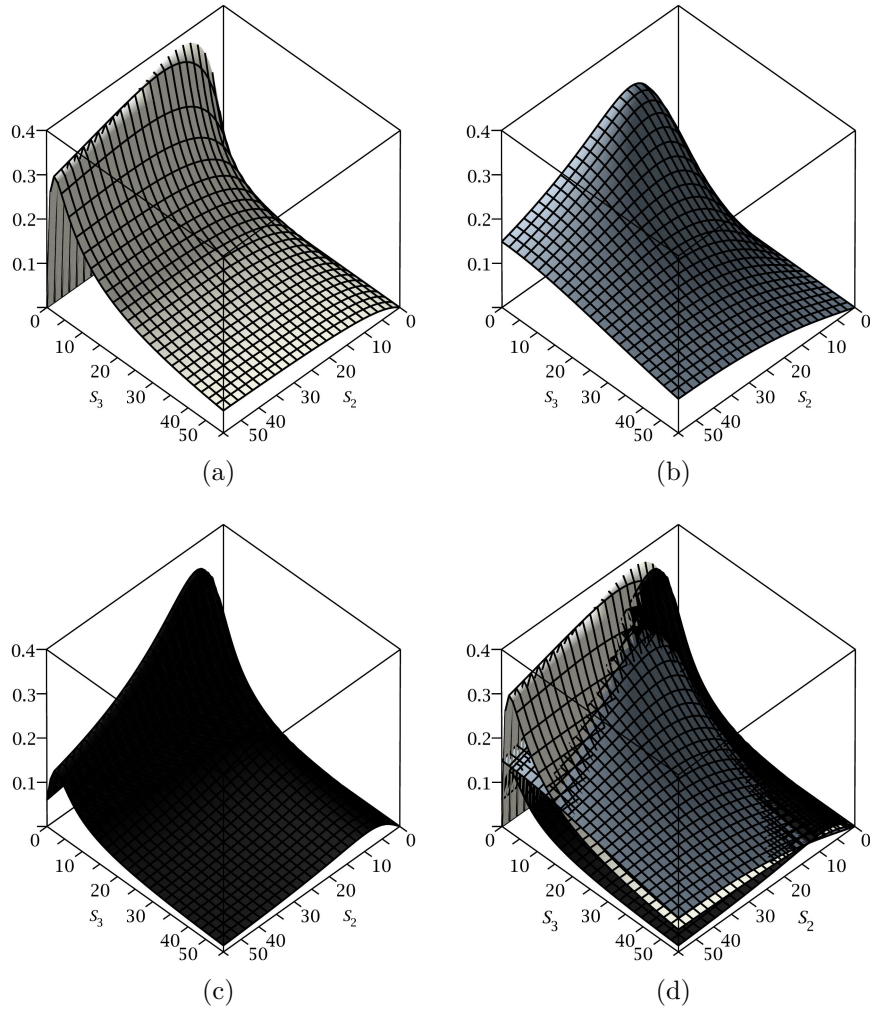


FIGURE 2.3: Plots of each prototype in 3-dimensions: (a)  $\mu_{2,I}(S_2, S_3)$ , (b)  $\mu_{2,II}(S_2, S_3)$ , (c)  $\mu_{2,III}(S_2, S_3)$ . (d) shows all three prototypes on the same axes for comparison. Parameters values used are given in Table 2.1.

$\mu_{2,I}(S_2, S_3)$ , but is non-zero when  $S_2 > 0$  and  $S_3 = 0$ , like  $\mu_{2,II}(S_2, S_3)$ .

The substrate input concentration,  $S^{(0)}$ , and dilution rate,  $D$ , are the two parameters that the operator of a reactor has the ability to control. In our bifurcation analysis, we focus on how the dynamics of the full system (2.1) change when these parameters vary. We note that  $\lambda_2$  and  $\lambda_3$  depend on  $S^{(0)}$  (see (2.3) and (2.4)), and hence,  $\max_{S_2 > 0} \mu_2(S_2, \lambda_3)$  changes when  $S^{(0)}$  changes. From the stability analysis in Section 2.3, two scenarios are possible. In the first scenario (see Figure 2.4), there is a transcritical bifurcation when  $\lambda_2 = \sigma_1$ , a transcritical bifurcation when  $\lambda_2 = \sigma_2$ , and a saddle-node bifurcation when  $\max_{S_2 > 0} \mu_2(S_2, \lambda_3) = D_2$ . In the second scenario (see Figure 2.5) there are two saddle node bifurcations as  $\lambda_3$  increases. This sequence of bifurcations occurs because  $\mu_{2,I}(S_2, S_3)$  and  $\mu_{2,III}(S_2, S_3)$  are unimodal in  $S_3$ . With the parameters listed in Table 2.1, the second prototype,  $\mu_{2,II}(S_2, S_3)$ , is strictly decreasing in  $S_3$ , and so only the first scenario is possible. The other two prototypes,  $\mu_{2,I}(S_2, S_3)$  and  $\mu_{2,III}(S_2, S_3)$ , are unimodal in  $S_3$ , and either scenario is possible.

In the bifurcation diagrams shown in Figures 2.4 and 2.5,

$$\mu_1(S_1) = \frac{\kappa S_1}{r_1 + S_1}, \quad (2.12)$$

and the parameters are the ones used in [4]. Any parameters not given in [4] (e.g.,  $m_{II}$ ,  $m_{III}$ ,  $r$ , and  $a$ ), were chosen so that the functions,  $\mu_{2,II}$  and  $\mu_{2,III}$ , closely resemble the function  $\mu_{2,I}$  given in [4]. See Table 2.1 for the parameter values used. A plot of each function is shown in Figure 2.3. The bifurcation diagrams in Figure 2.4 are qualitatively similar for each uptake function. The bifurcation

TABLE 2.1: The parameter values used in the following bifurcation diagrams are the ones used in [4], except  $m_{II}, m_{III}, r$ , and  $a$ , which were chosen so that the response functions  $\mu_{2,II}$  and  $\mu_{2,III}$  closely resemble  $\mu_{2,I}$ . The parameter  $D$  is the bifurcation parameter in Figures 2.4(a), 2.4(c) and 2.4(e), and  $S^{(0)}$  is the bifurcation parameter in Figures 2.4(b), 2.4(d) and 2.4(f).

Parameter	$S^{(0)}$	$D$	$D_i, i = 1, 2$		$\kappa$	$K$	$k_1$	$k_2$	$r$	$r_1$
Value	50	0.15	0.16		1.2	9.28	0.05	0.5	0.1	7.1
Parameter	$m_I$	$m_{II}$	$m_{III}$	$y_1$	$y_2$	$y_3$	$y_4$	$a$		
Value	1.64	0.4	3	42.14	116.5	268	1.165	12		

diagrams corresponding to  $\mu_{2,II}(S_2, S_3)$  and  $\mu_{2,III}(S_2, S_3)$  resemble the diagram for ADM1 in [4] more closely than the diagram for  $\mu_{2,I}(S_2, S_3)$ .

In the diagrams where  $D$  was used as the bifurcation parameter (Figures 2.4(a), 2.4(c) and 2.4(e)), there are three clear regions. In the first region when  $0 < D < D_1^*$ , only the equilibria  $\mathcal{E}_1$  and  $\mathcal{E}_0$  lie in the positive cone,  $\mathcal{E}_1$  is globally asymptotically stable and therefore all non-stationary solutions converge to  $\mathcal{E}_1$ . When  $D = D_1^*$  the washout equilibrium  $\mathcal{E}_0$  undergoes a transcritical bifurcation. In the second region, where  $D_1^* < D < D_2^*$  all three equilibria lie in the positive cone.  $\mathcal{E}_1$  and  $\mathcal{E}_0$  are locally asymptotically stable and  $\mathcal{E}_2$  is a saddle. All solutions (except the stable manifold of  $\mathcal{E}_2$ ) converge to one of  $\mathcal{E}_1$  or  $\mathcal{E}_0$ , depending on initial conditions. When  $D = D_2^*$ , the two interior equilibria  $\mathcal{E}_1$  and  $\mathcal{E}_2$  undergo a saddle node bifurcation. In the third region, where  $D_2^* < D$  only  $\mathcal{E}_0$  exists, and it is globally asymptotically stable. Therefore all solutions tend to  $\mathcal{E}_0$ .

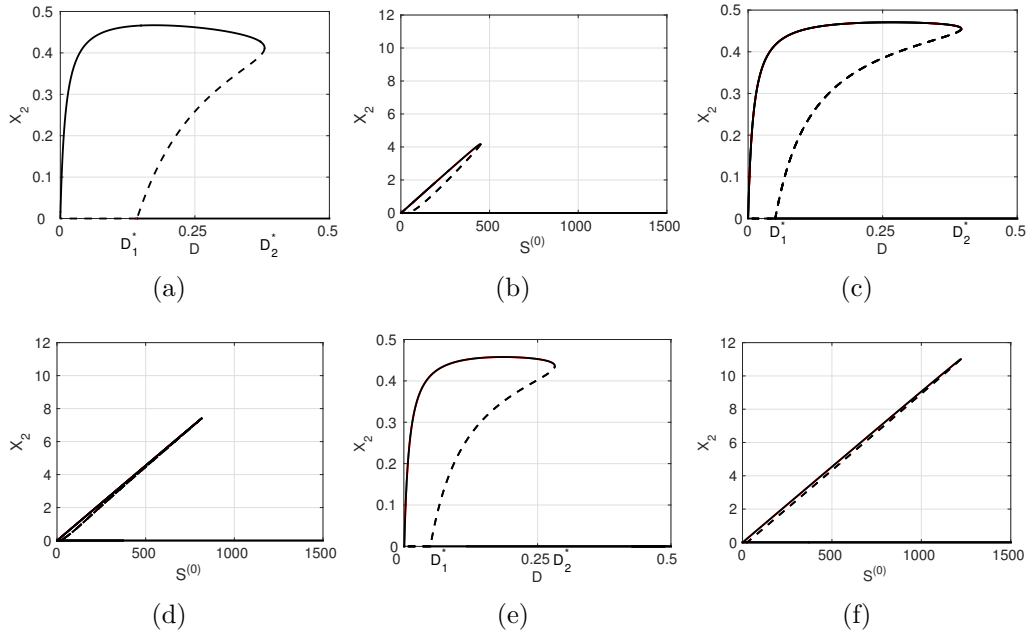


FIGURE 2.4: Bifurcation diagrams with bifurcation parameter  $D$  in (a), (c), (e) and  $S^{(0)}$  in (b),(d), (f) and response function  $\mu_2(S_2, S_3) = \mu_{2,I}(S_2, S_3)$  in (a) and (b), and  $\mu_2(S_2, S_3) = \mu_{2,II}(S_2, S_3)$  in (c) and (d) and  $\mu_2(S_2, S_3) = \mu_{2,III}(S_2, S_3)$  in (e) and (f).

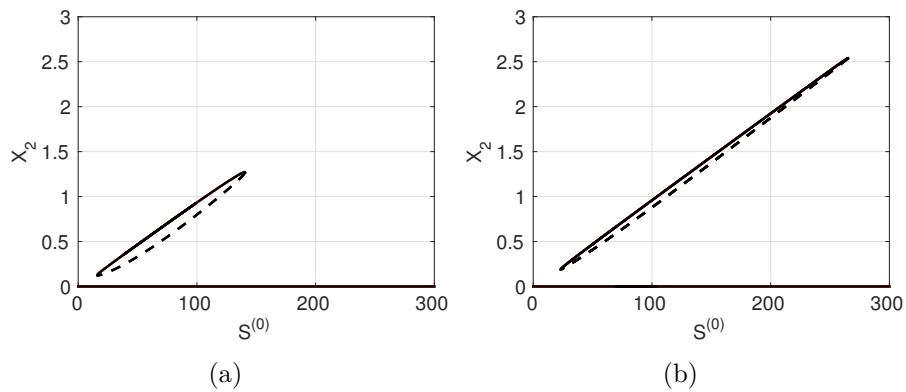


FIGURE 2.5: Bifurcation diagrams with bifurcation parameter  $S^{(0)}$  illustrating two saddle node bifurcations. (a)  $\mu_2(S_2, S_3) = \mu_{2,I}(S_2, S_3)$ . (b)  $\mu_2(S_2, S_3) = \mu_{2,III}(S_2, S_3)$ . The diagrams with  $\mu_{2,II}(S_2, S_3)$  do not exhibit this behaviour.

## 2.6 Stochastic Simulations of the Full System (2.1)

We describe two stochastic algorithms to capture stochasticity in the parameters. For comparison we also include simulations done with Gillespie’s stochastic simulation algorithm [8] and the adaptive tau-leaping algorithm [9].

The simulations in this section are all done for the full system (2.1) with

$$\mu_1(S_1) = \frac{\kappa S_1}{r_1 + S_1}$$

and  $\mu_2(S_2, S_3) = \mu_{2,\text{III}}(S_2, S_3)$ . The parameters are listed in Table 2.1. With these parameters, the deterministic system has two stable equilibria,  $E_0$  and  $E_1$ , and so the long-term behaviour of the solutions is initial condition dependent. If

$$(S_1(0), X_1(0), S_2(0), S_3(0), X_2(0)) = (50, 0.4, 0, 0, 1.16), \quad (2.13)$$

the solution of the deterministic system converges to  $E_1$  (see Table 2.2), and if

$$(S_1(0), X_1(0), S_2(0), S_3(0), X_2(0)) = (50, 0.4, 0, 0, 1.14), \quad (2.14)$$

the solution of the deterministic system converges to  $E_0$  (see Table 2.2). Thus, for one set of initial conditions, the deterministic system (2.1) predicts that the methanogens survive and produce biogas, and for the other it predicts that they do not. These initial conditions simulate the start up and inoculation of the reactor. The only difference between the initial conditions in (2.13) and (2.14) is the value of  $X_2(0)$ . Both initial conditions are close to the separatrix. We only

include figures that show the population of methanogens,  $X_2(t)$ , to compare the effect of stochasticity on biogas production, which only occurs if  $X_2$  is positive. In simulations (not shown) with initial conditions farther from the separatrix, solutions converged to the same equilibrium predicted by the deterministic model every time. The figures were produced using Matlab [17].

TABLE 2.2: Equilibria for system (2.1) with parameters given in Table 2.1, with  $\mu_2(S_2, S_3) = \mu_{2,\text{III}}(S_2, S_3)$ .

Equilibria	
$E$	(50, 0, 0, 0, 0)
$E_0$	(1.092, 1.088, 135.2, 1.352, 0)
$E_1$	(1.092, 1.088, 3.304, 1.352, 0.4614)
$E_2$	(1.092, 1.088, 28.09, 1.352, 0.3747)

We use two different approaches to study the behavior of (2.1) under stochastic perturbations. The first method is meant to model fluctuations in the parameters due, for example, to fluctuations in the environment. The second method captures the effect of potential mutations in members of the populations. In both schemes, multiple parameters are perturbed at randomly chosen times. Because we are varying many parameters, some of which appear in the non-linearities of the system, we are unable to write the resulting stochastic equations as a linear stochastic perturbation of the original system as was done in [23, 27] for chemostat models. In [23], the dilution rate and in [27], the dilution rate and the decay rates are assumed to vary stochastically. In one algorithm the perturbations are from the mean and in the other the perturbations are accumulative. Between perturbations the system is treated as a deterministic system that is solved numerically.

Let  $\tau_0 = 0$  and  $\tau_{i+1} = \tau_i - \ln(T_i)$ , where  $T_i \in (0, 1)$  is a uniformly distributed random variable. Therefore,  $\{\tau_i\}$  describes a monotone increasing sequence of times.

Let  $P_0$  be a row vector containing the parameter values present in the deterministic system that are affected by stochasticity. At each randomly chosen time  $\tau_i$ , these parameters values are updated to obtain a sequence of vectors  $\{P_{\tau_i}\}_{i=1}^{\infty}$ , and we set the parameters equal to  $P_t = P_{\tau_i}$ , for  $t \in [\tau_i, \tau_{i+1})$ .

In the first stochastic algorithm, which we call the environmental based fluctuation algorithm, we assume that the parameter values are influenced by the environment. As such, they cannot be perfectly controlled and so at random intervals of time they undergo small random changes. However, the parameters remain near their mean values given in the row vector  $P_0$ . Following this interpretation, we let  $N_t$  be a diagonal matrix with entries given by Gaussian random variables with mean  $\mu = 1$  and standard deviation,  $\sigma$ . We assume that  $N_t = N_{\tau_i}$  for  $t \in [\tau_i, \tau_{i+1})$ . Then

$$P_{\tau_{i+1}} = P_0 N_{\tau_i}. \quad (2.15)$$

Figures 2.6(a) and 2.6(b) show five simulations using the environmental based algorithm with  $\sigma = \frac{1}{10}$  and

$$P_0 = [S_0, D, y_1, y_2, y_3, y_4, K, k_1, m_{II}, r]$$

In Figure 2.6(a) the initial conditions are given by (2.14) and the solution to the deterministic system converges to  $E_0$ . In Figure 2.6(b), the initial conditions are given by (2.13) and solutions converge to  $E_1$ . The solutions for the deterministic system are shown in bold for comparison.

In the second stochastic algorithm, which we call the mutation based algorithm,

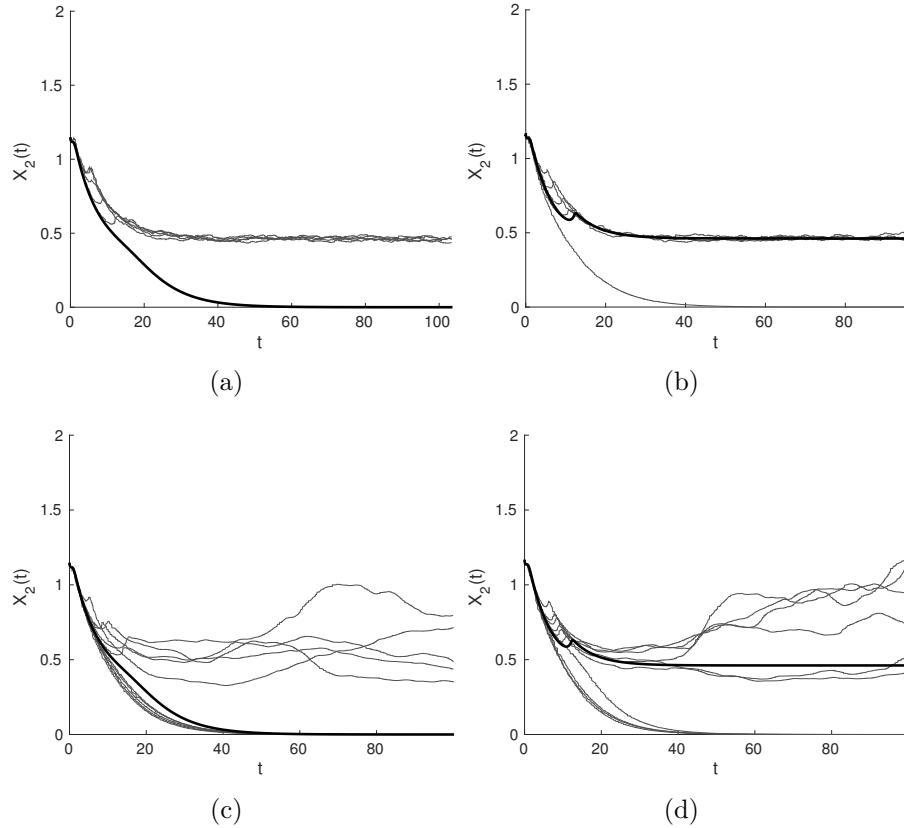


FIGURE 2.6: Sample paths of system (2.1) for the methanogens,  $X_2(t)$ , using the environmental fluctuation based method in Figures 2.6(a) and 2.6(b), and using the mutation based method in Figures 2.6(c) and 2.6(d). On the left, the initial conditions are given in (2.14) and are in the basin of attraction of  $E_0$  for the deterministic system. On the right, the initial conditions are given in (2.13) and are in the basin of attraction of  $E_1$  for the deterministic system. The darker curve in each graph is the solution of the deterministic system and the lighter curves show the results of different stochastic runs.

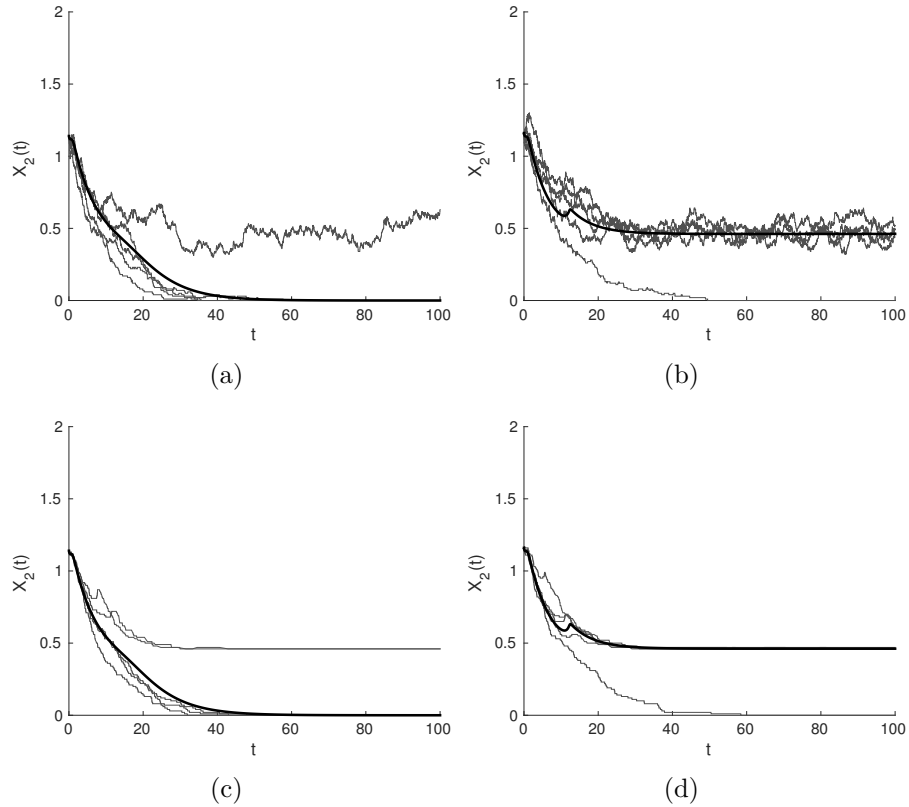


FIGURE 2.7: Sample paths of system (2.1) for the methanogens,  $X_2(t)$ , using Gillespie's SSA in Figures 2.7(a) and 2.7(b), and using the tau-leaping method in Figures 2.7(c) and 2.7(d). On the left, the initial conditions are given in (2.14) and are in the basin of attraction of  $E_0$  for the deterministic system. On the right, the initial conditions are given in (2.13) and are in the basin of attraction of  $E_1$  for the deterministic system. The darker curve in each graph is the solution of the deterministic system and the lighter curves show the results of different stochastic runs.

we assume that the parameters are dependent on properties of the microorganisms that can mutate, and therefore are subject to changes at random times that accumulate. In this case, many of the parameters are beyond the control of the operator, however we assume that the operator has complete control of the dilution rate  $D$  and the input concentration  $S_0$ . Following this interpretation, we update the parameters at random times to obtain,

$$P_{\tau_{i+1}} = P_{\tau_i} N_{\tau_i} = P_0 \prod_{n=1}^i N_{\tau_n}, \quad (2.16)$$

where again  $\sigma = \frac{1}{10}$ ,

$$P_0 = [y_1, y_2, y_3, y_4, K, k_1, m_{II}, r],$$

and  $N_{\tau_i}$  are as before. Using this algorithm,  $\{P_{\tau_i}\}_{i=1}^{\infty}$  is a random walk with mean  $P_0$ , and the mutations accumulate. Random walks have the property that  $\sigma^2 \rightarrow \infty$  as  $t \rightarrow \infty$ , and therefore the system is subject to wild fluctuations as time increases. Care must be taken so that the parameters, which have interpretations as positive quantities only, do not become negative. We ensure non-negativity by taking  $P_{\tau_{i+1}} = \max\{0, P_{\tau_i} N_{\tau_i}\}$ , and control the wild fluctuations by limiting the difference between current parameter values  $P_{\tau_i}$  and the initial parameter values  $P_0$  to be less than four standard deviations. Figures 2.6(c) and 2.6(d) shows five simulations using the mutation based algorithm.

We also include simulations using Gillespie's stochastic simulation algorithm (SSA) [8], in Figures 2.7(a) and 2.7(b). The SSA is an essentially exact description for systems with a finite number of interacting particles. The SSA is based on the principle of mass action, and as such the deterministic system must be converted

to an equivalent system that is of the form

$$\dot{S}_1 = \sum_{i,j,k,\ell,m} a_{ijklm} X_1^i S_1^j S_2^k S_3^\ell X_2^m, \quad (2.17a)$$

$$\dot{X}_1 = \sum_{i,j,k,\ell,m} b_{ijklm} X_1^i S_1^j S_2^k S_3^\ell X_2^m, \quad (2.17b)$$

$$\dot{S}_2 = \sum_{i,j,k,\ell,m} c_{ijklm} X_1^i S_1^j S_2^k S_3^\ell X_2^m, \quad (2.17c)$$

$$\dot{S}_3 = \sum_{i,j,k,\ell,m} d_{ijklm} X_1^i S_1^j S_2^k S_3^\ell X_2^m, \quad (2.17d)$$

$$\dot{X}_2 = \sum_{i,j,k,\ell,m} e_{ijklm} X_1^i S_1^j S_2^k S_3^\ell X_2^m. \quad (2.17e)$$

To do so, we rescale the time variable by  $dt = (r_1 + S_1)(K + k_1 S_2 + r S_2^2)(a + S_3^2) d\hat{t}$ . The resulting system has 104 different reaction terms that must be accounted for. As such, reporting the system here would be impractical. Although we have rescaled the time variable, the dynamics of system (2.17) are identical to those of (2.1). The SSA assumes that each reaction occurs independent of the others, and occurs with rates given by the coefficients of the differential equations. The SSA determines a time until each reaction takes place using the rate coefficients and the population of individuals relevant to that reaction, and increases or decreases the population(s) of the fastest reaction by a set step size. Once we have realized the simulation, we scale time back to the original time variable before plotting in order to compare with the other stochastic algorithms. Five simulations with a step size of  $\frac{1}{100}$  are shown in Figures 2.7(a) and 2.7(b). In reality, the step size is meant to represent a single individual in the population, but since SSA is notoriously slow, modelling a population of trillions of microorganisms and on the order of  $10^{23}$  molecules in this way is computationally impossible. It is also well known that as

you decrease the step size, the SSA will approach the deterministic solution [8].

Finally, we include simulations using the adaptive tau-leaping algorithm in Figures 2.7(c) and 2.7(d). The tau-leaping algorithm is an improvement on the SSA in terms of speed, and is generally easier to implement, although it is less accurate. One interpretation of the tau-leaping algorithm is that it is analogous to Euler's method, but instead of the derivative, a Poisson random variable with mean proportional to the derivative is used. Here, (2.1) takes the form

$$S_1(t + \tau) = S_1(t) + \delta P(\tau \dot{S}_1(t)), \quad (2.18a)$$

$$X_1(t + \tau) = X_1(t) + \delta P(\tau \dot{X}_1(t)), \quad (2.18b)$$

$$S_2(t + \tau) = S_2(t) + \delta P(\tau \dot{S}_2(t)), \quad (2.18c)$$

$$S_3(t + \tau) = S_3(t) + \delta P(\tau \dot{S}_3(t)), \quad (2.18d)$$

$$X_2(t + \tau) = X_2(t) + \delta P(\tau \dot{X}_2(t)), \quad (2.18e)$$

where  $\delta$  is the step size (typically interpreted to be an individual particle, as with the SSA). There has been much discussion on how to choose  $\tau$  appropriately [7, 9].

We chose

$$\tau = \min \left\{ \frac{1}{|\dot{S}_1|}, \frac{1}{|\dot{X}_1|}, \frac{1}{|\dot{S}_2|}, \frac{1}{|\dot{S}_3|}, \frac{1}{|\dot{X}_2|} \right\} \quad (2.19)$$

so that the fastest reaction determines  $\tau$ .

The stochasticity as simulated in the environmental based fluctuation algorithm and the mutation based algorithm stems from uncertainty in the system parameters, whether due to environmental noise or from mutations. The stochasticity of the SSA and tau-leaping algorithm is derived from the fact that the populations

are treated as discrete quantities. Since the populations are very large in practice, it may be more realistic to implement stochasticity using continuous hybrid algorithms that reflect the uncertainty in the parameters.

In the simulations using all four algorithms, if the stochasticity caused the system to predict a different outcome than the deterministic system, it usually happened while the system was transient. Once the system neared an equilibrium, the behaviour was usually quite stable. In rare instances, noise caused the system to destabilize after nearing an equilibrium, but this seemed only to occur for the mutation based method when the noise was quite large.

## **2.7 Conclusion**

We analyze the system introduced by Bornhöft et al. [4], which was proposed as a qualitative reduction of the ADM1 model, and claimed to capture the most relevant qualitative features of the ADM1 model. We give a complete global analysis of the dynamics of the model. If the concentration of the simple substrates is too low, both the acidogenic and methanogenic populations of microorganisms are eliminated from the reactor and no biogas is produced. Even if the input concentration of simple substrates is high enough, if the equilibrium concentration of VFAs produced by the acidogenic microorganisms is too low, then the methanogenic microorganisms will be eliminated from the reactor, and the system will converge to an equilibrium where no biogas is produced. If the VFA concentration is in a proper range, the system has a single globally stable interior equilibrium. Finally, if the equilibrium concentration of VFAs is very high, then the system possesses

two stable equilibria and one unstable equilibrium, and no sustained oscillatory behaviour is possible. In this case the long-term behavior is initial condition dependent. Only one of the two stable equilibria corresponds to the production of biogas meaning that it depends on the initial conditions whether the reactor will produce biogas in the long-term. The system does not allow bistability involving two or more biogas producing equilibria, previously shown to be possible for the ADM1 model [1] and for the models studied in [24, 25]

The dynamics predicted by a bifurcation analysis of the model is qualitatively similar for all three prototype functions. Ammonia inhibition is included in the ADM1 model, however, in ADM1 ammonia is not included as a dynamic variable. Ammonia concentration in ADM1 is computed as the difference of the concentration of inorganic nitrogen and  $NH_4^+$ . In the present model, ammonia is included as a dynamic variable and it is important to determine how to best model the effect of ammonia on the growth of the methanogens to capture the behaviour of ADM1. For all three prototype functions, inhibition of the growth of acetoclastic methanogens due to ammonia is unimodal with respect to the ammonia concentration. However, for  $\mu_{2,I}(S_2, S_3)$ , acetoclastic methanogens will not grow in the absence of ammonia, while for  $\mu_{2,II}(S_2, S_3)$  and  $\mu_{2,III}(S_2, S_3)$  the organisms grow even if the ammonia concentration is zero. Based on a comparison with Fig. 10 in [4], using  $\mu_{2,II}$  or  $\mu_{2,III}$  in model (2.1), the behavior resembles the behavior of the ADM1 model shown in [4] more closely than using  $\mu_{2,I}(S_2, S_3)$ . This indicates that these two functions are better suited to model the dependence of acetoclastic methanogens on ammonia.

We consider two algorithms that simulate stochastic effects in system (2.1).

The aim of these two algorithms is to model the uncertainty and variation in environmental and biological parameters that are hard to control with numerical algorithms that are easy to implement and run relatively quickly. We compare the resulting graphs with the graphs produced using the well-known Gillespie algorithm and the tau-leaping algorithm. The stochastic simulations from all four algorithms seem to indicate that a failure of the reactor is most likely to occur early in the reactors operating cycle, and that once the reactor has reached a steady state, it is quite resilient and less affected by minor perturbations due to mutations or small fluctuations in the environment. The one possible exception is in our mutation based stochastic algorithm that is intended to simulate the accumulation of mutations within the microbial population. Therefore, it appears to be most important to control the environment of the reactor during start up, and then to carefully monitor the characteristics of the microorganisms within the reactor after start up.

The analysis of the model of anaerobic digestion proposed by Bornhöft et al. [4] involved studying the limiting system (2.8), a model of growth in the chemostat in the case of a non-monotone response function with species decay rate added to the dilution rate. Armstrong and McGehee [18] considered model (2.8) extended to  $n$  species competition in the case of monotone response functions. By ignoring the species decay rate, they were able to apply a conservation law to obtain a limiting system. They then studied the resulting limiting system, but did not apply the theory of asymptotically autonomous systems to obtain results for the full system. Butler and Wolkowicz [5] used a different method, provided a complete global analysis of this  $n$  species model for both arbitrary monotone and non-monotone

response functions, and applied results for asymptotically autonomous systems so that their results applied to the full system, not just the limiting system. They proved that competitive exclusion holds, i.e., all solutions approach an equilibrium that can be initial condition dependent in the non-monotone case. In Wolkowicz and Lu [26], the decay rates were no longer ignored. There it was proved that for a large class of monotone and non-monotone response functions, again competitive exclusion holds and all populations approach equilibrium. However, in the case of non-monotone response they only considered the case when the species with the lowest break-even concentration also has its larger break-even concentration larger than the substrate input concentration. In the case of only one species, their method works for all monotone response functions, but for non-monotone response functions still requires the assumption that the larger break-even concentration is larger than the input concentration. In this paper we were able to eliminate this assumption, and hence complete the analysis for the model of growth in the basic chemostat.

## 2.A Proofs

*Proof of Proposition 2.2.1*

*i)* Assume first that  $X_1(0) = 0$  and all other initial conditions are non-negative. It follows that  $X_1(t) = 0$ , for all  $t \geq 0$ . Hence, (2.1) reduces to the system of first

order differential equations

$$\dot{S}_1 = (S^{(0)} - S_1)D, \quad (2.20a)$$

$$\dot{S}_2 = -DS_2 - y_3\mu_2(S_2, S_3)X_2, \quad (2.20b)$$

$$\dot{S}_3 = -DS_3, \quad (2.20c)$$

$$\dot{X}_2 = -D_2X_2 + \mu_2(S_2, S_3)X_2. \quad (2.20d)$$

Equations (2.20a) and (2.20c) imply that  $S_1$  and  $S_3$  converge exponentially to  $S^{(0)}$  and 0, respectively. The hyperplane given by  $S_2 = 0$  is invariant under (2.20b) by (H6), and the hyperplane given by  $X_2 = 0$  is invariant under (2.20d). By uniqueness of solutions to initial value problems, if  $S_2(0) \geq 0$  and  $X_2(0) \geq 0$ , then  $S_2(t) \geq 0$  and  $X_2(t) \geq 0$  for all  $t \geq 0$ . Consider  $\Sigma = S_2 + y_3X_2$ . Then  $\dot{\Sigma} = -DS_2 - y_3D_2X_2 \leq -D\Sigma$  and thus  $\Sigma(t) \rightarrow 0$  as  $t \rightarrow \infty$ , implying  $X_2(t)$  and  $S_2(t)$  must each converge to 0 as  $t \rightarrow \infty$ .

*ii) and iii)* Assume that  $X_1(0) > 0$  and  $X_2(0) \geq 0$ , with all other initial conditions non-negative. Notice first that (2.1a) and (2.1b) decouple from the system. They describe a simple chemostat, for which it is known that if  $X_1(0) > 0$  and  $S_1(0) \geq 0$ , then  $S_1(t) > 0$  and  $X_1(t) > 0$  for all  $t > 0$  (e.g., see [20, 26, 11]). Note that the hyperplane  $X_2 = 0$  is invariant under (2.20d), and so if  $X_2(0) = 0$ ,  $X_2(t) = 0$  for all  $t \geq 0$ , and if  $X_2(0) > 0$ , then  $X_2(t) > 0$  for all  $t \geq 0$ . If  $S_3(0) = 0$ , then by (2.1d),  $\dot{S}_3(0) > 0$ , and so there exists  $\epsilon > 0$  such that  $S_3(t) > 0$  for all  $t \in (0, \epsilon)$ . Let  $S_3(0) \geq 0$ . Suppose that there exists  $\hat{t} > 0$  such that  $S_3(t) > 0$  for all  $t \in (0, \hat{t})$  and  $S_3(\hat{t}) = 0$ . Then,  $\dot{S}_3(\hat{t}) \leq 0$ , but again from (2.1d),  $\dot{S}_3(\hat{t}) = y_4\mu_1(S_1(\hat{t}))X_1(\hat{t}) > 0$ , a contradiction. Hence,  $S_3(t) > 0$  for all  $t > 0$ .

Using (2.1c), a similar argument applies to  $S_2$ .

*iv)* It is known (e.g., see [20, 26, 11]) that solutions to the simple chemostat ((2.1a) and (2.1b)) are bounded. Hence, there exists  $0 < M < \infty$  such that  $S_1(t) < M$  and  $X_1(t) < M$  for all  $t \geq 0$ . Thus,  $S_3$  satisfies

$$\dot{S}_3 \leq -DS_3 + y_4\tilde{M}, \quad (2.21)$$

where  $\tilde{M} = \mu_1(M)M$ . This differential inequality implies that  $S_3(t) \leq \frac{y_4\tilde{M}}{D} + S_3(0)e^{-Dt}$  for all  $t \geq 0$ , and thus  $S_3(t)$  is bounded for  $t > 0$ . Since  $D_i \geq D$  the following differential inequality holds

$$\dot{X}_2 \leq -DX_2 + \mu_2(S_2, S_3)X_2. \quad (2.22)$$

Let  $\Sigma = y_3X_2 + S_2 - \frac{y_2}{y_4}S_3$ . Using (2.22), we see that  $\dot{\Sigma} \leq -D\Sigma$ , which implies that  $\Sigma(t) \leq \Sigma(0)e^{-Dt}$ . Since  $S_3(t)$  is bounded above and we know that  $S_2(t), X_2(t) \geq 0$  for all  $t \geq 0$ , they too must be bounded above.  $\square$

### *Proof of Proposition 2.2.2*

Since (2.1a) and (2.1b) depend only on  $S_1(t)$  and  $X_1(t)$ , these equations decouple from the full system (2.1), and it follows from known results on the basic model of the chemostat (e.g., see [20, 11]) that if  $\lambda_1 \geq S^{(0)}$ , then  $(S_1(t), X_1(t)) \rightarrow (S^{(0)}, 0)$  as  $t \rightarrow \infty$ . Therefore, for any  $\epsilon > 0$ , there is a  $T > 0$  such that for  $t > T$ ,  $S_1(t) < S^{(0)} + \epsilon$  and  $X_1(t) < \epsilon$ . Then, for  $t > T$ ,  $\dot{S}_3(t) \leq -DS_3(t) + y_4\mu_1(S^{(0)} + \epsilon)\epsilon$ , which gives  $S_3(t) \leq S_3(T)e^{-Dt} + \frac{y_4}{D}\mu_1(S^{(0)} + \epsilon)\epsilon(1 - e^{-D(t-T)})$ . Then,  $\lim_{t \rightarrow \infty} S_3(t) = \frac{y_4}{D}\mu_1(S^{(0)} + \epsilon)\epsilon$ . Since this holds for all  $\epsilon > 0$ , letting

$\epsilon \rightarrow 0$ , gives  $\lim_{t \rightarrow \infty} S_3(t) = 0$ . Next, let  $\Sigma_2(t) = S_2(t) + \frac{1}{y_3} X_2(t)$ . Since  $D \leq D_2$ ,  $\dot{\Sigma}_2(t) \leq -D\Sigma_2(t) + y_2\mu_1(S_1(t))X_1(t)$ . The same argument as before proves that  $\lim_{t \rightarrow \infty} \Sigma_2(t) = 0$ . Since for all  $t$ ,  $S_2(t) \geq 0$  and  $X_2(t) \geq 0$ , it follows that  $\lim_{t \rightarrow \infty} S_2(t) = \lim_{t \rightarrow \infty} X_2(t) = 0$ .  $\square$

To show that system (2.1) is a quasi-autonomous system with limiting system (2.7), we first prove a lemma. We call

$$\dot{x}(t) = f(t, x(t)) \tag{2.23}$$

with  $x(t) \in X$  a *quasi-autonomous system* with limiting system

$$\dot{y}(t) = g(y(t)) \tag{2.24}$$

if for any compact set  $K \subset X$

$$\int_{t_0}^{\infty} \sup_{x(t) \in K} \|f(t, x(t)) - g(x(t))\| dt < \infty. \tag{2.25}$$

**Lemma 2.A.1.** *Let  $\dot{x}(t) = f(t, x(t))$  be quasi-autonomous with limiting system  $\dot{y}(t) = g(y(t))$  and assume that there exists  $h(x(t))$  such that for all  $K \subset X$  compact*

$$\int_{t_0}^{\infty} \sup_{x(t) \in K} \|g(x(t)) - h(x(t))\| dt < \infty. \tag{2.26}$$

*Then  $\dot{x}(t) = f(t, x(t))$  is quasi-autonomous with limiting system  $\dot{y}(t) = h(y(t))$ .*

*Proof.* By the triangle inequality,

$$\begin{aligned}
\int_{t_0}^{\infty} \sup_{x \in K} \|f(t, x) - h(x)\| dt &\leq \int_{t_0}^{\infty} \sup_{x \in K} \|f(t, x) - h(x) + g(x) - g(x)\| dt \\
&\leq \int_{t_0}^{\infty} \sup_{x \in K} \|f(t, x) - g(x)\| + \|g(x) - h(x)\| dt \\
&\leq \int_{t_0}^{\infty} \sup_{x \in K} \|f(t, x) - g(x)\| dt + \int_{t_0}^{\infty} \sup_{x \in K} \|g(x) - h(x)\| dt \\
&< \infty. \qquad \square
\end{aligned}$$

*Proof of Proposition 2.2.3*

First we show that (2.1) is quasi-autonomous with limiting system:

$$\dot{S}_2 = (-S_2 + \lambda_2)D - y_3\mu_2(S_2, S_3)X_2, \quad (2.27a)$$

$$\dot{S}_3 = -DS_3 + \lambda_3D, \quad (2.27b)$$

$$\dot{X}_2 = -D_2X_2 + \mu_2(S_2, S_3)X_2. \quad (2.27c)$$

Since we are assuming that  $\mu_1(S_1)$  is a monotone response function, the results in [26] can be applied to the first two equations in (2.1) to prove that  $(S_1(t), X_1(t))$  converge exponentially to  $(\lambda_1, X_1^*)$  as  $t \rightarrow \infty$ . (The restriction that the results in [26] only apply to a general class of monotone response functions rather than any monotone response function does not apply to the single species growth model.)

Let  $x(t) = (S_1(t), X_1(t), S_2(t), S_3(t), X_2(t))$  be any solution of (2.1),  $K \subset \mathbb{R}_+^5$  be a compact set, and let  $\|\cdot\|$  denote the Euclidean norm. For  $t_0 \geq 0$ , consider

$$\mathcal{Q}_1 = \int_{t_0}^{\infty} \sup_{x \in K} \|(Y_1(t), Y_2(t), Y_3(t), Y_4(t), 0)\| dt,$$

where

$$Y_1(t) = (S^{(0)} - S_1(t))D - y_1\mu_1(S_1(t))X_1(t),$$

$$Y_2(t) = -D_1X_1(t) + \mu_1(S_1(t))X_1(t),$$

$$Y_3(t) = y_2\mu_1(S_1(t))X_1(t) - D\lambda_2,$$

$$Y_4(t) = y_4\mu_1(S_1(t))X_1(t) - D\lambda_3.$$

If  $t_0 = 0$ , then for any  $0 < t_1 < \infty$ , by continuity of the norm,

$$\int_0^{t_1} \sup_{x \in K} \|(Y_1(t), Y_2(t), Y_3(t), Y_4(t), 0)\| dt < \infty. \quad (2.28)$$

Thus, we need only consider the case  $t_0 > 0$ . By the Cauchy-Schwartz inequality,

$$\mathcal{Q}_1 \leq \left( \int_{t_0}^{\infty} \frac{1}{t^2} dt \right)^{\frac{1}{2}} \left( \int_{t_0}^{\infty} t^2 \sup_{x \in K} (Y_1(t)^2 + Y_2(t)^2 + Y_3(t)^2 + Y_4(t)^2) dt \right)^{\frac{1}{2}}. \quad (2.29)$$

The first integral,  $\int_{t_0}^{\infty} \frac{1}{t^2} dt$ , is finite. Since all of the terms of

$$\int_{t_0}^{\infty} t^2 \sup_{x \in K} (Y_1(t)^2 + Y_2(t)^2 + Y_3(t)^2 + Y_4(t)^2) dt, \quad (2.30)$$

are positive, we can consider them individually. We begin with the second term,

$$\int_{t_0}^{\infty} t^2 \sup_{x \in K} Y_2(t)^2 dt = \int_{t_0}^{\infty} t^2 \sup_{x \in K} X_1^2(t) [-D_1 + \mu_1(S_1(t))]^2 dt.$$

Since  $\mu_1(S_1) \in C^1$ , by the Mean Value Theorem, for every  $t > 0$ , there exists  $\theta(t)$ , such that  $S_1(\theta(t))$  lies between  $S_1(t)$  and  $\lambda_1$ . Let  $M_0 = \sup_{t \in [0, \infty)} |\mu_1'(S_1(\theta(t)))| > 0$ . Since  $S_1(t) \rightarrow \lambda$  as  $t \rightarrow \infty$ ,  $\mu_1'(S_1(\theta(t)))$  remains bounded,  $M_0$  is finite and

$|-D_1 + \mu_1(S_1(t))| = |-\mu_1(\lambda_1) + \mu_1(S_1(t))| = |\mu_1'(S_1(\theta(t)))| |-\lambda_1 + S_1(t)| \leq M_0 |-\lambda_1 + S_1(t)| \rightarrow 0$ , exponentially as  $t \rightarrow 0$ . Thus, there is a  $k > 0$ , such that

$$\int_{t_0}^{\infty} t^2 \sup_{x \in K} X_1^2(t) [-D_1 + \mu_1(S_1(t))]^2 dt \leq \overline{X_1} \widetilde{M_0}^2 \int_{t_0}^{\infty} t^2 e^{-2kt} dt < \infty,$$

where  $\overline{X_1}$  is the maximum value of  $X_1(t) \in K$ , and  $\widetilde{M_0} = M_0 |S_1(0) - \lambda_1|$ .

We now consider the first term,

$$\begin{aligned} \int_{t_0}^{\infty} t^2 \sup_{x \in K} Y_1(t) dt &= \int_{t_0}^{\infty} t^2 \sup_{x \in K} \left[ (S^{(0)} - S_1(t))D - y_1 \mu_1(S_1(t))X_1(t) \right]^2 dt \\ &\leq \int_{t_0}^{\infty} t^2 \sup_{x \in K} \left[ (\lambda_1 - S_1(t))D - y_1 \mu_1(S_1(t))X_1(t) + (S^{(0)} - \lambda_1)D \right]^2 dt. \end{aligned}$$

By Young's inequality and using  $S^{(0)} - \lambda_1 = y_1 X_1^*$ ,

$$\int_{t_0}^{\infty} t^2 \sup_{x \in K} Y_1(t) dt \leq \int_{t_0}^{\infty} 2t^2 \sup_{x \in K} \left[ (\lambda_1 - S_1(t))^2 D^2 + y_1^2 (\mu_1(S_1(t))X_1(t) - X_1^* D)^2 \right] dt.$$

Since this integral is a sum of positive terms we may consider each term individually. The first term is bounded above by the integral of a decaying exponential, and so is finite. We use Young's inequality to bound the second term,

$$\begin{aligned} &2 \int_{t_0}^{\infty} t^2 \sup_{x \in K} \left[ y_1^2 (\mu_1(S_1(t))X_1(t) - D_1 X_1(t) + D_1 X_1(t) - X_1^* D)^2 \right] dt \\ &\leq 4y_1^2 \int_{t_0}^{\infty} t^2 \sup_{x \in K} \left[ X_1(t)^2 (\mu_1(S_1(t)) - D_1)^2 + D_1^2 \left( X_1(t) - X_1^* \frac{D}{D_1} \right)^2 \right] dt, \quad (2.31) \end{aligned}$$

where both of the terms in (2.31) are bounded above by a decaying exponential and so this integral is finite. For the third term in (2.30), write

$$\begin{aligned} & \int_{t_0}^{\infty} t^2 \sup_{x \in K} [y_2 \mu_1(S_1(t)) X_1(t) - D\lambda_2]^2 dt \\ &= \int_{t_0}^{\infty} t^2 y_2^2 \sup_{x \in K} \left[ \mu_1(S_1(t)) X_1(t) - D_1 X_1(t) + D_1 X_1(t) - \frac{D\lambda_2}{y_2} \right]^2 dt \\ &\leq \int_{t_0}^{\infty} t^2 y_2^2 \sup_{x \in K} [\mu_1(S_1(t)) X_1(t) - D_1 X_1(t)]^2 dt + \int_{t_0}^{\infty} t^2 \sup_{x \in K} [y_2 D_1 X_1(t) - D\lambda_2]^2 dt. \end{aligned}$$

Noting that  $y_2 D_1 X_1^* = D\lambda_2$ , the exponential decay of  $(X_1(t) - X_1^*)^2$ , and the same decay arguments as with the first term in (2.30). The finiteness of the fourth term in (2.30) follows from a similar idea, noting that  $y_4 D_1 X_1^* = D\lambda_3$ . Thus, (2.1) is quasi-autonomous with limiting system (2.27).

Now we finally show that (2.1) has limiting system (2.7). From (2.27b), it follows that

$$|S_3(t) - \lambda_3| = |S_3(0) - \lambda_3| e^{-Dt}. \quad (2.32)$$

We use this to argue that

$$\mathcal{Q}_2 = \int_{t_0}^{\infty} \sup_{x \in K} \sqrt{(y_3^2 + 1) Y_5(t)^2 + D^2 Y_6(t)^2} dt < \infty,$$

where,  $Y_5(t) = \mu_2(S_2(t), \lambda_3) - \mu_2(S_2(t), S_3(t)) X_2(t)$ , and  $Y_6(t) = S_3(t) - \lambda_3$ . The Cauchy-Schwartz inequality allows us to split the integral into more manageable pieces,

$$\mathcal{Q}_2 \leq \left( \int_{t_0}^{\infty} \frac{1}{t^2} dt \right)^{\frac{1}{2}} \left( \int_{t_0}^{\infty} t^2 \sup_{x \in K} [(y_2^2 + 1)Y_5(t)^2 + D^2 Y_6(t)^2] dt \right)^{\frac{1}{2}}.$$

By (2.32), the term containing  $Y_6(t)$  is bounded above. In order to show the integral containing  $Y_5(t)$  is bounded above we use the fact that  $\mu_2(S_2, S_3) \in C^1$  and (2.32) to argue that there exists  $M_1 \geq 0$  such that

$$|\mu_2(S_2(t), \lambda_3) - \mu_2(S_2(t), S_3(t))| \leq M_1 |S_3(0) - \lambda_3| e^{-Dt}.$$

Since  $X_2(t)$  is bounded we have

$$\int_{t_0}^{\infty} t^2 \sup_{x \in K} \left[ (y_3^2 + 1) \overline{X}_2 M_1 |S_3(0) - \lambda_3| e^{-Dt} \right] dt, \quad (2.33)$$

Where  $\overline{X}_2$  is the maximum value of  $X(t)$  in  $K$ . The integral on the right is finite and therefore, by Lemma 2.A.1, (2.1) is quasi-autonomous with limiting system (2.7).  $\square$

# Bibliography

- [1] D. Batstone, J. Keller, I. Angelidaki, S. Kalyuzhnyi, S. Pavlosthathis, A. Rozzi, W. Sanders, H. Siegrist, and V. Vavilin. *Anaerobic Digestion Model No.1 (ADM1)*. IWA Publishing, London UK, 2002.
- [2] B. Benyahia, T. Sari, B. Cherki, and J. Harmand. Bifurcation and stability analysis of a two-step model for monitoring anaerobic digestion processes. *J. Process Contr.*, 22:1008–1019, 2012.
- [3] O. Bernard, Z. Hadj-Sadok, D. Dochain, A. Genovesi, and J.-P. Steyer. Dynamic model development and parameter identification for an anaerobic wastewater treatment process. *Biotechnol. Bioeng.*, 75:440–47, 2001.
- [4] A. Bornhöft, R. Hanke-Rauschenbach, and K. Sundmacher. Steady-state analysis of the anaerobic digestion model no.1 (ADM1). *Nonlinear Dyn.*, 73:535–549, 2013.
- [5] G. J. Butler and G. S. K. Wolkowicz. A mathematical model of the chemostat with a general class of functions describing nutrient uptake. *SIAM J. Appl. Math.*, 45:138–151, 1985.
- [6] F. Campillo, M. Joannides, and I. Larramendy-Valverde. Stochastic modelling

## BIBLIOGRAPHY

---

- of the chemostat. *Ecol. Model.*, 222:2676–2689, 2011.
- [7] Y. Cao, D. Gillespie, and L. Petzold. Efficient step size selection for the tau-leaping simulation method. *J. Chem. Phys.*, 124:044109–1–11, 2006.
- [8] D. Gillespie. Exact stochastic simulation of coupled chemical reactions. *J. Chem. Phys.*, 81:2340–2361, 1977.
- [9] D. Gillespie. Approximate accelerated stochastic simulation of chemically reacting systems. *J. Chem. Phys.*, 115:1716–1733, 2001.
- [10] M. E. Hajji, F. Mazenc, and J. Harmand. A mathematical study of syntrophic relationship of a model of anaerobic digestion process. *Math. Biosci. Eng.*, 7:641–656, 2010.
- [11] J. Harmand, C. Lobry, A. Rapaport, and T. Sari. *The chemostat: Mathematical theory of microorganism cultures*, volume 1 of *Chemical engineering series*. Wiley, 2017.
- [12] J. Hess and O. Bernard. Design and study of a risk management criterion for an unstable wastewater treatment process. *J. Process Contr.*, 18:71–79, 2008.
- [13] L. Imhof and S. Walcher. Exclusion and persistence in deterministic and stochastic chemostat models. *J. Differ. Equations*, 217:26–53, 2005.
- [14] S. Jeyaseelan. A simple mathematical model for anaerobic digestion process. *Water Sci. Technol.*, 35:185–191, 1997.
- [15] L. Y. Lokshina, V. A. Vavilin, R. H. Kettunen, J. Rintala, C. Holliger, and

## BIBLIOGRAPHY

---

- A. N. Nozhevnikova. Evaluation of kinetic coefficients using integrated Monod and Haldane models for low-temperature acetoclastic methanogenesis. *Water Res.*, 35:2913–2922, 2001.
- [16] MAPLE. *Maplesoft, a division of Waterloo Maple Inc.* Waterloo, Ontario, 2017.
- [17] MATLAB. *version 8.5.0 (R2015a)*. The MathWorks Inc., Natick, Massachusetts, 2015.
- [18] R. McGehee and R. A. Armstrong. Some mathematical problems concerning the ecological principle of competitive exclusion. *J. Differ. Equations*, 23:30–52, 1977.
- [19] S. Shen, G. C. Premier, A. Guwy, and R. Dinsdale. Bifurcation and stability analysis of an anaerobic digestion model. *Nonlinear Dyn.*, 48:391–408, 2007.
- [20] H. Smith and P. Waltman. *The theory of the chemostat: dynamics of microbial competition*. Cambridge University Press, 1995.
- [21] S. Sötermann, N. Ristow, M. Wentzel, and G. Ekama. A steady-state model for anaerobic digestion of sewage sludges. *Water SA*, 31:511–527, 2005.
- [22] H. Thieme. Asymptotically autonomous differential equations in the plane II. Stricter Poincaré-Bendixson type results. *Diff. Int. Eq.*, 7:1625–1640, 1994.
- [23] L. Wang and D. Jiang. The threshold and ergodicity of a stochastic chemostat model with regime switching in washout rate. To Appear.

## BIBLIOGRAPHY

---

- [24] M. Weedermann, G. Seo, and G. S. K. Wolkowicz. Mathematical model of anaerobic digestion in a chemostat: Effects of syntrophy and inhibition. *J. Biol. Dyn.*, 7:59–85, 2013.
- [25] M. Weedermann, G. S. K. Wolkowicz, and J. Sasara. Optimal biogas production in a model for anaerobic digestion. *Nonlinear Dyn.*, 81:1097–1112, 2015.
- [26] G. S. K. Wolkowicz and Z. Lu. Global dynamics of a mathematical model of competition in the chemostat: general response function and differential death rates. *SIAM J. Appl. Math.*, 52:222–233, 1992.
- [27] C. Xu, S. Yuan, and T. Zhang. Asymptotic behaviour of a chemostat model with stochastic perturbation on the dilution rate. *Abstr. Appl. Anal.*, ID 423154:11 pages, 2013.

## Chapter 3

# Growth on two essential nutrients in a self-cycling fermenter

### Abstract

A system of impulsive differential equations with state-dependent impulses is used to model the growth of a single population on two limiting essential resources in a self-cycling fermentor. Potential applications include water purification and biological waste remediation. The self-cycling fermentation process is a semi-batch process and the model is an example of a hybrid system. In this case, a well-stirred tank is partially drained, and subsequently refilled using fresh medium when the concentration of both resources (assumed to be pollutants) falls below some acceptable threshold. We consider the process successful if the threshold for emptying/refilling the reactor can be reached indefinitely without the time between successive emptying/refillings becoming unbounded and without interference by the

operator. We prove that whenever the process is successful, the model predicts that the concentrations of the population and the resources converge to a positive periodic solution. We derive conditions for the successful operation of the process that are shown to be initial condition dependent and prove that if these conditions are not satisfied, then the reactor fails. We show numerically that there is an optimal fraction of the medium drained from the tank at each impulse that maximizes the output of the process.

## **3.1 Introduction**

The self-cycling fermentation (SCF) process can be described in two stages: In the first stage, a well-stirred tank is filled with resources and inoculated with microorganisms that consume the resources. When a threshold concentration of one or more indicator quantities is reached, the second stage is initiated. The first stage is a batch culture [5]. During the second stage, the tank is partially drained, and subsequently refilled with fresh resources before repeating the first stage.

SCF is most often applied to wastewater treatment processes, where the goal is to reduce the concentration of one or more harmful compounds [10, 16]. In this application the concentration of harmful compounds is the most reasonable threshold quantity, since acceptable concentrations would typically be given by some government agency. More recently, the SCF process has been used as a means to improve production of some biologically derived compounds [20, 23]. In these instances, dissolved  $O_2$  content, or dissolved  $CO_2$  content have been used as

threshold quantities, since they are good indicators of when the microorganism approaches the stationary phase in its growth cycle. In both scenarios, the end goal is to maximize the amount of substrate processed by the reactor, while maintaining stable operating conditions. SCF has also been used to culture synchronized microbial cultures [17], where stability of the operating conditions is much more important than output of the reactor. It is the first scenario that we model, i.e. we consider the case that the microbial population is used to reduce two harmful compounds to an acceptable level.

Assuming that the time taken to empty and refill the tank is negligible, we can model the SCF process using a system of impulsive differential equations. Smith and Wolkowicz [18] used this approach to model the growth of a single species with one limiting resource. Fan and Wolkowicz [7] extended this model to include the possibility that the resource is limiting at large concentrations. Córdova-Lepe, Del Valle, and Robledo [6] also modeled single species growth in the SCF process, but used impulse dependent impulse times instead of the state dependent impulses used by the other models. For references on the theory of impulsive differential equations, see e.g. [1, 2, 3, 9, 15].

When there are two (or more) resources in limited supply, it is important to think about how the resources interact to promote growth. If any of the resources can be used interchangeably with the same outcome, we say the resources are substitutable. For instance, both glucose and fructose are carbon sources for many bacteria, and can fulfill the same purpose in bacterial growth. If all of the resources are required in some way for growth, and the bacteria will die out if any were missing, we say the resources are essential. For instance, both carbon and

nitrogen are required for growth of many bacteria, but glucose cannot be used as a nitrogen source, so some other compound such as nitrate is required. Growth and competition with two essential resources has been studied in the chemostat [4], in the chemostat with delay [12], and in the unstirred chemostat [24]. In all of the aforementioned studies, the interaction of essential resources is through Liebig's law of the minimum [22]. To illustrate the law of the minimum, consider a barrel with several staves of unequal length. Growth is limited by the resource in shortest supply in the same way that the capacity of the barrel is limited by length of the shortest stave.

In this paper we investigate the dynamics of the self-cycling fermentation process in a semi-batch culture with two essential resources that are assumed to be pollutants. The goal is to reduce both pollutant concentrations to acceptable levels. In Section 3.2, we introduce the model. In Section 3.3, we analyze the system of ordinary differential equations (ODEs) associated with the model introduced in Section 3.2. In Section 3.4, we analyze the system of impulsive differential equations introduced in Section 3.2, and obtain our main results: Theorem 3.4.6, which gives necessary and sufficient conditions for the existence of a unique periodic orbit, and Theorem 3.4.15, which summarizes all of the possible long term dynamics of the model. In Section 3.5, we demonstrate numerically that the emptying/refilling fraction can be used to maximize the output of the SCF process. In Section 3.6, we summarize our results and discuss the implications of our analysis. All figures were produced using Matlab [13].

## 3.2 Model Formulation

For a given function  $y(t)$  and time  $\tau$ , using the standard notation for impulsive equations we denote by  $\Delta y(\tau) = y(\tau^+) - y(\tau^-)$ , where

$$y(\tau^+) \equiv \lim_{t \rightarrow \tau^+} y(t) \quad \text{and} \quad y(\tau^-) \equiv \lim_{t \rightarrow \tau^-} y(t).$$

Our model takes the form

$$\left. \begin{aligned} \frac{ds_1(t)}{dt} &= -\frac{1}{Y_1} \min\{f_1(s_1(t)), f_2(s_2(t))\}x(t), \\ \frac{ds_2(t)}{dt} &= -\frac{1}{Y_2} \min\{f_1(s_1(t)), f_2(s_2(t))\}x(t), \\ \frac{dx(t)}{dt} &= (-D + \min\{f_1(s_1(t)), f_2(s_2(t))\})x(t), \end{aligned} \right\} t \neq t_k \quad (3.1)$$

$$\left. \begin{aligned} \Delta s_1(t_k) &= -rs_1(t_k^-) + rs_1^{\text{in}}, \\ \Delta s_2(t_k) &= -rs_2(t_k^-) + rs_2^{\text{in}}, \\ \Delta x(t_k) &= -rx(t_k^-), \end{aligned} \right\} t = t_k$$

where  $t_k$  are the times at which

$$\text{either } (s_1(t_k) = \bar{s}_1, s_2(t_k) \leq \bar{s}_2) \quad \text{or} \quad (s_1(t_k) \leq \bar{s}_1, s_2(t_k) = \bar{s}_2). \quad (3.2)$$

Here,  $t$  denotes time. The variables  $s_i$ ,  $i = 1, 2$  denote the concentration of the limiting resources (assumed to be pollutants) in the fermentor as a function of  $t$ , with associated parameters  $Y_i$ , the cell yield constants,  $s_i^{\text{in}}$ , the concentrations of each limiting resource in the medium added to the tank at the beginning of each

new cycle, and  $\bar{s}_i$  the threshold concentrations of limiting resource that trigger the emptying and refilling process. Since we are considering the scenario where both  $s_1$  and  $s_2$  are pollutants, the emptying and refilling process is only triggered when both concentrations reach the acceptable levels  $\bar{s}_1$  and  $\bar{s}_2$  set by some environmental protection agency. The variable  $x$  denotes the biomass concentration of the population of microorganisms that consume the resource at time  $t$ , assumed to have death rate  $D$ . The emptying/refilling fraction is denoted by  $r$ . It is assumed that  $D > 0$ ,  $0 < r < 1$  and for  $i = 1, 2$ ,  $Y_i > 0$ , and  $s_i^{\text{in}} > \bar{s}_i > 0$ .

We call the times  $t_k > 0$ , impulse times, and when they exist they form an increasing sequence that we denote  $\{t_k\}_{k=1}^N$ . If (3.2) is satisfied at  $t = 0$  or  $s_i(0) < \bar{s}_i$ ,  $i = 1, 2$ , then we assume that there is an immediate impulse at time  $t = 0$ . We consider the process to be successful if  $N = \infty$  and the time between impulses,  $t_k - t_{k-1}$  remains bounded. We consider the process a failure if either there are a finite number of impulses, and hence  $N$  is finite, or if the time between impulses becomes unbounded.

The two resources are assumed to be limiting essential resources (see e.g., Tilman [21] or Grover [8]) also called complementary resources (see Leon and Tumpson [11]), and as in those studies we use Liebig's law of the minimum [22] to model the uptake and growth of the microbial population.

We assume that each response function  $f_j(s)$ ,  $j = 1, 2$ , in (3.1) satisfies:

- (i)  $f_j : \mathbb{R}_+ \rightarrow \mathbb{R}_+$  is continuously differentiable;
- (ii)  $f_j(0) = 0$  and  $f'_j(s) > 0$  for  $s > 0$ ;

Define  $\lambda_i$ ,  $i = 1, 2$ , to be the value of each resource that satisfies  $f_i(\lambda_i) = D$ , and refer to each  $\lambda_i$  as a “break-even concentration”. If  $f_j$  is bounded below  $D$ , then we define the corresponding  $\lambda_j = \infty$ .

Between two consecutive impulses the system is governed by a system of ordinary differential equations (ODE) that models a batch fermentor [5],

$$\begin{aligned}\frac{ds_1(t)}{dt} &= -\frac{1}{Y_1} \min\{f_1(s_1(t)), f_2(s_2(t))\}x(t), \\ \frac{ds_2(t)}{dt} &= -\frac{1}{Y_2} \min\{f_1(s_1(t)), f_2(s_2(t))\}x(t), \\ \frac{dx(t)}{dt} &= (-D + \min\{f_1(s_1(t)), f_2(s_2(t))\})x(t).\end{aligned}\tag{3.3}$$

We will refer to system (3.3) as the associated ODE system.

### 3.3 Dynamics of System (3.3)

First we show that system (3.3) is well-posed.

**Proposition 3.3.1.** *Given any positive initial conditions  $(s_1(0), s_2(0), x(0))$ , the solution  $(s_1(t), s_2(t), x(t))$  of (3.3) is defined for all  $t \geq 0$  and remains positive.*

*Furthermore,  $\lim_{t \rightarrow \infty} (s_1(t), s_2(t), x(t))$  exists, is initial condition dependent,  $\lim_{t \rightarrow \infty} x(t) = 0$ , and  $\lim_{t \rightarrow \infty} s_i(t) < \lambda_i$  for at least one  $i \in \{1, 2\}$ .*

*Proof.* Since the vector field in (3.3) is locally Lipschitz, the positivity of  $(s_1(t), s_2(t), x(t))$  follows from the standard theory for the existence and uniqueness

of solutions of ODEs (see e.g., [14]). Also observe that

$$\frac{d}{dt} \left( x(t) + \frac{Y_1}{2} s_1(t) + \frac{Y_2}{2} s_2(t) \right) = -Dx(t) < 0,$$

so the solution  $(s_1(t), s_2(t), x(t))$  exists and is bounded for  $t$  in  $[0, \infty)$ .

From (3.3),  $s'_i(t) < 0$ ,  $i = 1, 2$ . By the positivity of  $s_i(t)$ ,  $\lim_{t \rightarrow \infty} s_i(t) \geq 0$  exists. Denote  $\lim_{t \rightarrow \infty} s_i(t) = s_i^*$ ,  $i = 1, 2$ .

We claim that  $\min\{f_1(s_1^*), f_2(s_2^*)\} < D$ . Suppose not. Then,  $\min\{f_1(s_1^*), f_2(s_2^*)\} \geq D$ . Since both  $s_1(t)$  and  $s_2(t)$  are strictly decreasing functions, it follows that  $\min\{f_1(s_1(t)), f_2(s_2(t))\} > D$  for all  $t \geq 0$ . From the equation of  $x'(t)$  in (3.3),  $x(t)$  would be a strictly increasing function. Then,  $s'_1(t) < \frac{-D}{Y_1}x(0)$  for all  $t \geq 0$ , contradicting the positivity of  $s_1(t)$ . Hence,  $s_i^* < \lambda_i$  for at least one  $i \in \{1, 2\}$ .

Since  $\min\{f_1(s_1^*), f_2(s_2^*)\} < D$ , define  $\gamma = -D + \min\{f_1(s_1^*), f_2(s_2^*)\} < 0$ . By the equation for  $x'(t)$  in (3.3),  $x'(t) < \frac{\gamma}{2}x(t) < 0$ , for all sufficiently large  $t$ . Hence  $x(t) \rightarrow 0$  as  $t \rightarrow \infty$ .  $\square$

Note that from (3.3),  $Y_1 \frac{ds_1}{dt} = Y_2 \frac{ds_2}{dt}$ . Define

$$R_{12} = \frac{Y_2}{Y_1} \quad \text{and} \quad R_{21} = \frac{Y_1}{Y_2} = \frac{1}{R_{12}}. \quad (3.4)$$

Then, every trajectory of (3.3) satisfies  $\frac{ds_2}{ds_1} = R_{21}$ .

**Lemma 3.3.2.** *Let  $(s_1(t), s_2(t), x(t))$  be a solution of (3.3) on an interval  $t \in [t_0, t_1]$  with positive initial conditions. Then,*

$$s_1(t) = s_1(t_0) + R_{12}(s_2(t) - s_2(t_0)), \quad (3.5)$$

or equivalently

$$s_2(t) = s_2(t_0) + R_{21}(s_1(t) - s_1(t_0)), \quad (3.6)$$

$$x(t_1) - x(t_0) = Y_1 \int_{s_1(t_1)}^{s_1(t_0)} \left( 1 - \frac{D}{\min\{f_1(v), f_2(s_2(t_1) + R_{21}(v - s_1(t_1)))\}} \right) dv, \quad (3.7)$$

or equivalently

$$x(t_1) - x(t_0) = Y_2 \int_{s_2(t_1)}^{s_2(t_0)} \left( 1 - \frac{D}{\min\{f_1(s_1(t_1) + R_{12}(v - s_2)), f_2(v)\}} \right) dv. \quad (3.8)$$

*Proof.* Solving the separable ODE,  $\frac{ds_1}{ds_2} = R_{12}$ , yields (3.5), and solving  $\frac{ds_2}{ds_1} = R_{21}$ , yields (3.6). Dividing the  $s_1'(t)$  equation in (3.3) by the  $x'(t)$  equation, substituting for  $s_2(t)$  using (3.6), and then integrating both sides, yields (3.7). We obtain (3.8) similarly.  $\square$

### 3.4 Analysis of the Full System (3.1)

First we visualize solutions of (3.1) in the  $s_1$ - $s_2$  plane as illustrated in Figure 3.1. Given any solution  $(s_1(t), s_2(t), x(t))$  of (3.1) with positive initial conditions, let

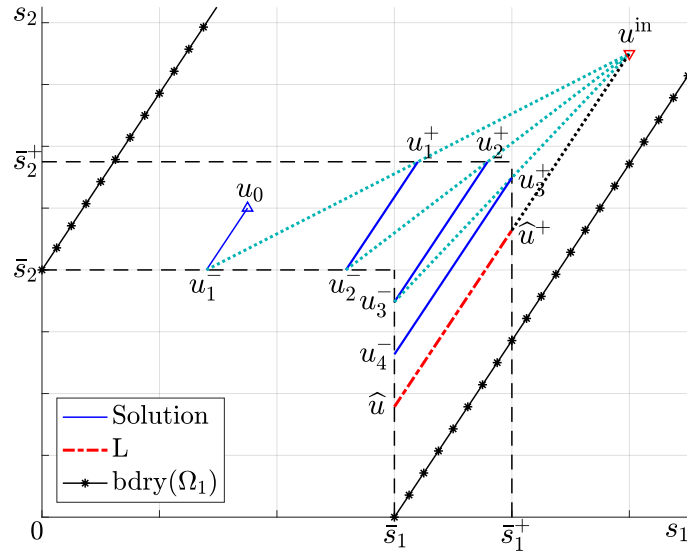


FIGURE 3.1:  $u_0 = (s_1^0, s_2^0)$ , indicated by  $\triangle$ , is the initial condition.  $u^{\text{in}} = (s_1^{\text{in}}, s_2^{\text{in}})$ , indicated by  $\nabla$ , is the input concentration.  $u_k^\pm = (s_1(t_k^\pm), s_2(t_k^\pm))$ ,  $k = 1, 2, \dots$ , satisfy  $u_k^+ = (1 - r)u_k^- + ru^{\text{in}}$ , where  $u^{\text{in}} = (s_1^{\text{in}}, s_2^{\text{in}})$ . Each connected piece of the solution has slope  $R_{21}$ .  $\hat{u} = (\bar{s}_1, \hat{s}_2) = (\bar{s}_1, s_2^{\text{in}} - R_{21}(s_1^{\text{in}} - \bar{s}_1))$  and  $\hat{u}^+ = (\bar{s}_1^+, \hat{s}_2^+) = ((1 - r)\bar{s}_1 + rs_1^{\text{in}}, s_2^{\text{in}} - (1 - r)R_{21}(s_1^{\text{in}} - \bar{s}_1))$ . The set  $\Omega_1$  lies above and to the right of  $\Gamma^-$  and between the two lines with slope  $R_{21}$ , through  $(0, \bar{s}_2)$  and  $(\bar{s}_1, 0)$ , respectively.

$t_0 = 0$  and let  $t_k$ ,  $k \in \mathbb{N}$ , denote the  $k$ th impulse time if it exists.

Let  $u_k^\pm = (s_1(t_k^\pm), s_2(t_k^\pm))$ . By (3.6), the trajectory of  $(s_1(t), s_2(t))$ ,  $t \in (t_k, t_{k+1})$ , is a line segment with slope  $R_{21}$  and endpoints  $u_k^+$  and  $u_{k+1}^-$ . The conditions for impulses to occur are given in (3.2). Therefore, each point  $u_k^-$  lies in the following union of the two horizontal and vertical line segments:

$$\Gamma^- \equiv \{(s_1, \bar{s}_2) : s_1 \in [0, \bar{s}_1]\} \cup \{(\bar{s}_1, s_2) : s_2 \in [0, \bar{s}_2]\}.$$

Define

$$u^{\text{in}} = (s_1^{\text{in}}, s_2^{\text{in}}) \quad \text{and} \quad \bar{s}_i^+ = (1-r)\bar{s}_i + rs_i^{\text{in}}, \quad i = 1, 2.$$

By the definition of  $\Delta s_i$  given in (3.1),

$$u_k^+ = (1-r)u_k^- + ru^{\text{in}}. \tag{3.9}$$

This implies that each  $u_k^+$  lies in the following union of horizontal and vertical line segments:

$$\Gamma^+ \equiv \{(s_1, \bar{s}_2^+) : s_1 \in [0, \bar{s}_1^+]\} \cup \{(\bar{s}_1^+, s_2) : s_2 \in [0, \bar{s}_2^+]\}.$$

Therefore, if impulses occur indefinitely, then the total trajectory of  $(s_1(t), s_2(t))$ ,  $t \in [t_1, \infty)$ , is a countable union of line segments with slope  $R_{21}$  and endpoints in  $\Gamma^- \cup \Gamma^+$ , (i.e.,  $u_k^+ \in \Gamma^+$  and  $u_k^- \in \Gamma^-$ .)

For any positive solution  $(s_1(t), s_2(t), x(t))$  of (3.1) with  $(s_1(0), s_2(0))$  lying between the coordinate axes and  $\Gamma^-$ , i.e.,  $0 \leq s_1(0) \leq \bar{s}_1$  and  $0 \leq s_2(0) \leq \bar{s}_2$ , an

impulse occurs immediately at  $t = 0$ , and so, after at most a finite number of impulses,  $(s_1(0^+), s_2(0^+))$  lies above or to the right of  $\Gamma^-$ . In the rest of this section, we therefore assume  $(s_1(0), s_2(0))$  lies above or to the right of  $\Gamma^-$ , i.e.,  $s_i(0) > \bar{s}_i$ , for at least one  $i \in \{1, 2\}$ .

The following proposition asserts that system (3.1) does not exhibit the phenomenon of *beating*. That is, the system possesses no solution with impulse times that form an increasing sequence with a finite accumulation point.

**Proposition 3.4.1.** *Assume that  $(s_1(t), s_2(t), x(t))$  is a positive solution of (3.1) with an infinite number of impulse times,  $\{t_k\}_{k=1}^\infty$ . Then  $\lim_{k \rightarrow \infty} t_k = \infty$ .*

*Proof.* Between impulses,  $s_1$  and  $s_2$  are strictly decreasing for all  $x(t) > 0$ , and therefore we can solve the first equation in (3.3) for the time between impulses:

$$t_{k+1} - t_k = Y_1 \int_{s_1(t_{k+1})}^{s_1(t_k)} \frac{1}{\min\{f_1(v), f_2(s_2(t_{k+1}) + R_{21}(v - s_1(t_{k+1})))\}} X_k(v) dv \quad (3.10)$$

where  $X_k(v)$  is defined by  $X_k(s_1(t)) = x(t)$  for  $t \in (t_k, t_{k+1})$ .

To show that  $\{t_k\}_{k=1}^\infty$  has no finite accumulation point, it suffices to show that there exists positive constants,  $M_1$ ,  $M_2$  and  $m$ , such that

$$s_1(t_k^+) - s_1(t_{k+1}^-) > m \quad \text{for } k = 1, 2, \dots$$

and

$$\min\{f_1(s_1(t)), f_2(s_2(t))\} < M_1, \quad x(t) < M_2, \quad \text{for } t \geq 0,$$

since then the difference  $t_{k+1} - t_k$  is greater than  $\frac{Y_1 m}{M_1 M_2}$ .

Since  $s_1(t_k^-) \leq \bar{s}_1$ ,  $s_2(t_k^-) \leq \bar{s}_2$ , and either  $s_1(t_k^+) = \bar{s}_1^+$  or  $s_2(t_k^+) = \bar{s}_2^+$ , we have

$$\text{either } s_1(t_k^+) - s_1(t_{k+1}^-) \geq \bar{s}_1^+ - \bar{s}_1 \quad \text{or} \quad s_2(t_k^+) - s_2(t_{k+1}^-) \geq \bar{s}_2^+ - \bar{s}_2.$$

From (3.5) it follows that

$$s_1(t_k^+) - s_1(t_{k+1}^-) \geq \min\{\bar{s}_1^+ - \bar{s}_1, R_{12}(\bar{s}_2^+ - \bar{s}_2)\} \equiv m.$$

Since after the first impulse occurs,  $(s_1(t), s_2(t))$  is bounded by  $\Gamma^+$ , the existence of  $M_1$  follows from the continuity of  $f_1$  and  $f_2$ . By (3.7), there exists  $M_0 > 0$  such that

$$x(t) < x(t_k^+) + M_0, \quad \text{for } t \in (t_k, t_{k+1}). \quad (3.11)$$

From the relation that  $x(t_k^+) = (1 - r)x(t_k^-)$ , we obtain

$$x(t_{k+1}^+) < (1 - r)(x(t_k^+) + M_0), \quad \text{for } k = 1, 2, \dots$$

By the comparison principle applied to  $x(t_k)$  and the sequence  $\{y_k\}$  defined by  $y_0 = x(0)$  and  $y_{k+1} = (1 - r)(y_k + M_0)$ ,  $k = 1, 2, \dots$ ,

$$\limsup_{k \rightarrow \infty} x(t_k^+) \leq \lim_{k \rightarrow \infty} y_k = \frac{(1 - r)M_0}{r}. \quad (3.12)$$

The existence of  $M_2$  follows from (3.11) and (3.12).  $\square$

Define  $\Omega_1$  to be the set of points  $(s_1^0, s_2^0)$  such that, for some  $x^0 > 0$ , the forward trajectory of the solution of (3.3) with initial value  $(s_1^0, s_2^0, x^0)$  intersects  $\Gamma^-$ . Then the boundary of  $\Omega_1$  is the union of  $\Gamma^-$  and the two lines of slope  $R_{21}$  passing

through  $(\bar{s}_1, 0)$  and  $(0, \bar{s}_2)$ , respectively. Then,

$$\Omega_1 = \left\{ (s_1, s_2) : \begin{array}{l} s_1 > \bar{s}_1 \text{ or } s_2 > \bar{s}_2, \text{ and} \\ s_2 - \bar{s}_2 < R_{21}s_1, \ s_2 > R_{21}(s_1 - \bar{s}_1) \end{array} \right\}.$$

Define  $\Omega_0$  to be the open set complementary to  $\Omega_1$  in the first quadrant above and to the right of  $\Gamma^-$ . Then,

$$\Omega_0 = \left\{ (s_1, s_2) : \begin{array}{l} s_1 > \bar{s}_1 \text{ or } s_2 > \bar{s}_2, \text{ and} \\ s_2 - \bar{s}_2 > R_{21}s_1 \text{ or } s_2 < R_{21}(s_1 - \bar{s}_1) \end{array} \right\}.$$

**Remark 3.4.2.** The sets  $\Omega_0$  and  $\Omega_1$  do not include the marginal cases where  $(s_1(0), s_2(0))$  lies on the lines of slope  $R_{21}$  passing through  $(\bar{s}_1, 0)$  or  $(0, \bar{s}_1)$ . If  $(s_1(0), s_2(0))$  lies on one of these lines and  $s_i(0) > 0$  for  $i = 1, 2$ , then no impulses occur, since the solution curve does not reach  $\Gamma^-$  in finite time. If  $(s_1(0), s_2(0)) = (\bar{s}_1, 0)$  or  $(s_1(0), s_2(0)) = (0, \bar{s}_2)$ , then an impulse occurs immediately, and  $(s_1(0^+), s_2(0^+))$  may be in either  $\Omega_0$  or  $\Omega_1$ , depending on the location of  $u^{\text{in}}$ .

In the following case, the fermentation process fails.

**Lemma 3.4.3.** *If  $(s_1(t), s_2(t), x(t))$  is a solution of (3.1) with  $(s_1(0), s_2(0)) \in \Omega_0$ , then no impulses occur.*

*Proof.* Since  $\Omega_0$  is complementary to  $\Omega_1$ ,  $(s_1(t), s_2(t)) \notin \Gamma^-$  for any  $t \geq 0$ , and hence no impulses occur.  $\square$

Next we define a Lyapunov-type function

$$V(s_1, s_2) = Y_2(s_2^{\text{in}} - s_2) - Y_1(s_1^{\text{in}} - s_1). \quad (3.13)$$

Then,

$$\Omega_1 = \left\{ (s_1, s_2) : \begin{array}{l} s_1 > \bar{s}_1 \text{ or } s_2 > \bar{s}_2, \text{ and} \\ V(0, \bar{s}_2) < V(s_1, s_2) < V(\bar{s}_1, 0) \end{array} \right\}$$

and

$$\Omega_0 = \left\{ (s_1, s_2) : \begin{array}{l} s_1 > \bar{s}_1 \text{ or } s_2 > \bar{s}_2, \text{ and} \\ V(s_1, s_2) < V(0, \bar{s}_2) \text{ or } V(s_1, s_2) > V(\bar{s}_1, 0) \end{array} \right\}.$$

Note that the level sets of  $V$  are straight lines with slope  $R_{21}$  in the  $s_1$ - $s_2$  plane. For any fixed value of  $s_1$ ,  $V(s_1, s_2)$  is a decreasing function of  $s_2$ , and for any fixed value of  $s_2$ ,  $V(s_1, s_2)$  is an increasing function of  $s_1$ .

**Lemma 3.4.4.** *Assume  $(s_1(t), s_2(t), x(t))$  is a solution of (3.1) with positive initial conditions. Let  $t_0 = 0$  and  $t_k$ ,  $k \in \mathbb{N}$ , denote the  $k$ th impulse time, if it exists; otherwise set  $t_k = \infty$ . Define  $V(t) = V(s_1(t), s_2(t))$ . Then,*

$$(i) \quad \frac{d}{dt}V(t) = 0 \text{ for } t \in (t_k, t_{k+1}),$$

$$(ii) \quad V(t_k^+) = (1 - r)V(t_k^-), \text{ if } t_k < \infty.$$

*Proof.* (i) By the equations for  $ds_i/dt$  in (3.3),

$$\frac{d}{dt}V(t) = \left( \frac{Y_2}{Y_2} - \frac{Y_1}{Y_1} \right) \min\{f_1(s_1(t)), f_2(s_2(t))\}x(t) = 0.$$

(ii) Substituting (3.9) into (3.13),

$$V(t_k^+) = (1 - r)(s_1(t_k^-) - s_1^{\text{in}}, s_2(t_k^-) - s_2^{\text{in}}) \cdot (Y_1, -Y_2) = (1 - r)V(t_k^-),$$

where  $\cdot$  denotes the inner product in  $\mathbb{R}^2$ . □

By the definition of  $V(s_1, s_2)$  in (3.13) and Lemma 3.4.4, the line

$$\{(s_1, s_2) : V(s_1, s_2) = 0\} = \{(s_1^{\text{in}} + vY_2, s_2^{\text{in}} + vY_1) : v \in \mathbb{R}\} \quad (3.14)$$

is invariant under (3.3) for all  $x(0)$ . By symmetry, we may assume the point  $(\bar{s}_1, \bar{s}_2)$  lies on or above this invariant line, i.e.,  $V(\bar{s}_1, \bar{s}_2) \leq 0$ , or

$$s_2^{\text{in}} - \bar{s}_2 \leq R_{21}(s_1^{\text{in}} - \bar{s}_1). \quad (3.15)$$

Next we show that in the case that  $(s_1^{\text{in}}, s_2^{\text{in}})$  lies in  $\Omega_0$ , once again the fermentation process is doomed to fail.

**Lemma 3.4.5.** *If  $(s_1^{\text{in}}, s_2^{\text{in}}) \in \Omega_0$ , then every solution of (3.1) with positive initial conditions has at most finitely many impulses.*

*Proof.* Note that,  $V(s_1^{\text{in}}, s_2^{\text{in}}) = 0$ , so the condition  $(s_1^{\text{in}}, s_2^{\text{in}}) \notin \Omega_1$  implies that either  $V(0, \bar{s}_2) > 0$  or  $V(\bar{s}_1, 0) < 0$ . Since  $V(0, \bar{s}_2) < V(\bar{s}_1, \bar{s}_2) \leq 0$ , by assumption (3.15),  $V(\bar{s}_1, 0) < 0$ .

We proceed using proof by contradiction. Suppose that a solution

$(s_1(t), s_2(t), x(t))$  of (3.1) with positive initial conditions has infinitely many impulses. Denote the impulse times by  $t_1 < t_2 < \dots$ . By Lemma 3.4.4(ii),  $V(s_1(t_k^-), s_2(t_k^-)) \rightarrow 0$  as  $k \rightarrow \infty$ . Hence,  $V(s_1(t_k^-), s_2(t_k^-)) > V(\bar{s}_1, 0)$  for some  $k \geq 1$ . By Lemma 3.4.3, no more impulses can occur.  $\square$

In the case of  $(s_1^{\text{in}}, s_2^{\text{in}}) \in \Omega_1$ , under assumption (3.15), the line given by (3.14) intersects  $\Gamma^-$  at the point  $(\bar{s}_1, \hat{s}_2)$  given by

$$\hat{s}_2 = s_2^{\text{in}} - R_{21}(s_1^{\text{in}} - \bar{s}_1).$$

Define  $L$  to be the portion of the line given by (3.14) from the point  $(\bar{s}_1, \hat{s}_2)$  to its image via the impulsive map, namely

$$\begin{aligned} L &= \{(s_1, s_2) : \bar{s}_1 \leq s_1 \leq \bar{s}_1^+, V(s_1, s_2) = 0\} \\ &= \{(s_1, s_2) : \bar{s}_1 \leq s_1 \leq \bar{s}_1^+, s_2 = \hat{s}_2 + R_{21}(s_1 - \bar{s}_1)\}. \end{aligned}$$

Then  $L$  is invariant under (3.1) for all  $x(0)$ .

### 3.4.1 Existence of Periodic Orbits

Next we investigate under what conditions the reactor has a periodic solution and the process has the potential to succeed.

We regard the emptying/refilling fraction  $r \in (0, 1)$  as a variable. Without loss of generality, from now on we assume that  $(\bar{s}_1, \bar{s}_2)$  lies on or above  $L$ . Otherwise, from (3.15), by symmetry we can relabel the resources. Therefore, the right

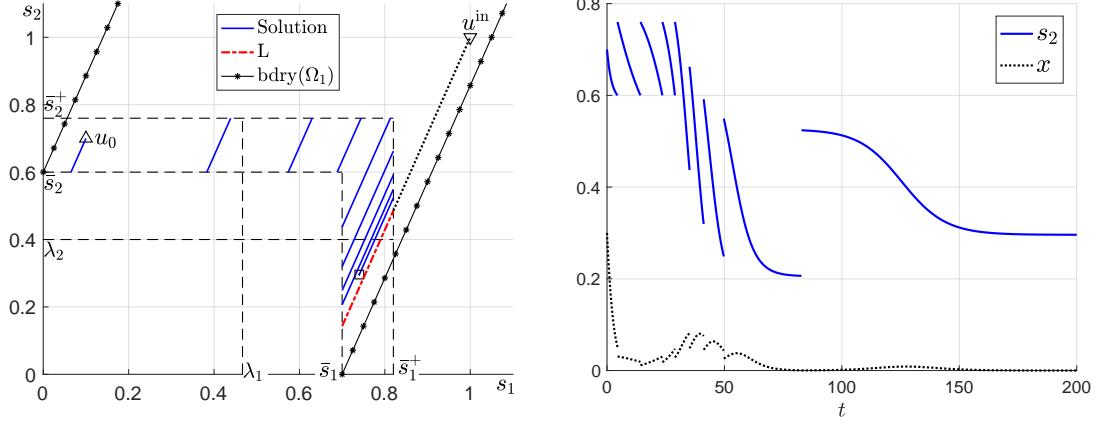


FIGURE 3.2: No periodic solution exists, and the  $x$ -component of every solution tends to 0 as  $t \rightarrow \infty$ . In the simulation, the response functions are  $f_i(s_i) = \frac{m_i s_i}{a_i + s_i}$ ,  $i = 1, 2$ , with  $(m_1, m_2, a_1, a_2) = (2, 2, 1.4, 1.2)$ . The parameters are  $(Y_1, Y_2, D) = (2, 0.7, 0.5)$  and  $(\bar{s}_1, \bar{s}_2, s_1^{\text{in}}, s_2^{\text{in}}, r) = (0.7, 0.6, 1, 1, 0.4)$ . The initial condition is  $u_0 = (s_1(0), s_2(0), x(0)) = (0.1, 0.7, 0.3)$ . After a finite number of impulses, the orbit converges before reaching the threshold for an impulse, indicated by  $\square$ . The value of  $\mu(r) \approx -0.08 < 0$ .

endpoint of  $L$  is  $(\bar{s}_1^+(r), \hat{s}_2^+(r))$  given by

$$\bar{s}_1^+(r) = (1 - r)\bar{s}_1 + r s_1^{\text{in}} \quad \text{and} \quad \hat{s}_2^+(r) = (1 - r)\hat{s}_2 + r s_2^{\text{in}}.$$

By (3.7), the net change in  $x(t)$  over one cycle with impulse at  $(\bar{s}_1, \hat{s}_2)$  is

$$\mu(r) = Y_1 \int_{\bar{s}_1}^{\bar{s}_1^+(r)} \left( 1 - \frac{D}{\min\{f_1(v), f_2(\hat{s}_2 + R_{21}(v - \bar{s}_1))\}} \right) dv. \quad (3.16)$$

We prove the following theorem concerning the existence and the uniqueness of periodic solutions.

**Theorem 3.4.6.** *Assume  $(s_1^{\text{in}}, s_2^{\text{in}}) \in \Omega_1$ . If  $r \in (0, 1)$  and  $\mu(r) > 0$ , then system (4.1) has a periodic orbit that is unique up to time translation and has one impulse*

per period. On a periodic orbit,  $x(t_k^+) = \frac{(1-r)}{r}\mu(r)$  and  $x(t_k^-) = \frac{1}{r}\mu(r)$ , for all  $k \in \mathbb{N}$ .

If  $\mu(r) \leq 0$ , then system (4.1) has no periodic orbits.

See Figure 3.2 for an illustration of the case with  $\mu(r) < 0$ .

*Proof.* Suppose that there is a positive periodic solution  $(s_1(t), s_2(t), x(t))$ . Since (3.3) has no periodic orbits, the solution has at least one impulse. By periodicity there are infinitely many impulses. Denote the impulse times by  $t_1 < t_2 < \dots$  and the number of impulses within a period by  $N$ . Then  $x(t_{N+k}^\pm) = x(t_k^\pm)$  for all  $k \in \mathbb{N}$ . By (3.1),

$$x(t_{k+1}^-) = x(t_k^+) + \mu(r) \quad \text{and} \quad x(t_k^+) = (1-r)x(t_k^-).$$

Thus,

$$x(t_{k+1}^-) = (1-r)x(t_k^-) + \mu(r). \tag{3.17}$$

If  $x(t_1^-) > \mu(r)$  (resp.  $x(t_1^+) < \mu(r)$ ), then from (3.17) it can be shown by induction that  $x(t_k^-)$  is a strictly decreasing (resp. strictly increasing) sequence, contradicting  $x(t_{N+k}^-) = x(t_k^-)$ . Hence, on any periodic orbit there is only one impulse, and it follows from (3.17), on a periodic orbit  $x(t_k^-) = \frac{1}{r}\mu(r)$  for all  $k \in \mathbb{N}$ . Therefore,  $\mu(r) > 0$ , since the solution must be positive, and if a periodic orbit exists it is unique.

If  $\mu(r) > 0$ , the solution of (3.1) with initial condition  $(\bar{s}_1^+, \hat{s}_2^+, \frac{1-r}{r}\mu(r))$  is

periodic, since if  $x(t_{k+1}^-) = \frac{1}{r}\mu(r)$ , then  $x(t_{k+1}^+) = \frac{1-r}{r}\mu(r)$  and if  $x(t_k^+) = \frac{1-r}{r}\mu(r)$ , then  $x(t_{k+1}^-) = \frac{1}{r}\mu(r)$ .  $\square$

**Proposition 3.4.7.** *If  $\mu(1) > 0$ , then there exists a unique  $r^* \in [0, 1)$  such that  $\mu(r) > 0$  for all  $r \in (r^*, 1]$  and  $\mu(r) \leq 0$  for all  $r \in (0, r^*]$ .*

*Proof.* Let

$$r_* = \max\{r \in [0, 1] : \mu(v) \leq 0 \ \forall v \in [0, r]\}. \quad (3.18)$$

Note that  $r_*$  is well-defined, since  $\mu(r)$  is continuous and  $\mu(0) = 0$ . By definition,  $\mu(r) \leq 0$  for all  $r \in [0, r_*]$ . Since  $\mu(r)$  is continuous, if  $\mu(1) > 0$  then  $r_* < 1$ . Furthermore,  $\mu(r) > 0$  for all  $r \in (r_*, 1]$ , since  $f_1(s_1)$  and  $f_2(s_2)$  are monotone increasing, and so the integrand in (3.16) with  $v = \bar{s}_1^+(r_*)$  must be positive. Otherwise,  $r_*$  can be increased, contradicting definition (3.18). By the monotonicity of  $f_1(s_1)$  and  $f_2(s_2)$ , the integrand in (3.16) with  $v = \bar{s}_1^+(r)$  remains positive for  $r_* < r \leq 1$ . Hence,  $\mu(r) > 0$  for  $r \in (r_*, 1]$ .  $\square$

**Remark 3.4.8.** If  $\lambda_1 \leq \bar{s}_1$  and  $\lambda_2 \leq \hat{s}_2$ , then  $\mu(r) > 0$  for all  $r \in (0, 1)$ , i.e.,  $r_* = 0$ , because the integrand in (3.16) is then positive for all  $v \in (\bar{s}_1, s^{\text{in}})$ .

### 3.4.2 Global Stability of Periodic Orbits

In this subsection we fix an  $r \in (r_*, 1)$ , where  $r_*$  is the number given in Theorem 3.4.6. Hence,  $\mu(r) > 0$  and a unique periodic orbit exists.

For each point  $(s_1, s_2) \in \Omega_1$ , we denote by  $\pi^-(s_1, s_2)$ , the point of intersection of the line through  $(s_1, s_2)$  of slope  $R_{21}$  with  $\Gamma^-$ , i.e.,

$$\pi^-(s_1, s_2) = \begin{cases} (s_1 + R_{12}(\bar{s}_2 - s_2), \bar{s}_2), & \text{if } V(s_1, s_2) \leq V(\bar{s}_1, \bar{s}_2), \\ (\bar{s}_1, s_2 + R_{21}(\bar{s}_1 - s_1)), & \text{if } V(s_1, s_2) \geq V(\bar{s}_1, \bar{s}_2). \end{cases}$$

For each point  $(s_1, s_2) \in \Gamma^-$ , we denote by  $\pi^+(s_1, s_2)$  the pre-image of  $(s_1, s_2)$  in  $\Gamma^+$  under  $\pi^-$ . Hence,  $\pi^+(s_1, s_2) \in \Gamma^+$  satisfies  $\pi^-(\pi^+(s_1, s_2)) = (s_1, s_2)$  for all  $(s_1, s_2) \in \Gamma^-$ . Let  $g : \Gamma^- \rightarrow \Gamma^+$ , be the image of  $(s_1, s_2) \in \Gamma^-$  under the impulsive map, i.e.,

$$g(s_1, s_2) = (1 - r)(s_1, s_2) + r(s_1^{\text{in}}, s_2^{\text{in}}).$$

For each point  $(s_1^0, s_2^0) \in \Omega_1$ , let  $I(s_1^0, s_2^0)$  denote the net change in  $x(t)$ , over the time interval from  $t = 0$  to the first impulse time. Therefore, for a solution  $(s_1(t), s_2(t), x(t))$  of (3.1) satisfying  $(s_1(0), s_2(0)) = (s_1^0, s_2^0)$  that has at least one impulse, by Lemma 3.3.2,

$$\begin{aligned} I(s_1^0, s_2^0) &= \begin{cases} Y_2 \int_{\bar{s}_2}^{s_2^0} \left(1 - \frac{D}{\min\{f_1(s_1^0 + R_{12}(v - s_2^0), f_2(v))\}}\right) dv, & \text{if } V(s_1, s_2) \leq V(\bar{s}_1, \bar{s}_2), \\ Y_1 \int_{\bar{s}_1}^{s_1^0} \left(1 - \frac{D}{\min\{f_1(v), f_2(s_2^0 + R_{21}(v - s_1^0))\}}\right) dv, & \text{if } V(s_1, s_2) \geq V(\bar{s}_1, \bar{s}_2). \end{cases} \end{aligned}$$

Note that  $\mu(r) = I(\pi^+(\bar{s}_1, \hat{s}_2))$ .

If  $(s_1(t), s_2(t), x(t))$  is a solution of (3.3) with  $(s_1(t_0), s_2(t_0)) = (s_1^0, s_2^0) \in \Gamma^+$  and  $(s_1(t_1), s_2(t_1)) = (s_1^1, s_2^1) \in \Gamma^-$  for some  $t_0 < t_1$ , then  $(s_1^0, s_2^0) = \pi^+(s_1^1, s_2^1)$  and the net change in  $x(t)$  over the time interval  $[t_0, t_1]$  is  $I(\pi^+(s_1^1, s_2^1))$ . Since  $V(\bar{s}_1, \bar{s}_2) <$

$V(\bar{s}_1^+, \bar{s}_2^+) < V(s_1^{\text{in}}, s_2^{\text{in}})$ , from  $V(s_1^{\text{in}}, s_2^{\text{in}}) = V(\bar{s}_1, \hat{s}_2)$  there exists  $\tilde{s}_2 \in (\hat{s}_2, \bar{s}_2)$  such that  $V(\bar{s}_1, \tilde{s}_2) = V(\bar{s}_1^+, \bar{s}_2^+)$ . Define

$$\Gamma_A^- = \{(\bar{s}_1, s_2) : 0 < s_2 \leq \tilde{s}_2 : I(\pi^+(s_1, s_2)) > 0\}. \quad (3.19)$$

**Lemma 3.4.9.** *Assume  $(s_1^{\text{in}}, s_2^{\text{in}}) \in \Omega_1$  and  $\mu(r) > 0$ . Then,*

$$\Gamma_A^- = \{\bar{s}_1\} \times (s_{2\sharp}, \tilde{s}_2] \quad (3.20)$$

for some  $s_{2\sharp} \in (0, \hat{s}_2)$ .

*Proof.* By assumption (3.15), for any  $s_2 \in [0, \tilde{s}_2]$ ,

$$I(\pi^+(\bar{s}_1, s_2)) = Y_1 \int_{\bar{s}_1}^{\bar{s}_1^+} \left( 1 - \frac{D}{\min\{f_1(v), f_2(s_2 + R_{21}(v - \bar{s}_1))\}} \right) dv.$$

Let

$$\Lambda = \{s_2 \in (0, \tilde{s}_2) : I(\pi^+(\bar{s}_1, s_2)) > 0\}.$$

By the monotonicity of  $f_1(s_1)$  and  $f_2(s_2)$ , since  $I(\pi^+(\bar{s}_1, \hat{s}_2)) = \mu(r) > 0$ ,  $\Lambda$  is an interval containing  $\hat{s}_2$  with right endpoint  $\tilde{s}_2$ . Hence,  $\Gamma_A^-$  takes the form (3.20) for some  $s_{2\sharp} \in (0, \hat{s}_2)$ .  $\square$

Let  $\Omega_{1A}$  be the set of points  $(s_1^0, s_2^0)$  such that, for some  $x^0 > 0$ , the forward trajectory of the solution of (3.3) with initial value  $(s_1^0, s_2^0, x^0)$  passes through  $\Gamma_A^-$ .

Then,

$$\Omega_{1A} = \{(s_1, s_2) \in \Omega_1 : \pi^-(s_1, s_2) \in \Gamma_A^-\}. \quad (3.21)$$

In the case  $\mu(r) > 0$ , by (3.20),

$$\Omega_{1A} = \{(s_1, s_2) \in \Omega_1 : V_- < V(s_1, s_2) < V_+\}, \quad (3.22)$$

where  $V_- = V(\bar{s}_1, \tilde{s}_2)$  and  $V_+ = V(\bar{s}_1, s_{2\sharp})$ .

**Lemma 3.4.10.** *Assume  $(s_1^{\text{in}}, s_2^{\text{in}}) \in \Omega_1$  and  $\mu(r) > 0$ . Let  $(s_1(t), s_2(t), x(t))$  be a solution of (3.1) with  $x(0) > 0$  and*

$$(s_1(0), s_2(0)) \in \Omega_{1A}.$$

*The solution converges to the unique periodic solution given by Theorem 3.4.6, if and only if  $x(0) > -I(s_1(0), s_2(0))$ . If  $x(0) \leq -I(s_1(0), s_2(0))$ , then no impulses occur.*

*Proof.* If  $x(0) \leq -I(s_1(0), s_2(0))$ , then by Lemma 3.3.2 the value of  $x(t)$  approaches 0 before any impulses occur.

If  $x(0) > -I(s_1(0), s_2(0))$ , then the first impulse occurs at some finite time  $t_1 > 0$ . The condition  $(s_1(0), s_2(0)) \in \Omega_{1A}$  implies that  $(s_1(t_1^+), s_2(t_1^+)) \in \Omega_{1A}$ . Hence,  $I(s_1(t_1^+), s_2(t_1^+)) > 0$ . This implies that the net change of  $x(t)$  is positive over any time interval from  $t_1$  to a time before the next impulse. Hence, another impulse occurs at some finite time  $t_2 > t_1$ . Inductively, it follows that impulses occur indefinitely. By Lemma 3.4.4,  $\lim_{t \rightarrow \infty} V(s_1(t), s_2(t)) = 0$ . Hence,

$$(s_1(t_k^-), s_1(t_k^-)) \rightarrow (\bar{s}_1, \hat{s}_2) \quad \text{and} \quad (s_1(t_k^+), s_1(t_k^+)) \rightarrow (\bar{s}_1^+, \hat{s}_2^+).$$

Therefore, by Lemma 3.3.2 and the relation  $I(\pi^+(\bar{s}_1, \hat{s}_2)) = \mu(r)$ ,

$$\lim_{k \rightarrow \infty} (x(t_{k+1}^-) - x(t_k^+)) = \mu(r).$$

On the other hand, the impulsive map in (3.1) gives  $\lim_{k \rightarrow \infty} x(t_k^+) - (1-r)x(t_k^-) = 0$ . This gives

$$\lim_{k \rightarrow \infty} (x(t_{k+1}^-) - (1-r)x(t_k^-)) = \mu(r),$$

which implies  $\lim_{k \rightarrow \infty} x(t_k^-) = \frac{1}{r}\mu(r)$  and  $\lim_{k \rightarrow \infty} x(t_k^+) = \frac{1-r}{r}\mu(r)$ . We conclude that the solution converges to the periodic orbit.  $\square$

**Corollary 3.4.11.** *If  $(s_1^{\text{in}}, s_2^{\text{in}}) \in \Omega_1$  and  $\mu(r) > 0$ , then all solutions to (3.1) with  $(s_1(0), s_2(0)) = (s_1^{\text{in}}, s_2^{\text{in}})$  and  $x(0) > 0$  converge to the periodic orbit given by Theorem 3.4.6.*

*Proof.* By the definitions of  $\Gamma_A^-$  and  $\Omega_{1A}$  given in (3.19) and (3.21), respectively,  $(s_1^{\text{in}}, s_2^{\text{in}}) \in \Omega_{1A}$ . Since  $I(s_1^{\text{in}}, s_2^{\text{in}}) > I(\pi^+(\bar{s}_1, \hat{s}_2)) = \mu(r) > 0$ , the desired result follows from Lemma 3.4.10.  $\square$

For each  $(s_1^0, s_2^0) \in \Omega_1$ , let  $N_0 = N_0(s_1^0, s_2^0)$  be the smallest positive integer such that

$$(g \circ \pi^-)^{N_0}(s_1^0, s_2^0) \in \Omega_{1A}. \quad (3.23)$$

In particular,  $N_0(s_1^0, s_2^0) = 1$  for all  $(s_1^0, s_2^0) \in \Omega_{1A}$ . For  $(s_1^0, s_2^0) \in \Omega_1 \setminus \Omega_{1A}$ , by the identities  $V(g(s_1, s_2)) = (1-r)V(s_1, s_2)$  and  $V(\pi^-(s_1, s_2)) = V(s_1, s_2)$ ,

$$V((g \circ \pi^-)^n(s_1^0, s_2^0)) = (1-r)^n V(s_1^0, s_2^0), \quad n = 1, 2, \dots. \quad (3.24)$$

If  $V(s_1^0, s_2^0) < 0$ , then by (3.22), the condition  $(s_1^0, s_2^0) \notin \Omega_{1A}$  is equivalent to  $V(s_1^0, s_2^0) \leq V_-$ . Thus, by (3.24), condition (3.23), is equivalent to

$$(1 - r)^{N_0} V(s_1^0, s_2^0) > V_-.$$

Similarly, if  $V(s_1^0, s_2^0) > 0$  and  $(s_1(0), s_2(0)) \in \Omega_{1A}$ , then condition (3.23) is equivalent to

$$(1 - r)^{N_0} V(s_1^0, s_2^0) < V_+.$$

Hence,

$$N_0(s_1^0, s_2^0) = \begin{cases} \left\lceil \frac{\ln(V(s_1^0, s_2^0)/V_-)}{-\ln(1-r)} \right\rceil, & \text{if } V(s_1^0, s_2^0) < V_-, \\ \left\lceil \frac{\ln(V(s_1^0, s_2^0)/V_+)}{-\ln(1-r)} \right\rceil, & \text{if } V(s_1^0, s_2^0) > V_+, \end{cases} \quad (3.25)$$

where  $\lceil y \rceil$  is the least integer greater than or equal to  $y$ .

For any solution  $(s_1(t), s_2(t), x(t))$  of (3.1) with  $(s_1(0), s_2(0)) = (s_1^0, s_2^0) \in \Omega_1$ , and  $x(0) > 0$ ,

$$x(t_1^-) = x(0) + I(s_1^0, s_2^0).$$

Note that  $x(t_k^+) = (1 - r)x(t_k^-)$  by the impulsive map in (3.1), and  $x(t_{k+1}^-) = x(t_k^+) + I(s_1(t_k^+), s_2(t_k^+))$  by Lemma 3.3.2. Hence, for any  $n = 2, 3, \dots$ , the left limit of  $x(t)$  at the  $n$ th impulse, if it exists, equals

$$x(t_n^-) = (1 - r)x(t_{n-1}^-) + I((g \circ \pi^-)^{n-1}(s_1^0, s_2^0)),$$

where  $t_0 = 0$ , and  $t_k$ ,  $k \geq 1$ , is the  $k$ th impulse time. By induction,

$$x(t_n^-) = (1 - r)^{n-1}x(0) + \sum_{k=1}^n (1 - r)^{n-k} I((g \circ \pi^-)^{k-1}(s_1^0, s_2^0)).$$

Thus the condition  $x(t_n^-) > 0$  is equivalent to

$$x(0) > - \sum_{k=1}^n (1 - r)^{-(k-1)} I((g \circ \pi^-)^{k-1}(s_1^0, s_2^0)).$$

We define  $X(s_1^0, s_2^0)$  to be the least value so that if  $x(0) > X(s_1^0, s_2^0)$  then  $(s_1(t_*^-), s_2(t_*^-)) \in \Gamma_A^-$  for some  $t_* > 0$ . Hence,

$$X(s_1^0, s_2^0) = - \left( \min_{1 \leq n \leq N_0(s_0, s_1)} \sum_{k=1}^n (1 - r)^{-(k-1)} I((g \circ \pi^-)^{k-1}(s_1^0, s_2^0)) \right). \quad (3.26)$$

In particular,

$$X(s_1^0, s_2^0) = -I(s_1^0, s_2^0) \quad \text{if } N_0(s_1^0, s_2^0) = 1.$$

The following proposition extends Lemma 3.4.10.

**Proposition 3.4.12.** *Assume  $(s_1^{\text{in}}, s_2^{\text{in}}) \in \Omega_1$  and  $\mu(r) > 0$ . Let  $(s_1(t), s_2(t), x(t))$  be a solution of (3.3) with  $(s_1(0), s_2(0)) \in \Omega_1$  and  $x(0) > 0$ .*

- (i) *If  $x(0) \leq X(s_1(0), s_2(0))$ , then there are at most  $N_0(s_1^0, s_2^0) - 1$  impulses.*
- (ii) *If  $x(0) > X(s_1(0), s_2(0))$ , then the solution converges to the unique periodic orbit given by Theorem 3.4.6.*

*Proof.* (i) Suppose  $x(0) \leq X(s_1(0), s_2(0))$  and the solution has at least  $N_0 = N_0(s_1^0, s_2^0)$  impulses. Denote the first  $N_0$  impulse times by  $t_1 < t_2 < \dots < t_{N_0}$ .

Then, by Lemma 3.3.2 and the definition of  $X(s_1, s_2)$ , for some  $k \in \{1, \dots, N_0\}$ ,

$$x(t_k^-) = x(0) - X(s_1(0), s_2(0)) \leq 0,$$

contradicting the positivity of the solution.

(ii) If  $x(0) > X(s_1(0), s_2(0))$ , then the solution has at least  $N_0$  impulses. Denote the  $N_0$ th impulse time by  $t_{N_0}$ . Then,

$$(s_1(t_{N_0}^+), s_2(t_{N_0}^+)) = (g \circ \pi^-)^{N_0}(s_1(0), s_2(0)) \in \Omega_{1A}.$$

Since  $(s_1(t_{N_0}^+), s_2(t_{N_0}^+)) \in \Gamma^+$ , by the definition of  $\Omega_{1A}$ ,  $I(s_1(t_{N_0}^+), s_2(t_{N_0}^+)) > 0$ .

Hence, the result follows from Lemma 3.4.10.  $\square$

**Example 3.4.13.** Consider (3.1) with the Monod functional responses  $f_i(s_i) = \frac{m_i s_i}{a_i + s_i}$ ,  $i = 1, 2$ , and parameters  $(m_1, m_2, a_1, a_2) = (2, 2, 1.9, 0.3)$ ,  $(Y_1, Y_2, D) = (4, 1.9, 0.5)$ , and  $(\bar{s}_1, \bar{s}_2, s_1^{\text{in}}, s_2^{\text{in}}, r) = (0.6, 0.5, 1, 1, 0.4)$ .

We compute the following quantities using their definition.

$$(\bar{s}_1^+, \bar{s}_2^+) = (0.76, 0.7), \quad \tilde{s}_2 \approx 0.36, \quad \hat{s}_2 \approx 0.16, \quad \mu(r) \approx 0.03, \quad V_- \approx -0.39.$$

Taking the initial values  $(s_1^0, s_2^0) = (0.23, 0.6)$ , we have  $V(s_1^0, s_2^0) = -2.32$ . Then,

$$N_0(s_1^0, s_2^0) = \left\lceil \frac{\ln(V(s_1^0, s_2^0)/V_-)}{-\ln(1-r)} \right\rceil = \lceil 3.4908 \rceil = 4.$$

The approximated values of  $I((g \circ \pi^-)^n(s_1^0, s_2^0))$ ,  $1 \leq n < N_0$ , are as follows.

$n$	0	1	2	3
$(1-r)^{-n}I((g \circ \pi^-)^n(s_1^0, s_2^0))$	-0.2970	-0.1785	-0.0441	0.0846

Therefore  $X(s_1^0, s_2^0) \approx 0.2970 + 0.1785 + 0.0441 = 0.5196$ .

In Figures 3.3 and 3.4, the initial data satisfies  $x(0) = 0.5 < X(s_1^0, s_2^0)$  and  $x(0) = 0.53 > X(s_1^0, s_2^0)$ , respectively. By Proposition 3.4.12 the fermentation succeeds only in the latter case.

If  $(s_1^{\text{in}}, s_2^{\text{in}}) \in \Omega_1$  and  $\mu(r) \leq 0$ , then, by Theorem 3.4.6, system (3.1) has no periodic solution. The following proposition asserts that the fermentation fails in this case.

**Proposition 3.4.14.** *Assume  $(s_1^{\text{in}}, s_2^{\text{in}}) \in \Omega_1$ .*

- (i) *If  $\mu(r) < 0$ , then for every solution of (3.1) with positive initial conditions, only finitely many impulses occur.*
- (ii) *If  $\mu(r) = 0$ , then for every solution of (3.1) with positive initial conditions, either only finitely many impulses occur, or the time between impulses tends to infinity.*

*Proof.* Let  $(s_1(t), s_2(t), x(t))$  be a solution of (3.1) with positive initial conditions. Suppose the solution has infinitely many impulses. Denote the impulse times by  $t_1 < t_2 < \dots$ . Then by Lemma 3.4.4,  $(s_1(t_k^-), s_2(t_k^-)) \rightarrow (\bar{s}_1, \hat{s}_2)$  and  $(s_1(t_k^+), s_2(t_k^+)) \rightarrow (\bar{s}_1^+, \hat{s}_2^+)$  as  $k \rightarrow \infty$ .

(i) In the case  $\mu(r) < 0$ , by Lemma 3.3.2 and the relation  $I(\pi^+(\bar{s}_1, \hat{s}_2)) = \mu(r)$ ,

$$\lim_{k \rightarrow \infty} (x(t_{k+1}^-) - x(t_k^+)) = \mu(r).$$

(ii) On the other hand, the impulsive map in (3.1) gives  $x(t_k^+) = (1-r)x(t_k^-)$ . This implies  $\lim_{k \rightarrow \infty} x(t_k^-) = \frac{1}{r}\mu(r) < 0$ , contradicting to the positivity of the solution.

In the case  $\mu(r) = 0$ , by Lemma 3.3.2 and the relation  $I(\pi^+(\bar{s}_1, \hat{s}_2)) = \mu(r) = 0$ ,

$$\lim_{k \rightarrow \infty} (x(t_{k+1}^-) - x(t_k^+)) = 0.$$

By the relation  $x(t_k^+) = (1-r)x(t_k^-)$ , it follows that  $\lim_{k \rightarrow \infty} x(t_k^\pm) = 0$ . Hence, the trajectory of  $(s_1(t), s_2(t), x(t))$ ,  $t \in (t_k, t_{k+1})$ , approaches the heteroclinic orbit of (3.3) from  $(\bar{s}_1^+, \hat{s}_2^+, 0)$  to  $(\bar{s}_1, \hat{s}_2, 0)$ . This implies  $\lim_{k \rightarrow \infty} (t_{k+1} - t_k) = \infty$ .  $\square$

By (3.25), the function  $N_0(s_1, s_2)$  of  $(s_1, s_2) \in \Omega_1$  has an upper bound

$$\bar{N} = \max\{N_0(0, \bar{s}_2), N_0(\bar{s}_1, 0)\}.$$

We summarize our results as follows.

**Theorem 3.4.15.** *Consider system (3.1).*

- i) If  $(s_1^{\text{in}}, s_2^{\text{in}}) \in \Omega_0$ , then every solution has at most finitely many impulses.*
- ii) If  $(s_1^{\text{in}}, s_2^{\text{in}}) \in \Omega_1$  and  $\mu(r) \leq 0$ , then the fermentation fails in the sense that for every solution with positive initial conditions, either only finitely many impulses occur, or the time between impulses tends to infinity.*

iii) If  $(s_1^{\text{in}}, s_2^{\text{in}}) \in \Omega_1$  and  $\mu(r) > 0$ , then there is a unique periodic orbit. Moreover, for any solution  $(s_1(t), s_2(t), x(t))$ , with positive initial conditions, the number of impulse times is either infinite or is less than  $\bar{N}$ . The case with infinitely many impulses occurs if and only if

$$(s_1(0), s_2(0)) \in \Omega_1 \quad \text{and} \quad x(0) > X(s_1(0), s_2(0)).$$

*Proof.* The theorem follows from Lemmas 3.4.3 and 3.4.5 and Propositions 3.4.12 and 3.4.14. □

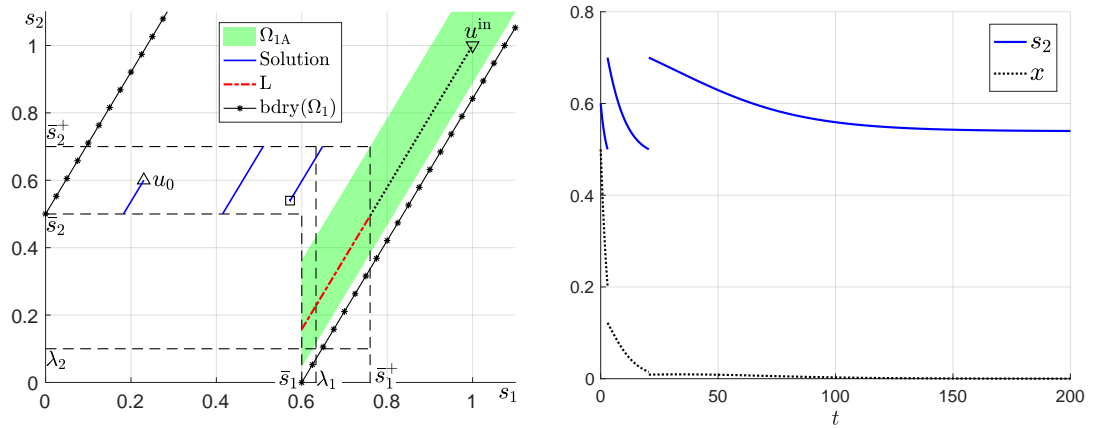


FIGURE 3.3: If  $x(0) \leq X(s_1(0), s_2(0))$ , then only finitely many impulses occur. The orbit converges, indicated by  $\square$ , after a finite number of impulses, and the  $x$ -component of the solution tends to 0 as  $t \rightarrow \infty$ . The parameters are the values given in Example 3.4.13, and the initial condition is  $(s_1(0), s_2(0), x(0)) = (0.23, 0.6, 0.5)$ .

In the following Corollary, we consider a case in which we are guaranteed that  $X(s_1^0, s_2^0) \leq 0$ . In this case, by Proposition 3.4.12, it follows that any solution of (3.1) with  $(s_1(0), s_2(0)) = \Omega_1$  and  $x(0) > 0$  converges to the periodic orbit.

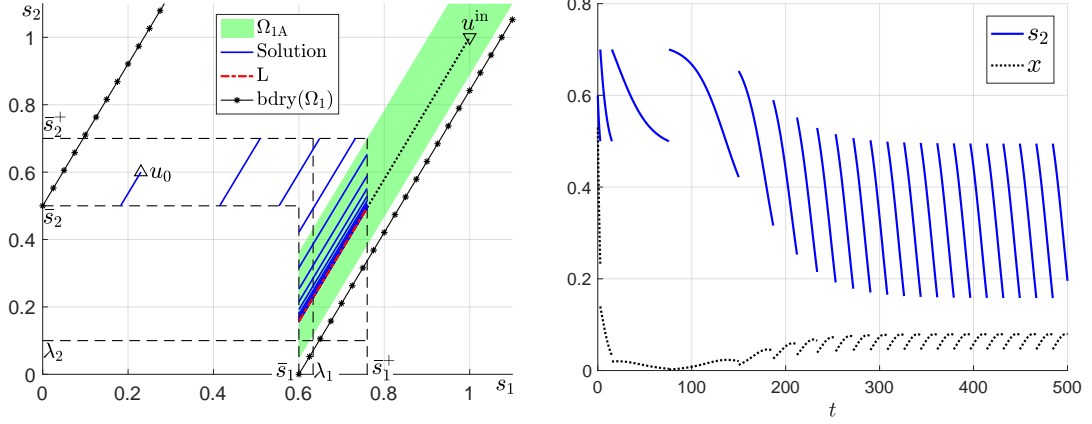


FIGURE 3.4: If  $L$  lies in  $\Omega_{1A}$  and  $x(0) > X(s_1(0), s_2(0))$ , then the solution converges to the periodic orbit. The parameters are the values given in Example 3.4.13, and the initial condition is  $(s_1(0), s_2(0), x(0)) = (0.23, 0.6, 0.53)$ .

If  $\bar{s}_1 > \lambda_1$  and  $\bar{s}_2 > \lambda_2$ , we define  $\Omega_\lambda$  to be the region in the  $s_1$ - $s_2$  plane that lies between the lines  $s_2 = \bar{s}_2 + R_{21}(s_1 - \lambda_1)$  and  $s_2 = \lambda_2 + R_{21}(s_1 - \bar{s}_1)$  and above or to the left of  $\Gamma^-$ , i.e.,

$$\Omega_\lambda = \left\{ (s_1, s_2) : \begin{array}{l} s_1 > \bar{s}_1 \text{ or } s_2 > \bar{s}_2, \text{ and} \\ V(\lambda_1, \bar{s}_2) \leq V(s_1, s_2) \leq V(\bar{s}_1, \lambda_2) \end{array} \right\}. \quad (3.27)$$

For every  $(s_1, s_2) \in \Omega_\lambda$ , we have  $\min\{f_1(s_1), f_2(s_2)\} > D$ , and so growth of  $x$  is always positive in this region.

**Corollary 3.4.16.** *Assume  $(s_1^{\text{in}}, s_2^{\text{in}}) \in \Omega_1$  and  $\mu(r) > 0$ . If  $\bar{s}_1 > \lambda_1$  and  $\tilde{s}_2 \geq \lambda_2$ , then any solution  $(s_1(t), s_2(t), x(t))$  with  $(s_1(0), s_2(0)) \in \Omega_\lambda$  and  $x(0) > 0$  converges to the unique periodic orbit of (3.1).*

*Proof.* First note that, since  $\tilde{s}_2 \geq \lambda_2$ , the line through  $(\bar{s}_1^+, \bar{s}_2^+)$  is in  $\Omega_\lambda$ , and  $\Omega_\lambda \cup \Omega_{1A}$  is connected. For any  $(s_1^0, s_2^0) \in \Omega_\lambda$ , we have  $I(s_1^0, s_2^0) > 0$  and  $(g \circ$

$\pi^-(s_1^0, s_2^0) \in \Omega_\lambda \cup \Omega_{1A}$ . By (3.26),  $X(s_1^0, s_2^0) < 0 < x(0)$ , and by Theorem 3.4.15,  $(s_1(t), s_2(t), x(t))$  converges to the periodic orbit.  $\square$

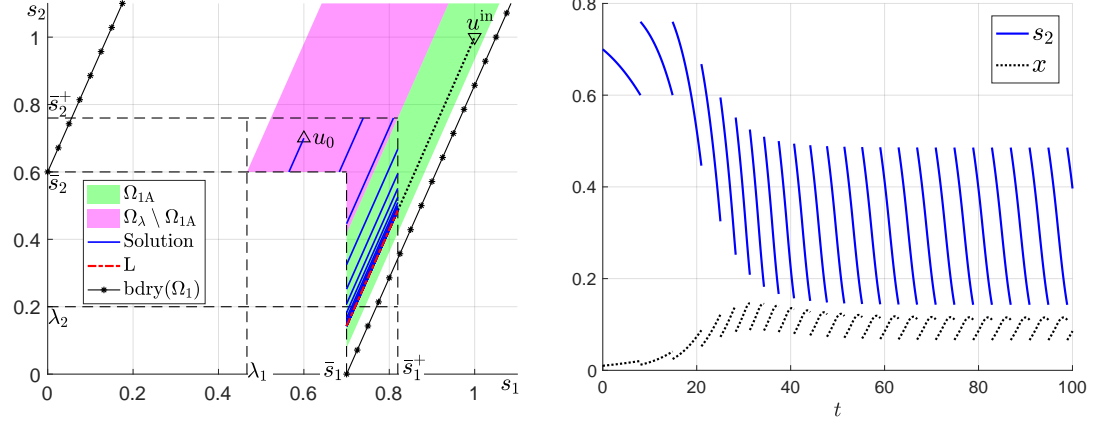


FIGURE 3.5: If  $u_0 \in \Omega_\lambda \setminus \Omega_{1A}$  and  $\Omega_\lambda \cup \Omega_{1A}$  is connected, when  $X(s_1^0, s_2^0) \leq 0$ , the fermentation is still always successful for all  $x(0) > 0$ . The parameters are the values given in Example 3.4.17. The initial condition is  $(s_1(0), s_2(0), x(0)) = (0.6, 0.7, 0.01)$ .

**Example 3.4.17.** Consider (3.1) with the Monod functional responses  $f_i(s_i) = \frac{m_i s_i}{a_i + s_i}$ ,  $i = 1, 2$ , and parameters  $(m_1, m_2, a_1, a_2) = (2, 2, 1.4, 0.6)$ ,  $(Y_1, Y_2, D) = (2, 0.7, 0.5)$ , and  $(\bar{s}_1, \bar{s}_2, s_1^{\text{in}}, s_2^{\text{in}}, r) = (0.7, 0.6, 1, 1, 0.4)$ . Then,

$$(\bar{s}_1^+, \bar{s}_2^+) = (0.82, 0.76), \quad \tilde{s}_2 \approx 0.42, \quad \hat{s}_2 \approx 0.14, \quad \mu(r) \approx 0.04, \quad V_- \approx -0.19.$$

The equation  $f_i(s_i) = D$ ,  $i = 1, 2$ , yields  $\lambda_i = \frac{a_i D}{D - m_i}$ , which gives  $\lambda_1 \approx 0.4677$  and  $\lambda_2 = 0.2$ . Since  $\lambda_1 < \bar{s}_1$  and  $\lambda_2 < \tilde{s}_2$ ,  $\Omega_\lambda \cup \Omega_{1A}$  is a connected set, and the hypotheses in Corollary 3.4.16 are satisfied.

We take the initial value  $(s_1^0, s_2^0) = (0.6, 0.7)$ . Then,  $V(s_1^0, s_2^0) = -0.59$ . A direct calculation gives  $V(\lambda_1, \bar{s}_2) \approx -0.79$ , so that  $V(\lambda_1, \bar{s}_2) < V(s_1^0, s_2^0) < 0$ . This

implies that  $(s_1^0, s_2^0) \in \Omega_\lambda$ . By Corollary 3.4.16, the fermentation succeeds for every initial value  $x(0) > 0$ . An illustration is shown in Figure 3.5.

**Remark 3.4.18.** If  $\lambda_2 > \tilde{s}_2$  then the set  $\Omega_{1A} \cup \Omega_\lambda$  is not connected. Then for some  $(s_1^0, s_2^0) \in \Omega_\lambda$ ,  $(g \circ \pi^-)(s_1^0, s_2^0)$  is in the gap between  $\Omega_\lambda$  and  $\Omega_{1A}$ . We are unable to rule out the possibility that the net growth in this gap is negative, and so it is conceivable that  $I((g \circ \pi^-)(s_1^0, s_2^0)) < 0$ . In particular, we can choose  $(s_1^0, s_2^0) \in \Omega_\lambda$  such that  $I(s_1^0, s_2^0) < -I((g \circ \pi^-)(s_1^0, s_2^0))$ . Therefore,

$$X(s_1^0, s_2^0) \geq -I(s_1^0, s_2^0) - (1 - r)^{-1}I((g \circ \pi^-)(s_1^0, s_2^0)) > 0. \quad (3.28)$$

Therefore, for some positive initial concentrations of biomass, the reactor will fail, even though the initial conditions are in  $\Omega_\lambda$ .

## 3.5 Maximizing the Output

In this section we regard  $r$  as a variable in the interval  $(r_*, 1)$ , where  $r_*$  is the number given in Proposition 4.3.8.

For each  $r \in (r_*, 1)$ , there is a periodic orbit. In each period, there is exactly one impulse. As shown in the proof of Theorem 3.4.6, the left and right limits at an impulse are, respectively,

$$(\bar{s}_1, \hat{s}_2, x_-(r)) \quad \text{and} \quad (\bar{s}_1^+(r), \hat{s}_2^+(r), x_+(r)),$$

where

$$x_-(r) = \frac{1}{r}\mu(r) \quad \text{and} \quad x_+(r) = \frac{1-r}{r}\mu(r). \quad (3.29)$$

The trajectory of the periodic orbit can be parameterized by

$$s_2 = \hat{s}_2 + R_{21}(s_1 - \bar{s}_1)$$

and

$$x = X(s_1; r) = x_-(r) - Y_1 \int_{\bar{s}_1}^{s_1} 1 - \frac{D}{\min\{f_1(v), f_2(\hat{s}_2 + R_{21}(v - \bar{s}_1))\}} dv \quad (3.30)$$

$$= x_+(r) + Y_1 \int_{s_1}^{\bar{s}_1^+} 1 - \frac{D}{\min\{f_1(v), f_2(\hat{s}_2 + R_{21}(v - \bar{s}_1))\}} dv \quad (3.31)$$

with  $s_1 \in (\bar{s}_1, \bar{s}_1^+)$  and  $\bar{s}_1^+ = \bar{s}_1 + r(s_1^{\text{in}} - \bar{s}_1)$ .

Denote the minimal period of the periodic orbit by  $T(r)$ . Then

$$T(r) = Y_1 \int_{\bar{s}_1}^{\bar{s}_1^+(r)} \frac{1}{\min\{f_1(v), f_2(\hat{s}_2 + R_{21}(v - \bar{s}_1))\}} X(v; r) dv. \quad (3.32)$$

In the long run, the average amount of output divided by the total volume is

$$Q(r) = \frac{r}{T(r)}.$$

Maximizing  $Q(r)$  for  $r \in (r_*, 1)$  is equivalent to maximizing the output.

**Lemma 3.5.1.** *The minimal period  $T(r)$ ,  $r \in (r_*, 1)$  of the periodic orbit of (3.1) satisfies  $\lim_{r \rightarrow 1^-} T(r) = \infty$ . Also  $\lim_{r \rightarrow r_*} T(r) = \infty$  if  $r_* > 0$ .*

*Proof.* As  $r \rightarrow 1$ , we have  $x_+(r) \rightarrow 0$ . By (3.32) and (3.31),  $T(r) \rightarrow \infty$ .

If  $r_* > 0$ , then by (3.29),  $x_-(r) \rightarrow 0$  as  $r \rightarrow r_*$ . Along the periodic orbit,  $x \geq x_-(r) > 0$  and

$$\min\{f_1(s_1), f_2(s_2)\} \geq \min\{f_1(\bar{s}_1), f_2(\bar{s}_2)\} > 0.$$

By (3.32) we conclude that  $T(r) \rightarrow \infty$  as  $r \rightarrow r_*$ . □

**Proposition 3.5.2.** *The function  $Q(r) = r/T(r)$ ,  $r \in (r_*, 1)$ , satisfies  $\lim_{r \rightarrow 1} Q(r) = 0$ . If  $r_* > 0$ , then  $\lim_{r \rightarrow r_*} Q(r) = 0$ . If  $r_* = 0$ ,  $\bar{s}_1 \geq \lambda_1$ , and  $\hat{s}_2 \geq \lambda_2$ , then  $\lim_{r \rightarrow r_*} Q(r) = \min\{f_1(\bar{s}_1), f_2(\hat{s}_2)\} - D \geq 0$ .*

*Proof.* By Lemma 3.5.1,  $\lim_{r \rightarrow 1} Q(r) = 1/(\lim_{r \rightarrow 1} T(r)) = 0$ .

If  $r_* > 0$ , then, by Lemma 3.5.1,  $\lim_{r \rightarrow r_*} Q(r) = r_*/(\lim_{r \rightarrow r_*} T(r)) = 0$ .

Next we assume  $r_* = 0$ . By (3.32)

$$Q(r) = r \left/ \left( Y_1 \int_{\bar{s}_1}^{\bar{s}_1^+(r)} \frac{1}{\min\{f_1(v), f_2(\hat{s}_2 + R_{21}(v - \bar{s}_1))\}} X(v; r) dv \right) \right., \quad (3.33)$$

where  $X$  is defined by (3.30). Since  $X(\bar{s}_1; r) = x_-(r) = \frac{\mu(r)}{r}$ , using L'Hôpital's rule and the definition of  $\mu(r)$  in (3.16),

$$\lim_{r \rightarrow 0} X(\bar{s}_1; r) = Y_1 \left. \frac{d\bar{s}_1^+(r)}{dr} \right|_{r=0} \left( 1 - \frac{D}{\min\{f_1(\bar{s}_1), f_2(\hat{s}_2)\}} \right).$$

Since  $\bar{s}_1^+ = \bar{s}_1 + r(s_1^{\text{in}} - \bar{s}_1)$ , we have

$$\left. \frac{d\bar{s}_1^+(r)}{dr} \right|_{r=0} = s_1^{\text{in}} - \bar{s}_1, \quad (3.34)$$

and it follows that

$$\lim_{r \rightarrow 0} X(\bar{s}_1; r) = Y_1(s_1^{\text{in}} - \bar{s}_1) \left( 1 - \frac{D}{\min\{f_1(\bar{s}_1), f_2(\hat{s}_2)\}} \right). \quad (3.35)$$

Furthermore, we have

$$\begin{aligned} T'(r) &= \frac{Y_1(s_1^{\text{in}} - \bar{s}_1)}{\min\{f_1(\bar{s}_1^+), f_2(\hat{s}_2 + rR_{21}(s_1^{\text{in}} - \bar{s}_1))\}} X(\bar{s}_1^+; r) \\ &\quad - \frac{Y_1}{r^2} \int_{\bar{s}_1}^{\bar{s}_1^+(r)} \frac{\mu'(r)r - \mu(r)}{\min\{f_1(v), f_2(\hat{s}_2 + R_{21}(v - \bar{s}_1))\}} X(v; r)^2 dv. \end{aligned} \quad (3.36)$$

Since  $\bar{s}_1^+(0) = \bar{s}$  and  $X(\bar{s}_1; 0) \neq 0$ , by (3.35) and (3.36) we obtain

$$T'(0) = \frac{Y_1(s_1^{\text{in}} - \bar{s}_1)}{\min\{f_1(\bar{s}_1), f_2(\hat{s}_2)\}} X(\bar{s}_1; 0) = \frac{1}{\min\{f_1(\bar{s}_1), f_2(\hat{s}_2)\} - D}.$$

From the expression  $Q(r) = r/T(r)$ , using L'Hôpital's rule, we conclude that  $\lim_{r \rightarrow 0} Q(r) = 1/T'(0) = \min\{f_1(\bar{s}_1), f_2(\hat{s}_2)\} - D$ .  $\square$

Assume  $r_* > 0$ . Since  $\lim_{r \rightarrow r_*} Q(r) = \lim_{r \rightarrow 1} Q(r) = 0$ , by Proposition 3.5.2,  $Q(r)$  attains its maximum at some value of  $r$  in  $(r_*, 1)$ . Unfortunately, the analytical expression of the derivative  $\frac{d}{dr} Q(r)$  is too complicated for finding a critical point of  $Q(r)$ . We have only obtained the maximum value using a numerical simulation. An illustration of the maximal value of  $Q(r)$  is given in Figure 3.6.

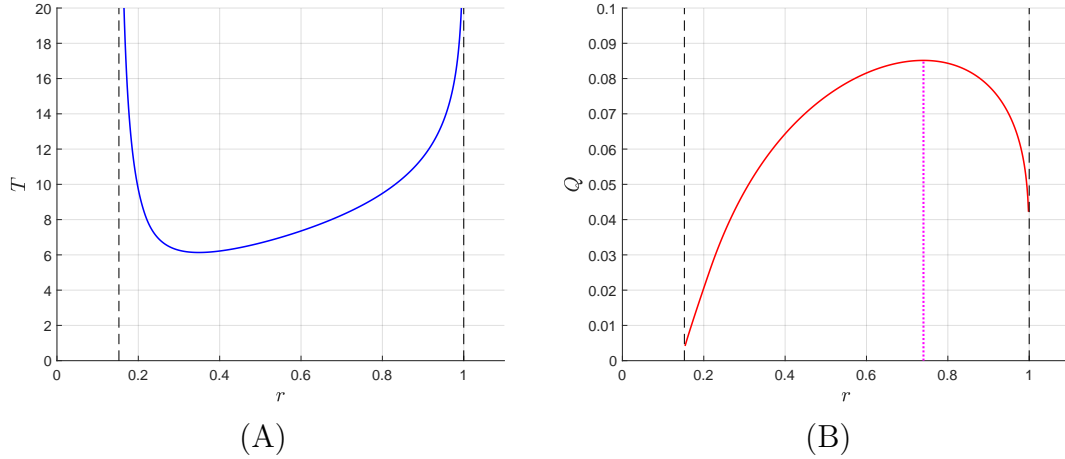


FIGURE 3.6: (A)  $T(r)$  is the minimal period of the periodic orbit,  $r \in (r_*, 1)$ . The dashed line is  $r = r_*$ . As  $r \rightarrow r_*$  or  $r \rightarrow 1$ ,  $T(r) \rightarrow \infty$ . (B) The maximum of  $Q(r)$  is attained at  $r \approx 0.6416$ , indicated by the dotted line. In the simulation, the response functions are  $f_i(s_i) = \frac{m_i s_i}{a_i + s_i}$ ,  $i = 1, 2$ , with parameters given in Example 3.4.17.

### 3.6 Discussion

We have modeled the self-cycling fermentation process assuming that there are two essential resources  $s_1$  and  $s_2$  that are growth limiting for a population of microorganisms,  $x$ , using a system of impulsive differential equations with state-dependent impulses. Assuming that the process is used for an application such as water purification, where the resources  $s_1$  and  $s_2$  are the pollutants, we assume that the threshold for emptying and refilling a fraction of the contents of the fermentor, resulting in the release of treated water, occurs when the concentrations of both pollutants reach an acceptable concentration set by some governmental agency. We called these thresholds,  $s_1 \leq \bar{s}_1$  and  $s_2 \leq \bar{s}_2$ . We consider the process successful if once initiated, it proceeds indefinitely without a need for any subsequent interventions by the operator.

By solving the associated ODE system for  $s_2$  in terms of  $s_1$ , we show that solutions, when projected onto the  $s_1$ - $s_2$  plane, are lines with slope given by the ratio of the growth yield constants. In order to derive necessary conditions for successful operation of the fermentor, we first divide the  $s_1$ - $s_2$  plane into two regions:  $\Omega_0$  and  $\Omega_1$ . The model predicts that solutions of the associated system of ODEs with initial conditions in  $\Omega_0$  approach the axes without ever reaching the thresholds for emptying and refilling and the reactor fails, independent of the initial concentration of microorganisms. Solutions of the associated system of ODEs with initial conditions in  $\Omega_1$  have the potential to reach the threshold for emptying and refilling, but in this case, successful operation can also depend on the initial concentration of the population of microorganisms.

In most cases, at startup the input concentration of the pollutant would be the concentration of the pollutant in the environment, which we are assuming is constant, i.e.,  $(s_1(0), s_2(0)) = (s_1^{\text{in}}, s_2^{\text{in}})$ . If, for any solution starting at these input concentrations of the resources,  $(s_1^{\text{in}}, s_2^{\text{in}})$ , and positive concentration of biomass,  $x(0) > 0$ , the threshold for emptying and refilling,  $s_1 \leq \bar{s}_1$  and  $s_2 \leq \bar{s}_2$ , is reached with net positive growth of the biomass, the model analysis predicts that we can choose an emptying/refilling fraction,  $r$ , so that the system cycles indefinitely. In this case the solution approaches a periodic solution with one impulse per period.

If the system has a periodic solution, the  $(s_1, s_2)$  components of the periodic orbit lie along the line with slope given by the ratio of the growth yield constants joining  $(s_1^{\text{in}}, s_2^{\text{in}})$  and the point in the  $s_1$ - $s_2$  plane where both thresholds are reached. The net change in the biomass on the periodic orbit, that we denote  $\mu(r)$ , must then also be positive.

For other initial conditions in  $\Omega_1$ , in order for the process to operate successfully, it is not enough that  $\mu(r) > 0$ . There is also a minimum concentration of biomass,  $X$ , that depends on the initial concentration of the resources, that is required for the reactor to be successful. If the initial concentration of biomass is larger than  $X$ , then our analysis predicts that the reactor will cycle indefinitely and solutions will converge to the periodic orbit. If the initial concentration of biomass is less than or equal to  $X$ , then the reactor will cycle a finite number of times and then fail. If there is no periodic orbit, then the reactor will either cycle a finite number of times and then fail, or will cycle indefinitely, but the time between cycles will approach infinity.

Besides depending on the initial concentration of the resources at start up, the minimum concentration of biomass at startup required for successful operation depends on the emptying/refilling fraction in an interesting way. The closer  $r$  is to one, the smaller the number of impulses that are required for solutions to get to the periodic orbit. However, the time spent in a region of negative growth could be larger, and so  $X$  would be larger. The closer  $r$  is to zero, results in less time spent in regions with negative growth, but more impulses are then required to get close to the periodic orbit. Each impulse removes biomass from the reactor, and so  $X$  would also increase. This implies that there is an optimal value of  $r$  for which the reactor has the best potential for success. The values of the growth yield constants,  $Y_1$  and  $Y_2$ , also play a role in the size of  $X$ . If their ratio is held constant, but each value is scaled by a constant  $c > 0$ , then  $X$  is also scaled by the same constant  $c$ . Knowing this is important when selecting the population of microorganisms to use in the process.

If the choice of potential microorganisms for use in the process is restricted, then it might be easier to treat more highly polluted water than less polluted water, provided the microorganisms are not inhibited at high concentrations of the pollutant. We have shown that for successful operation, it is necessary that an  $r$  exists such that  $\mu(r) > 0$ . One way to increase  $\mu(r)$  without changing anything else is to increase  $s_1^{\text{in}}$  and  $s_2^{\text{in}}$  in such a way that it still lies on the same line as before. It is also important to choose a population of microorganisms so that  $(s_1^{\text{in}}, s_2^{\text{in}})$  lies in  $\Omega_1$ . It might only be possible to do this by increasing the concentration of one of the pollutants. However, another possibility might be to pre-process the input with a different population of microorganisms that moves  $(s_1^{\text{in}}, s_2^{\text{in}})$  into an acceptable position so that a second population can then treat the water effectively.

We also make what might appear to be other surprising observations. Although the break-even concentrations play a role, it is not necessary for both break-even concentrations to be below their respective thresholds for emptying and refilling for the process to be successful (see Figure 3.4). Also, the process can still fail when both break-even concentrations are below their respective thresholds (see Figure 3.2).

For growth on a single, non-inhibitory, limiting resource in the self-cycling fermentation process, it has been shown that when the system has a periodic orbit, every solution either converges to the periodic orbit, or converges to an equilibrium without a single impulse [19]. If the resource is inhibitory at high concentrations, it has been shown that solutions may also converge to an equilibrium after a single impulse, but if there are at least two impulses then the solution is destined to converge to the periodic orbit [7]. In contrast, if there are two limiting essential

resources, we have shown that there may be many impulses before the system converges to an equilibrium, even when the system has a periodic orbit. The example in Figure 3.3 demonstrates failure after two impulses.

An important issue when setting up the self cycling fermentation process is the choice of the emptying and refilling fraction,  $r$ . In the application we considered we were interested in optimizing the total amount of output. In the example, shown in Section 3.5, we demonstrated that the optimal value of the emptying/refilling fraction is  $r \approx 0.64$ . This result is consistent with what was shown in the single resource cases [7, 19]. Another reason for implementing a self-cycling fermentation process instead of a continuous input process is to maximize the concentration of some microorganism in the output over some time period. For example, one recent ‘proof of concept’ study [23] investigated using the self-cycling fermentation process to improve the production of cellulosic ethanol production. In their investigation, and many other applications of self-cycling fermentation the emptying/refilling fraction  $r$  is set to one half. While this is convenient for experiments and measurements, our results indicate that this is might not be the optimal choice of  $r$ .

# Bibliography

- [1] D. D. Baïnov and P. S. Simeonov. *Systems with impulse effect*. Ellis Horwood Series: Mathematics and its Applications. Ellis Horwood Ltd., Chichester; Halsted Press [John Wiley & Sons, Inc.], New York, 1989. Stability, theory and applications.
- [2] D. D. Baïnov and P. S. Simeonov. *Impulsive differential equations: periodic solutions and applications*, volume 66 of *Pitman Monographs and Surveys in Pure and Applied Mathematics*. Longman Scientific & Technical, Harlow; copublished in the United States with John Wiley & Sons, Inc., New York, 1993.
- [3] D. D. Baïnov and P. S. Simeonov. *Impulsive differential equations*, volume 28 of *Series on Advances in Mathematics for Applied Sciences*. World Scientific Publishing Co., Inc., River Edge, NJ, 1995. Asymptotic properties of the solutions, Translated from the Bulgarian manuscript by V. Covachev [V. Khr. Kovachev].
- [4] G. J. Butler and G. S. K. Wolkowicz. Exploitative competition in a chemostat for two complementary, and possibly inhibitory, resources. *Math. Biosci.*, 83:1–48, 1987.

## BIBLIOGRAPHY

---

- [5] A. Cinar, S. J. Parulekar, C. Ündey, and G. Birol. *Batch fermentors, modeling, monitoring, and control*. Marcel Dekker, New York, 2003.
- [6] F. Córdovea-Lepe, R. D. Valle, and G. Robledo. Stability analysis of a self-cycling fermentation model with state-dependent impulses. *Math. Methods Appl. Sci.*, 37:1460–1475, 2014.
- [7] G. Fan and G. S. K. Wolkowicz. Analysis of a model of nutrient driven self-cycling fermentation allowing unimodal response functions. *Discrete Cont. Dyn. S.*, 8(4):801–831, 2007.
- [8] J. P. Grover. *Resource competition. Population and community biology series 19*. Chapman and Hall, New York, 1997.
- [9] A. Halanay and D. Wexler. *Teoria calitativa a sistemelor du impulsuri*. Ed. Acad. RSR, Bucharedt, 1968.
- [10] S. M. Hughes and D. G. Cooper. Biodegradation of phenol using the self-cycling fermentation process. *Biotechno. Bioeng.*, 51:112–119, 1996.
- [11] J. A. León and D. B. Tumpson. Competition between two species for two complementary or substitutable resources. *J. Theor. Biol.*, 50:185–2012, 1975.
- [12] B. Li, G. S. K. Wolkowicz, and Y. Kuang. Global asymptotic behavior of a chemostat model with two perfectly complementary resources with distributed delay. *SIAM J. Appl. math.*, 60(6):2058–2086, 2000.
- [13] MATLAB. *version 9.3.0 (R2017b)*. The MathWorks Inc., Natick, Massachusetts, 2017.

## BIBLIOGRAPHY

---

- [14] L. Perko. *Differential equations and dynamical systems*. Springer-Verlag, 1996.
- [15] A. Samoilenko and N. A. Perestyuk. *Impulsive differential equations*. World Scientific, Singapore, 1995.
- [16] B. E. Sarkas and D. G. Cooper. Biodegradation of aromatic compounds in a self-cycling fermenter. *Can. J. Chem. Eng.*, 72(5):874–880, 1994.
- [17] D. Sauvageau, Z. Storms, and D. G. Cooper. Synchronized populations of *Escherichia coli* using simplified self-cycling fermentation. *J. Biotechnol.*, 149:67–73, 2010.
- [18] H. L. Smith and P. Waltman. *The theory of the chemostat*, volume 13 of *Cambridge Studies in Mathematical Biology*. Cambridge University Press, Cambridge, 1995. Dynamics of microbial competition.
- [19] R. J. Smith and G. S. K. Wolkowicz. Analysis of a model of the nutrient driven self-cycling fermentation process. *Dyn. Contin. Discret. I.*, 11:239–265, 2004.
- [20] Z. J. Storms, T. Brown, D. Sauvageau, and D. G. Cooper. Self-cycling operation increases productivity of recombinant protein in *Escherichia coli*. *Biotechnol. Bioeng.*, 109(9):2262–2270, 2012.
- [21] D. Tilman. *Resource competition and community structure*. Princeton University Press, New Jersey, 1982.
- [22] J. Von Liebig. *Die organische Chemie in ihrer Anwendung auf Agrikultur und Physiologie*. Friedrich Vieweg, Braunschweig, 1840.

## BIBLIOGRAPHY

---

- [23] J. Wang, M. Chae, D. Sauvageau, and D. C. Bressler. Improving ethanol productivity through self-cycling fermentation of yeast: a proof of concept. *Biotechnol. Biofuels*, 10(1):193, 2017.
- [24] J. Wu, H. Nie, and G. S. K. Wolkowicz. A mathematical model of competition for two essential resources in the unstirred chemostat. *SIAM J. Appl. Math.*, 65:209–229, 2004.

# Chapter 4

## Growth on multiple essential limiting nutrients in a self-cycling fermentor

### Abstract

We introduce a model of the growth of a single microorganism in a self-cycling fermentor in which an arbitrary number of resources are limiting, and impulses are triggered when the concentration of one specific substrate reaches a predetermined level. The model is in the form of a system of impulsive differential equations. We consider the operation of the reactor to be successful if it cycles indefinitely without human intervention and derive conditions for this to occur. In this case, the system of impulsive differential equations has a periodic solution. We show that success is equivalent to the convergence of solutions to this periodic solution. We provide conditions that ensure that a periodic solution exists. When it exists, it is unique and

attracting. However, we also show that whether a solution converges to this periodic solution, and hence the model predicts that the reactor operates successfully, is initial-condition dependent. The analysis is illustrated with numerical examples.

## 4.1 Introduction

The self-cycling fermentation (SCF) process can be described as a sequential batch process and is an example of a hybrid system. In SCF, a tank is filled with a liquid medium that contains nutrients and microorganisms that use these nutrients to grow. The liquid medium is mixed to keep the concentrations uniform while the microorganisms feed on the nutrients and grow. If a predetermined decanting criterion is met, the tank is partially drained and subsequently refilled with fresh medium. Many different decanting criteria can be used to initiate the emptying/refilling sequence, such as elapsed time, a specific nutrient concentration, or a specific biomass concentration. For example, in [17], a specific dissolved oxygen concentration was used as the the decanting criterion. The goal was to choose the decanting criterion so that the fermentor would run indefinitely without operator input.

Self-cycling fermentors and sequential batch reactors are used to improve the efficiency of wastewater-treatment facilities [6, 8], to cultivate microorganisms [9], and to produce some biologically derived compounds [11, 16]. The process has been suggested as an addition to the sidestream partial nitritation process in order to reduce the competition pressure on the beneficial anammox bacteria [12]. It can

also be argued that the control mechanism that is implemented in a turbidostat is closer to a realization of the self-cycling fermentation process than to continuous flow.

The decanting criterion can have a profound effect on the successful operation of the reactor. If the decanting criterion is too strict (e.g., complete removal of a resource), it may never be reached, and if it is too lenient (e.g., a small increase in biomass concentration), it may be reached too often. Many studies have modelled the growth of a single species with a single limiting resource with different decanting criteria, such as: threshold biomass concentrations [13]; threshold nutrient concentrations [4, 10]; or after a certain time elapsed that depends on the nutrient concentrations after the previous decanting stage [3]. Under the assumption that the emptying/refilling process occurs on a much faster time scale than the other processes in the system, the system can be modelled using a system of impulsive differential equations. For a discussion on the qualitative theory of impulsive differential equations see [2, 7].

A more recent paper by Hsu et al. [5] investigated the dynamics of a model with two essential limiting nutrients in which the decanting criterion required both nutrient concentrations to reach or be below a prescribed threshold. When modelling with multiple resources, two resources are said to be *essential* if the microorganism cannot grow without both resources. Conversely, two resources are said to be *substitutable* if the presence of either resources is enough to promote growth. The different ways in which a species may respond to multiple limiting nutrients exist on a spectrum that was described in the book by Tilman [14]. In [5], nutrient uptake of two essential resources was modelled using Liebig's law of the minimum

[15], where the growth is limited by the nutrient concentration that results in the slowest individual growth rate. Many more modern engineering papers do not use Liebig's law and instead model nutrient uptake for essential nutrients using the product of individual uptake functions [1]. This may be problematic in the case when a large number of resources are growth limiting; the product of many uptake functions may predict much lower growth than what is actually observed if each uptake function is a small number. However, the product of uptake functions is advantageous because it is differentiable, whereas the minimum of uptake functions given by Liebig's law of the minimum is only Lipschitz continuous.

Implementation of a self-cycling fermentor can be difficult. Online measurements can be expensive, and measuring quantities of interest may be impractical. Operators of these reactors will often choose to make easier measurements that act as a proxy for the quantities of true interest. For example, in [17], the authors measured the dissolved oxygen concentration, since it was known to reach a minimum at the same time as the limiting substrate was exhausted. Alternatively, operators may not be aware that some nutrient concentrations are lower than required in the input medium, and, as a result, unanticipated resources may become limiting.

In this paper, we investigate the growth of a single microorganism with an arbitrary number of essential nutrients in a self-cycling fermentor. The decanting criterion is met when one specific tracked nutrient concentration falls below a prescribed threshold value. We model nutrient uptake using a general class of functions that includes both the product of uptake functions used in much of the engineering literature and the minimum of uptake functions preferred by biologists.

In the case with a single limiting resource, this model reduces to that given in [10]. In the case with two essential limiting resources and nutrient uptake modelled using Liebig's law of the minimum, this model is the same as the one in [5] where one threshold concentration is arbitrarily large.

The paper is organized as follows. In Section 4.2, we introduce the model and show that it is mathematically and biologically well-posed. In Section 4.3, we provide conditions for the system to have a unique periodic solution and find the basin of attraction for the periodic solution. We show that if the initial conditions lie outside of the basin of attraction, then the population of microorganisms will eventually die out, and the reactor will fail. In Section 4.4, we summarize what we have learned, compare with similar models and discuss what implications this may have for operators of self-cycling reactors.

## 4.2 The Model

We model the self cycling fermentor using the system of impulsive differential equations

$$\left. \begin{aligned} \dot{s}_i(t) &= -\frac{1}{y_i}F(\mathbf{s}(t))x(t), \quad i = 1, \dots, n \\ \dot{x}(t) &= (-D + F(\mathbf{s}(t)))x(t) \end{aligned} \right\} \quad \mathbf{s}(t_k^-) \notin \Gamma^-, \quad (4.1a)$$

$$\left. \begin{aligned} \mathbf{s}(t_k^+) &= r\mathbf{s}^{\text{in}} + (1-r)\mathbf{s}(t_k^-) \\ x(t_k^+) &= (1-r)x(t_k^-) \end{aligned} \right\} \quad \mathbf{s}(t_k^-) \in \Gamma^-, \quad (4.1b)$$

where  $\mathbf{s}(t) = (s_1(t), \dots, s_n(t))^T$ . Here,  $s_i(t)$  denotes the concentration of the  $i$ th nutrient and  $x(t)$  denotes the concentration of the biomass in the tank at time  $t$ .

The set  $\Gamma^-$  is called the *impulsive set*, and it represents the condition on  $\mathbf{s}$  that triggers the emptying/refilling process. We consider the case where only one of the nutrients is tracked by the operator and the tank is reset when the concentration of this nutrient reaches a prescribed threshold. Without loss of generality, we label this nutrient  $s_1$  and denote the prescribed threshold by  $\bar{s}_1$ . Therefore, we define the impulsive set

$$\Gamma^- = \{\mathbf{s} \in \mathbb{R}_+^n : s_1 = \bar{s}_1\}. \quad (4.2)$$

This is an  $(n-1)$ -dimensional hyperplane restricted to the positive cone,  $\mathbb{R}_+^n = \{z \in \mathbb{R}^n : z_i > 0 \text{ for } i = 1, \dots, n\}$ . For simplicity, we assume that  $s_1(0) > \bar{s}_1$ . The *impulse times* are then the times  $\{t_k\}$  such that  $\mathbf{s}(t_k^-) \in \Gamma^-$ , where  $\mathbf{s}(t_k^-) = \lim_{t \rightarrow t_k^-} \mathbf{s}(t)$ .

The parameter  $D$  is the decay rate (or maintenance coefficient) for the microorganism  $x$ ,  $\mathbf{s}^{\text{in}} = (s_1^{\text{in}}, \dots, s_n^{\text{in}})^T$ , where  $s_i^{\text{in}}$  is the concentration of the  $i$ th nutrient in the fresh medium,  $r \in (0, 1)$  is the fraction of the tank that is decanted and subsequently refilled, and  $y_i > 0$ ,  $i = 1, \dots, n$ , are the yield coefficients for each nutrient.

We assume  $F : \mathbb{R}_+^n \rightarrow \mathbb{R}_+$  is a Lipschitz-continuous function satisfying  $F(\mathbf{s}) = 0$  if  $s_i = 0$  for any  $i = 1, \dots, n$ ,  $F(\mathbf{s}) > 0$  if every  $s_i > 0$ , and increasing in each of its arguments (i.e.,  $F(\mathbf{s} + \varepsilon \mathbf{e}_i) > F(\mathbf{s})$  for any  $\varepsilon > 0$ , where  $\mathbf{e}_i$  is the  $i$ th positive unit vector in  $\mathbb{R}^n$ ).

This class of functions includes Liebig's minimum function,

$$F(\mathbf{s}) = \min\{f_i(s_i) : i = 1, \dots, n\}, \quad (4.3)$$

as well as the product of functions

$$F(\mathbf{s}) = \prod_{i=1}^n f_i(s_i), \quad (4.4)$$

where each  $f_i(s_i)$  denotes the rate at which the microorganism uptakes the  $i$ th nutrient and are assumed to be increasing functions. In Tilman's classification of resource types [14], Liebig's minimum function (4.3) describes perfectly essential nutrients, and the product of functions (4.4) describes interactive essential nutrients. In the engineering literature, it is common to use the Monod growth function,  $f_i(s_i) = \frac{\mu_i s_i}{k_i + s_i}$  to describe the uptake of the  $i$ th nutrient.

For  $\mathbf{s} \notin \Gamma^-$  the system is governed by the system of ordinary differential equations,

$$\dot{s}_i(t) = -\frac{1}{y_i} F(\mathbf{s}(t))x(t), \quad i = 1, \dots, n, \quad (4.5a)$$

$$\dot{x}(t) = (-D + F(\mathbf{s}(t)))x(t). \quad (4.5b)$$

**Lemma 4.2.1.** *Solutions of (4.5) with initial conditions  $(s_1(0), \dots, s_n(0), x(0)) \in \mathbb{R}_+^{n+1}$  are bounded and satisfy  $\mathbf{s}(t) \in \mathbb{R}_+^n$  for all  $t \geq 0$ . Furthermore,  $x(t) \rightarrow 0$  as  $t \rightarrow \infty$ .*

*Proof.* Noting that  $F(\mathbf{s}) = 0$  if  $s_i = 0$  for any  $i = 1, \dots, n$ , the faces of  $\mathbb{R}_+^{n+1}$

are invariant. Since the vector field in (4.5) is Lipschitz, solutions to initial value problems are unique. Therefore, any solution with initial conditions in the interior of  $\mathbb{R}_+^{n+1}$  is confined to the interior of  $\mathbb{R}_+^{n+1}$ . The right hand side of each nutrient equation is non-positive, and so the nutrient concentrations are nonincreasing, which implies that  $F(\mathbf{s}(t))$  is a nonincreasing function of  $t$ .

If  $x(0) > 0$ , then there exists  $t_* \geq 0$  such that  $F(\mathbf{s}(t)) < D$  for all  $t \geq t_*$ . If not, then  $F(\mathbf{s}(t)) \geq D$  for all  $t$ , and therefore

$$x'(t) = (F(\mathbf{s}(t)) - D)x(t) \geq 0.$$

Since  $x(t)$  is nondecreasing, it follows that  $x(t) \geq x(0)$  for all  $t$ . Therefore,

$$s'_i(t) \leq -\frac{1}{y_i} Dx(0).$$

This implies that  $s_i(t) \leq s_i(0) - \frac{1}{y_i} Dx(0)t$  for all  $t \geq 0$ , and hence  $s_i(t) \rightarrow -\infty$  as  $t \rightarrow \infty$ , a contradiction.

Therefore, there exists  $t_* \geq 0$  such that  $F(\mathbf{s}(t_*)) < D$  for all  $t \geq t_*$ . This implies that

$$x'(t) \leq (F(\mathbf{s}(t_*)) - D)x(t) < 0,$$

for all  $t \geq t_*$ . Integrating gives

$$x(t) \leq x(t_*)e^{(F(\mathbf{s}(t_*)) - D)(t - t_*)}.$$

Therefore,  $x(t) \rightarrow 0$  as  $t \rightarrow \infty$ .  $\square$

Dividing the other nutrient equations in (4.5a) by the equation for  $s_1(t)$  (i.e., considering  $\dot{s}_i/\dot{s}_1$ ,  $i = 2, \dots, n$ ) and integrating, it follows that the nutrient concentrations are linear functions of  $s_1(t)$ . In vector form,

$$\mathbf{s}(t) = \mathbf{s}^0 - y_1(s_1^0 - s_1(t))\mathbf{Y}, \quad (4.6)$$

where  $\mathbf{Y} = (1/y_1, \dots, 1/y_n)^T$  and  $\mathbf{s}^0 = (s_1(0), \dots, s_n(0))^T$ . Note that the equation for  $s_1$  in this form is trivial. For positive initial conditions,  $s_1(t)$  is strictly decreasing as a function of time, and so  $s_1(t)$  is invertible, allowing us to write  $t(s_1)$ . This means we can use  $s_1$  as a measure of time. With this in mind, dividing by the  $s_1$  equation we can write

$$\mathbf{s}(s_1) = \mathbf{s}^0 - y_1(s_1^0 - s_1)\mathbf{Y}, \quad (4.7a)$$

$$x(s_1) = x^0 - y_1 \int_{s_1^0}^{s_1} \left(1 - \frac{D}{F(\mathbf{s}(\tau))}\right) d\tau, \quad (4.7b)$$

where  $x^0 = x(s_1^0)$ . If there exists  $t_1$  such that  $s_1(t_1^-) = \bar{s}_1$ , then we can reparameterize (4.7) using the percentage of  $s_1$  consumed up to that point. Let  $\nu(s_1) = (s_1^0 - s_1)/(s_1^0 - \bar{s}_1)$ . Then  $\nu \in [0, 1]$  and

$$\begin{aligned} \mathbf{s}(\nu) &= \mathbf{s}^0 - \nu y_1(s_1^0 - \bar{s}_1)\mathbf{Y}, \\ x(\nu) &= x^0 + y_1(s_1^0 - \bar{s}_1) \int_0^\nu \left(1 - \frac{D}{F(\mathbf{s}(\tau))}\right) d\tau. \end{aligned}$$

After the first impulse,  $s_1 \in [\bar{s}_1, \bar{s}_1^+]$ , where  $\bar{s}_1^+ = r s_1^{\text{in}} + (1-r)\bar{s}_1$  is the image of  $\bar{s}_1$  under the impulsive map. In general, for each  $k \geq 1$  for which there exists  $t_k^-$

such that  $s_1(t_k^-) = \bar{s}_1$ , we write

$$\varphi_\nu(\mathbf{s}^k) = \mathbf{s}^k - \nu y_1(s_1^k - \bar{s}_1) \mathbf{Y}, \quad (4.8)$$

$$u_\nu(\mathbf{s}^k, x^k) = x^k + y_1(s_1^k - \bar{s}_1) \int_0^\nu \left( 1 - \frac{D}{F(\varphi_\tau(\mathbf{s}^k))} \right) d\tau, \quad (4.9)$$

with the understanding that  $s_1^k = \bar{s}_1^+$ . In this notation,

$$\varphi_0(\mathbf{s}^k) = \mathbf{s}^k = \mathbf{s}(t_k^+) \quad \text{and} \quad \varphi_1(\mathbf{s}^k) = \mathbf{s}(t_{k+1}^-).$$

$$u_0(\mathbf{s}^k, x^k) = x^k = x(t_k^+) \quad \text{and} \quad u_1(\mathbf{s}^k, x^k) = x(t_{k+1}^-).$$

First we prove that if there are an infinite number of impulses, then the reactor cycles indefinitely with finite cycle time. I.e., the phenomenon of beating is not possible for system (4.1).

**Lemma 4.2.2.** *Assume that  $(s_1(t), \dots, s_n(t), x(t)) \in \mathbb{R}_+^{n+1}$  is a solution to (4.1) with an infinite number of impulse times  $\{t_k\}_{k=1}^\infty$ . Then  $\lim_{k \rightarrow \infty} t_k = \infty$ .*

*Proof.* Since the  $s_i$  are strictly decreasing, if  $x(t) > 0$ , we can solve the  $s_1$  equation in (4.1) for the time between impulses (i.e., consider  $dt/ds_1$  and again use the substitution  $\nu(s_1) = (s_1^0 - s_1)/(s_1^0 - \bar{s}_1)$ ). After the first impulse, the time between impulses is given by

$$t_{k+1} - t_k = y_1(\bar{s}_1^+ - \bar{s}_1) \int_0^1 \frac{1}{F(\varphi_\nu(\mathbf{s}^k)) u_\nu(\mathbf{s}^k, x^k)} d\nu.$$

In order to show that the sequence  $\{t_k\}_{k=1}^\infty$  has no accumulation point, it is enough to show that there exists  $M > 0$ , independent of  $k$ , such that  $F(\varphi_\nu(\mathbf{s}^k)) u_\nu(\mathbf{s}^k, x^k) <$

$M$ . For  $\nu \in [0, 1]$ , each component of  $\varphi_\nu(\mathbf{s}^k)$  is decreasing in  $\nu$ ; i.e.,

$$(\varphi_\nu)_i(\mathbf{s}^k) \leq (\varphi_0)_i(\mathbf{s}^k) = s_i^k$$

for  $\nu \in [0, 1]$ , where  $(\varphi_\nu)_i$  is the  $i$ th component of  $\varphi_\nu$ ,  $i > 1$ . By the relationship,  $s_i^k = rs_i^{\text{in}} + (1-r)(\varphi_1)_i(\mathbf{s}^{k-1})$ , for  $i > 1$ , we obtain

$$s_i^{k+1} \leq rs_i^{\text{in}} + (1-r)s_i^k.$$

Let  $\{q_i^k\}_{k=0}^\infty$  be the sequence defined by  $q_i^0 = s_i^0$ ,  $q_i^{k+1} = rs_i^{\text{in}} + (1-r)q_i^k$ . Then,

$$\limsup_{t \rightarrow \infty} s_i(t) \leq \lim_{k \rightarrow \infty} \sup_{\nu \in [0,1]} (\varphi_\nu)_i(\mathbf{s}^k) \leq \lim_{k \rightarrow \infty} q_i^k = s_i^{\text{in}}, \quad (4.10)$$

and thus each  $s_i(t)$  is bounded above. It remains to show that  $x(t)$  is bounded.

By (4.9), there exists  $M_0 > 0$  such that

$$u_\nu(\mathbf{s}^k, x^k) \leq x^k + M_0, \quad \text{for all } \nu \in [0, 1].$$

Using the relations  $u_1(\mathbf{s}^k, x^k) = x(t_{k+1}^-)$  and  $x^k = (1-r)x(t_k^-)$ , it follows that

$$\frac{1}{1-r}x^{k+1} = x(t_{k+1}^-) = u_1(\mathbf{s}^k, x^k) \leq x^k + M_0 \quad (4.11)$$

and hence

$$x^{k+1} \leq (1-r)(x^k + M_0). \quad (4.12)$$

Consider the sequence  $\{y_k\}_{k=0}^{\infty}$ , defined by  $y(0) = x^0$  and  $y_{k+1} = (1-r)(y_k + M_0)$ , for  $k = 1, 2, \dots$ . Then

$$\limsup_{t \rightarrow \infty} x(t) \leq \lim_{k \rightarrow \infty} \sup_{\nu \in [0,1]} u_{\nu}(\mathbf{s}^k, x^k) \leq \lim_{k \rightarrow \infty} y_k = \frac{(1-r)M_0}{r}. \quad \square$$

**Corollary 4.2.3.** *Let  $(s_1(t), \dots, s_n(t), x(t)) \in \mathbb{R}_+^{n+1}$  be a solution of (4.1). Then, for all  $t \geq 0$ , the solution is bounded,  $s_i(t) > 0$ ,  $i = 1, 2, \dots, n$ , and  $x(t) > 0$ .*

*Proof.* That solutions to system (4.1) are bounded was part of the proof of Lemma 4.2.2.

It is also clear that the impulse map leaves solutions positive.  $\square$

### 4.3 The Periodic Solution

Define the component-wise Lyapunov-like function by

$$V_i(\mathbf{s}) = (s_1^{\text{in}} - s_1)y_1 - (s_i^{\text{in}} - s_i)y_i, \quad i = 1, \dots, n. \quad (4.13)$$

Each component,  $V_i(\mathbf{s})$ , can be seen as the signed distance from  $\mathbf{s}$  to the line through  $\mathbf{s}^{\text{in}}$  in the direction of  $\mathbf{Y}$  when both are projected onto the  $s_1$ - $s_i$  plane. If  $V_i(\mathbf{s}) > 0$ , then  $\mathbf{s}$  lies above the line through  $\mathbf{s}^{\text{in}}$  in the  $s_1$ - $s_i$  plane, and if  $V_i(\mathbf{s}) < 0$ , then  $\mathbf{s}$  lies below the line through  $\mathbf{s}^{\text{in}}$  in the  $s_1$ - $s_i$  plane. Note that  $V_1(\mathbf{s}) \equiv 0$  and if  $n = 2$ , then  $V_2(\mathbf{s})$  is the same Lyapunov-type function used in Chapter 3 (see also [5]).

While each  $V_i(\mathbf{s})$  is useful to determine the location of the projection of  $\mathbf{s}$  in the  $s_1$ - $s_i$  plane, they are not convex functions, and therefore  $\mathbf{V}(\mathbf{s})$  does not truly

constitute a vector-Lyapunov function. On the other hand, the supremum norm,

$$\|\mathbf{V}(\mathbf{s})\|_\infty = \max\{|V_i(\mathbf{s})| : i = 1, \dots, n\}, \quad (4.14)$$

is convex and is therefore a candidate Lyapunov function.

**Lemma 4.3.1.** *Assume that  $(s_1(t), \dots, s_n(t), x(t)) \in \mathbb{R}_+^{n+1}$  is a solution of (4.1).*

*Let  $t_0 = 0$  and  $t_k$  be the  $k$ th impulse time, if it exists. Otherwise, set  $t_k = \infty$ .*

*Then, for each  $i = 2, \dots, n$ ,*

1.  $\frac{d}{dt}V_i(\mathbf{s}(t)) = 0$  for  $t \in (t_k, t_{k+1})$ .

2.  $V_i(\mathbf{s}(t_k^+)) = (1 - r)V_i(\mathbf{s}(t_k^-))$ .

*Proof.* For each component of  $\mathbf{V}$ ,

$$\begin{aligned} \frac{d}{dt}V_i(\mathbf{s}(t)) &= \frac{d}{dt}y_1(s_1^{\text{in}} - s_1(t)) - \frac{d}{dt}y_i(s_i^{\text{in}} - s_i(t)), \\ &= -F(\mathbf{s}(t))x(t) + F(\mathbf{s}(t))x(t), \\ &= 0, \end{aligned}$$

and so  $\frac{d}{dt} \max\{|V_i(\mathbf{s}(t))| : i = 1, \dots, n\} = 0$ .

When  $t = t_k^+$ , using (4.1b),

$$\begin{aligned} V_i(\mathbf{s}(t_k^+)) &= y_1(s_1^{\text{in}} - s_1(t_k^+)) - y_i(s_i^{\text{in}} - s_i(t_k^+)), \\ &= y_1(s_1^{\text{in}} - r s_1^{\text{in}} - (1 - r)s_1(t_k^-)) - y_i(s_i^{\text{in}} - r s_i^{\text{in}} - (1 - r)s_i(t_k^-)), \\ &= (1 - r)V_i(\mathbf{s}(t_k^-)). \end{aligned} \quad \square$$

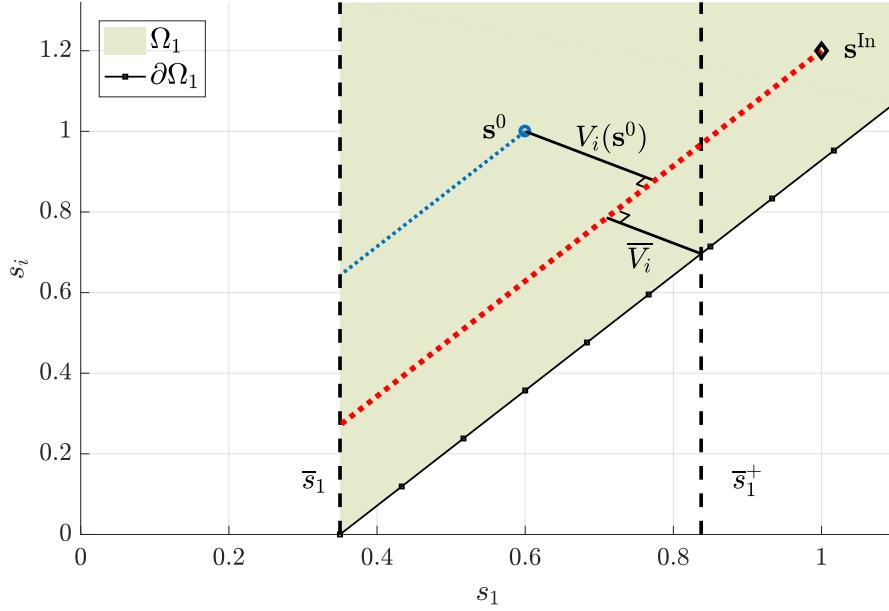


FIGURE 4.1: For any  $\mathbf{s}^0$ ,  $V_i(\mathbf{s}^0)$  is the length of the perpendicular line segment connecting  $\mathbf{s}^0$  to the solution segment through  $\mathbf{s}^{\text{in}}$  in the  $s_1$ - $s_i$  plane. For each  $i$ ,  $\bar{V}_i$  is the distance from  $\partial\Omega_1$  to  $\mathbf{s}^{\text{in}}$  in the  $s_1$ - $s_i$  plane.

**Corollary 4.3.2.** *If  $(s_1(t), \dots, s_n(t), x(t)) \in \mathbb{R}_+^{n+1}$  is a solution to (4.1) with an infinite number of impulses, then  $\mathbf{V}(\mathbf{s}(t)) \rightarrow \mathbf{V}(\mathbf{s}^{\text{in}}) = \mathbf{0}$  as  $t \rightarrow \infty$ .*

We can use the components of  $\mathbf{V}(\mathbf{s})$  to partition  $\mathbb{R}^n$  into two complementary pieces. Define

$$\bar{V}_i = y_1(s_1^{\text{in}} - \bar{s}_1) - y_i s_i^{\text{in}},$$

(i.e.,  $V_i(\mathbf{s})$  when  $s_1 = \bar{s}_1$  and  $s_i = 0$ ), and

$$\Omega_1 = \{\mathbf{s} \in \mathbb{R}_+^n : s_1 \geq \bar{s}_1, V_i(\mathbf{s}) > \bar{V}_i, \text{ for all } i = 2, \dots, n\},$$

$$\Omega_0 = \{\mathbf{s} \in \mathbb{R}_+^n : s_1 \geq \bar{s}_1, V_i(\mathbf{s}) < \bar{V}_i, \text{ for at least one } i = 2, \dots, n\}.$$

**Lemma 4.3.3.** *If  $(s_1(t), \dots, s_n(t), x(t)) \in \mathbb{R}_+^{n+1}$  is a solution of (4.1) with  $\mathbf{s}(0) \in \Omega_0$ , then there are no impulses.*

*Proof.* Without loss of generality, assume that  $V_2(\mathbf{s}^0) < \bar{V}_2$ . Suppose that the first impulse occurs at  $t = t_1$ ; i.e.,  $s_1(t_1^-) = \bar{s}_1$ . By Lemma 4.3.1,

$$y_1(s_1^{\text{in}} - \bar{s}_1) - y_2(s_2^{\text{in}} - s_2(t_1^-)) = V_2(\mathbf{s}(t_1^-)) = V_2(\mathbf{s}^0) < \bar{V}_2 = y_1(s_1^{\text{in}} - \bar{s}_1) - y_2 s_2^{\text{in}}.$$

This implies  $s_2(t_1^-) < 0$ , contradicting Corollary 4.2.3, and so there are no impulses.  $\square$

**Lemma 4.3.4.** *If  $\mathbf{s}^{\text{in}} \in \Omega_0$ , then there are at most a finite number of impulses and  $\lim_{t \rightarrow \infty} x(t) = 0$ .*

*Proof.* Suppose not. Then there exists an infinite sequence of impulse times  $\{t_k\}_{k=1}^{\infty}$ . Since  $\mathbf{s}^{\text{in}} \in \Omega_0$ , it follows that  $V_i(\mathbf{s}^{\text{in}}) = 0 < \bar{V}_i$  for at least one  $i = 2, \dots, n$ . By Corollary 4.3.2, there exists  $k \geq 0$  such that  $V_i(\varphi_0(\mathbf{s}^k)) < \bar{V}_i$ . Therefore,  $\varphi_0(\mathbf{s}^k) \in \Omega_0$ , and by Lemma 4.3.3, no more impulses can occur. Thus, the remaining dynamics are governed by (4.5). By Lemma 4.2.1,  $x(t) \rightarrow 0$  as  $t \rightarrow \infty$ .  $\square$

**Remark 4.3.5.** Both  $\Omega_1$  and  $\Omega_0$  are open sets, complementary in  $\mathbb{R}_n^+$ . We are therefore missing the marginal case on their shared boundary,

$$\begin{aligned} \partial\Omega_1 &= \{\mathbf{s} \in \mathbb{R}_+^n : s_1 \geq \bar{s}_1, V_i(\mathbf{s}) \geq \bar{V}_i, \text{ for all } i = 2, \dots, n, \\ &\text{and } V_i(\mathbf{s}) = \bar{V}_i \text{ for at least one } i = 2, \dots, n\}. \end{aligned}$$

While not covered here, it can be seen that if  $\mathbf{s}^0 \in \partial\Omega_1$ , then there are no impulses. If  $\mathbf{s}^{\text{in}} \in \partial\Omega_1$  and  $\mathbf{s}^0 \in \Omega_1$ , then either finitely many impulses occur or there are infinitely many impulses but the time between impulses tends to infinity.

In order to visualize solutions, we project them onto the  $s_1$ - $s_j$  plane, where  $j$  is such that  $\bar{V}_j = \max\{\bar{V}_i : i = 2, \dots, n\}$ . This allows us to see clearly whether  $\mathbf{s}^{\text{in}} \in \Omega_0$  or  $\mathbf{s}^{\text{in}} \in \Omega_1$ , since if  $\mathbf{s}^{\text{in}} \in \Omega_0$ , then at least one  $\bar{V}_i > 0$ .

**Example 4.3.6.** Consider (4.1) with  $n = 3$ ,

$$F(\mathbf{s}) = \min \left\{ \frac{0.4s_1}{0.25 + s_1}, \frac{1.3s_2}{0.3 + s_2}, \frac{0.5s_3}{0.5 + s_3} \right\},$$

$r = 0.7$ ,  $\mathbf{Y} = (1.00, 0.83, 1.25)^T$ ,  $\bar{s}_1 = 0.4$ ,  $D = 0.05$  and  $\mathbf{s}^{\text{in}} = (1, 1, 0.6)^T$ . Using its definition, we compute  $\bar{\mathbf{V}} = (0, -0.20, 0.52)^T$ . Since  $\bar{V}_3 = \max\{\bar{V}_i : i = 2, 3\}$ , we project solutions onto the  $s_1$ - $s_3$  plane and easily see that  $\mathbf{s}^{\text{in}} \in \Omega_0$ . The initial conditions,  $\mathbf{s}^0 = (0.6, 0.7, 0.8)^T$ ,  $x^0 = 0.5$  satisfy  $\mathbf{s}^0 \in \Omega_1$ , yet the conditions for Lemma 4.3.3 are satisfied, and so, as predicted, in Figure 4.2, we see that  $x(t) \rightarrow 0$  as  $t \rightarrow \infty$ .

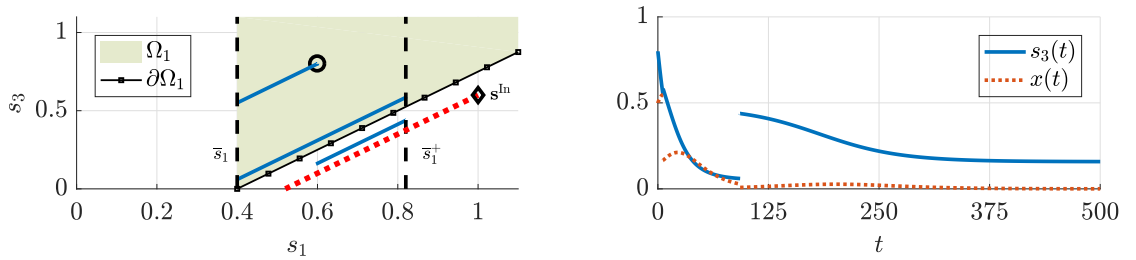


FIGURE 4.2: The dynamics of Example 4.3.6 illustrated by projecting orbits onto  $s_1$ - $s_3$  space, with the line through  $\mathbf{s}^{\text{in}}$  shown in dotted red on the left. Solutions of  $s_3$  and  $x$  as functions of time are shown on the right. As predicted by Lemma 4.3.3, only finitely many impulses occur and  $x(t) \rightarrow 0$  as  $t \rightarrow \infty$ .

If  $\mathbf{s}^{\text{in}} \in \Omega_1$ , then each component of  $\varphi_1(\mathbf{s}^{\text{in}})$  is positive. We define  $\widehat{\mathbf{s}}^+$  to be the point on  $\varphi_\nu(\mathbf{s}^{\text{in}})$  with  $s_1 = \overline{s}_1^+$ , i.e., for fixed  $r \in (0, 1)$

$$\widehat{\mathbf{s}}^+ := \widehat{\mathbf{s}}^+(r) = \mathbf{s}^{\text{in}} - (1 - r)y_1(s_1^{\text{in}} - \overline{s}_1)\mathbf{Y},$$

and define

$$\mu(r) = y_1(\overline{s}_1^+ - \overline{s}_1) \int_0^1 \left( 1 - \frac{D}{F(\varphi_\nu(\widehat{\mathbf{s}}^+))} \right) d\nu \quad (4.15)$$

to be the change in  $x$  as  $\mathbf{s}$  changes from  $\widehat{\mathbf{s}}^+$  to  $\widehat{\mathbf{s}} = \varphi_1(\widehat{\mathbf{s}}^+)$ . Note that, by Lemma 4.3.1,  $V_i(\widehat{\mathbf{s}}^+) = V_i(\mathbf{s}^{\text{in}}) = 0$  for all  $i = 1, \dots, n$  and for all  $r \in (0, 1)$ . Since  $\overline{s}_1^+ = rs_1^{\text{in}} + (1 - r)\overline{s}_1$ , an equivalent representation of (4.16) is

$$\mu(r) = ry_1(s_1^{\text{in}} - \overline{s}_1) \int_0^1 \left( 1 - \frac{D}{F(\varphi_\nu(\widehat{\mathbf{s}}^+))} \right) d\nu. \quad (4.16)$$

**Theorem 4.3.7.** *Assume  $\mathbf{s}^{\text{in}} \in \Omega_1$ . If  $r \in (0, 1)$  and  $\mu(r) > 0$ , then system (4.1) has a unique periodic solution that has one impulse per period. On a periodic solution,  $x(t_k^+) = \frac{(1-r)}{r}\mu(r)$  and  $x(t_k^-) = \frac{1}{r}\mu(r)$  for all  $k \in \mathbb{N}$ .*

*If  $\mu(r) \leq 0$ , then system (4.1) has no periodic solutions.*

*Proof.* First we show that if (4.1) has a periodic solution, then it is unique.

Assume that (4.1) has a periodic solution. From Corollary 4.3.2, the projection of the periodic solution onto the resource hyperplane has to lie on  $\varphi_\nu(\widehat{\mathbf{s}}^+)$ . Since system (4.5) has no cycles, there is at least one impulse, and, by periodicity, there are an infinite number of impulses. Denote by  $K$  the number of impulses in each period. Then  $u_\nu(\mathbf{s}^{K+k}, x^{K+k}) = u_\nu(\mathbf{s}^k, x^k)$  for every  $\nu \in [0, 1]$ ,  $k \in \mathbb{N}$ . By (4.1b)

and combining (4.9) with (4.15),

$$u_1(\mathbf{s}^k, x^k) = u_0(\mathbf{s}^k, x^k) + \mu(r), \quad x^{k+1} = (1-r)u_1(\mathbf{s}^k, x^k),$$

and therefore, using the relation  $u_0(\mathbf{s}^k, x^k) = x^k$ ,

$$x^{k+1} = (1-r)(x^k + \mu(r)).$$

If  $x^{k+1} > x^k$ , then we can show inductively that  $\{x^k\}_{k=0}^{\infty}$  is a strictly increasing sequence. Similarly, if  $x^{k+1} < x^k$  we can show that  $\{x^k\}_{k=0}^{\infty}$  is a strictly decreasing sequence. Therefore, if there is a periodic orbit, it is unique up to time translation and satisfies  $K = 1$ ,  $u_0(\mathbf{s}^k, x^k) = x^k = \frac{1-r}{r}\mu(r)$ , and  $u_1(\mathbf{s}^k, x^k) = \frac{1}{r}\mu(r)$  for all  $k \in \mathbb{N}$ .

If  $\mathbf{s}^{\text{in}} \in \Omega_1$  and  $\mu(r) > 0$ , then the solution with  $(\mathbf{s}^0, x^0) = (\widehat{\mathbf{s}}^+, \frac{1-r}{r}\mu(r))$  is periodic, since  $\varphi_1(\widehat{\mathbf{s}}^+) = \widehat{\mathbf{s}}$  and  $u_1(\widehat{\mathbf{s}}^+, \frac{1-r}{r}\mu(r)) = \frac{1}{r}\mu(r)$ .

If  $\mu(r) \leq 0$ , then by the uniqueness of periodic solutions and Corollary 4.2.3, (4.1) has no periodic solutions.  $\square$

**Proposition 4.3.8.** *If  $\mu(1) > 0$ , then there exists a unique  $r^* \in [0, 1)$  such that  $\mu(r) > 0$  for all  $r \in (r^*, 1]$  and  $\mu(r) \leq 0$  for all  $r \in [0, r^*]$ .*

*Proof.* Let

$$r_* = \max\{r \in [0, 1] : \mu(\tau) \leq 0 \text{ for all } \tau \in [0, r]\}. \quad (4.17)$$

Note that  $r_*$  is well defined, since  $\mu(0) = 0$  and  $\mu$  is a continuous function of  $r$ . Since  $\mu(1) > 0$ , it follows that  $r_* \in [0, 1)$ . By definition of  $r_*$ , there exists  $\varepsilon > 0$

such that

$$\mu(r) > \mu(r_*) = 0$$

for all  $r \in (r_*, r_* + \varepsilon)$ . If not, then  $r_*$  could be increased, violating the definition of  $r_*$ . For each  $\nu \in [0, 1]$ ,  $F(\varphi_\nu(\widehat{\mathbf{s}}^+(r)))$  is a nondecreasing function of  $r$ , since

$$\begin{aligned} \varphi_\nu(\widehat{\mathbf{s}}^+(r)) &= \widehat{\mathbf{s}}^+(r) - \nu y_1(s_1^{\text{in}} - \bar{s}_1)\mathbf{Y}, \\ &= \mathbf{s}^{\text{in}} - y_1(s_1^{\text{in}} - \bar{s}_1)\mathbf{Y} + r(1 - \nu)y_1(s_1^{\text{in}} - \bar{s}_1)\mathbf{Y}. \end{aligned}$$

It follows that  $\mu(r) > \mu(r_*)$  for all  $r \in (r_*, 1]$ . □

**Proposition 4.3.9.** *Assume  $\mathbf{s}^{\text{in}} \in \Omega_1$  and let  $(s_1(t), \dots, s_n(t), x(t))$  be a solution to (4.1) with positive initial conditions.*

(i) *If  $\mu(r) < 0$ , then there are finitely many impulses.*

(ii) *If  $\mu(r) = 0$ , then either finitely many impulses occur or the time between impulses tends to infinity.*

*Proof.* Suppose the solution has infinitely many impulses. By Corollary 4.3.2,  $\mathbf{s}^k \rightarrow \widehat{\mathbf{s}}^+$  as  $k \rightarrow \infty$ .

(i) If  $\mu(r) < 0$ , then

$$\lim_{k \rightarrow \infty} (x^{k+1} - x^k) \leq \lim_{k \rightarrow \infty} (x^{k+1} - (1 - r)x^k) = \mu(r) < 0.$$

Therefore,  $x^k$  eventually becomes negative, contradicting Corollary 4.2.3.

(ii) If  $\mu(r) = 0$ , then

$$\lim_{k \rightarrow \infty} x^{k+1} - (1-r)x^k = 0,$$

implying that  $x^k \rightarrow 0$  as  $k \rightarrow \infty$ . Using the relation  $x^{k+1} = (1-r)u_1(\mathbf{s}^k, x^k)$ , it follows that  $u_1(\mathbf{s}^k, x^k) \rightarrow 0$  as  $k \rightarrow \infty$ . Therefore,  $u_\nu(\mathbf{s}^k, x^k)$  converges to the heteroclinic orbit of (4.5) that connects  $(\widehat{\mathbf{s}}^+, 0)$  to  $(\widehat{\mathbf{s}}, 0)$  as  $k \rightarrow \infty$ . This implies that  $t_{k+1} - t_k \rightarrow \infty$ .  $\square$

**Example 4.3.10.** Consider (4.1) with  $n = 3$ ,

$$F(\mathbf{s}) = \frac{0.4s_1}{0.25 + s_1} \cdot \frac{1.3s_2}{0.3 + s_2} \cdot \frac{0.5s_3}{0.5 + s_3},$$

$r = 0.7$ ,  $\mathbf{Y} = (1.00, 0.83, 1.25)$ ,  $\bar{s}_1 = 0.4$ ,  $D = 0.1$  and  $\mathbf{s}^{\text{in}} = (1, 1, 1)$ . By definition  $\bar{V}_2 = -0.6$  and  $\bar{V}_3 = -0.2$ . Since  $\bar{V}_3 = \max\{\bar{V}_2, \bar{V}_3\}$ , we project solutions onto the  $s_1$ - $s_3$  plane, and see that  $\mathbf{s}^{\text{in}} \in \Omega_1$ . Since  $\mu(r) \approx -0.2924 < 0$ , by Proposition 4.3.9, there are a finite number of impulses and  $x(t) \rightarrow 0$  as  $t \rightarrow \infty$ . This is illustrated in Figure 4.3.

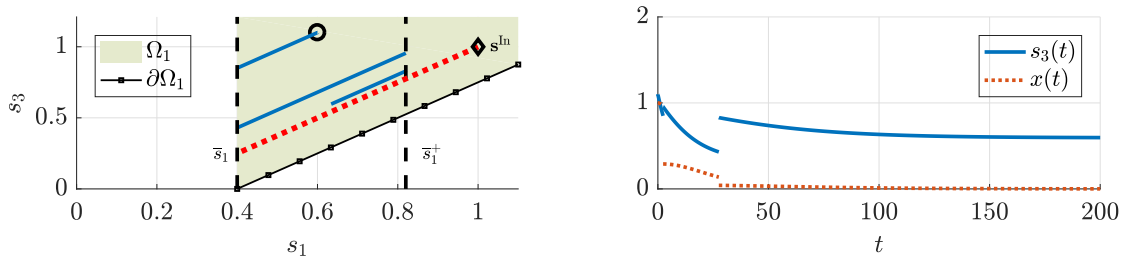


FIGURE 4.3: The dynamics of Example 4.3.10, in which  $\mu(r) < 0$ , illustrated by projecting orbits onto  $s_1$ - $s_3$  space, with the line through  $\mathbf{s}^{\text{in}}$  shown in dotted red on the left. Solutions of  $s_3$  and  $x$  as functions of time are shown on the right. As predicted by Proposition 4.3.9, only finitely many impulses occur and  $x(t) \rightarrow 0$  as  $t \rightarrow \infty$ .

### 4.3.1 Stability of the Periodic Solution

In this section, we assume that  $\mathbf{s}^{\text{in}} \in \Omega_1$  and  $\mu(1) > 0$ . We fix  $r \in (r_*, 1)$ , where  $r_*$  is given in Proposition 4.3.8, so that  $\mu(r) > 0$  and system (4.1) has a unique periodic solution.

For any  $\mathbf{s}^0 \in \Omega_1$ , we define the net change in  $x$  over the time until the first impulse by

$$I(\mathbf{s}^0) = y_1(s_1^0 - \bar{s}_1) \int_0^1 \left( 1 - \frac{D}{F(\varphi_\nu(\mathbf{s}^0))} \right) d\nu. \quad (4.18)$$

Since  $\mathbf{s}^0 \in \Omega_1$ ,  $I(\mathbf{s}^0)$  is finite and an impulse occurs as long as  $x^0$  is large enough.

Note that  $I(\widehat{\mathbf{s}}^+) = \mu(r)$ . Define

$$\Gamma^+ = \{\mathbf{s} \in \mathbb{R}_+^n : s_1 = \bar{s}_1^+\} \quad (4.19)$$

and

$$G^+ = \{\mathbf{s} \in \Gamma^+ \cap \Omega_1 : I(\mathbf{s}) > 0\}, \quad (4.20)$$

the subset of  $\Gamma^+$  with positive growth before the first impulse. Also define

$$G^- = \{\varphi_1(\mathbf{s}) \in \Gamma^- : \mathbf{s} \in G^+\} \quad (4.21)$$

the image of  $G^+$  under  $\varphi_1$  in  $\Gamma^-$ . Let  $g : \Gamma^- \rightarrow \Gamma^+$  be the impulse map acting on  $\mathbf{s}$ . I.e., for  $\mathbf{s} \in \Gamma^-$ ,

$$g(\mathbf{s}) = r\mathbf{s}^{\text{in}} + (1 - r)\mathbf{s}.$$

The composition  $(g \circ \varphi_1)(\mathbf{s}^0) = \mathbf{s}^1$ , and more generally  $(g \circ \varphi_1)(\mathbf{s}^k) = \mathbf{s}^{k+1}$  for  $k = 0, 1, \dots$

**Lemma 4.3.11.** *Assume that  $\mathbf{s}^{\text{in}} \in \Omega_1$  and  $\mu(r) > 0$ . Then there exists  $\rho > 0$  such that  $\Gamma_\rho^+ := \{\mathbf{s} \in \Gamma^+ : V_i(\mathbf{s}) > -\rho \text{ for all } i = 2, \dots, n\}$  is a subset of  $G^+$ .*

*Proof.* Let  $\tilde{\mathbf{s}}(z) = \widehat{\mathbf{s}}^+ - (0, z/y_2, \dots, z/y_n)^T$ . Then, by Lemma 4.3.1,

$$V_i(\tilde{\mathbf{s}}(z)) = y_1 \left( s_1^{\text{in}} - \bar{s}_1^+ \right) - y_i \left( s_i^{\text{in}} - \left( \widehat{s}_i^+ - \frac{z}{y_i} \right) \right) = V_i(\widehat{\mathbf{s}}^+) - z = -z$$

for  $i = 2, \dots, n$ . Since  $\mathbf{s}^{\text{in}} \in \Omega_1$ ,  $\bar{V}_i < 0$  for all  $i = 2, \dots, n$ . Let  $\sigma = \min\{-\bar{V}_i : i = 2, \dots, n\} > 0$ . Then  $\varphi_\nu(\tilde{\mathbf{s}}(\sigma))$  is in  $\mathbb{R}_+^n$  for all  $\nu \in [0, 1)$  and intersects the boundary of  $\mathbb{R}_+^n$  when  $\nu = 1$ . Thus,  $F(\varphi_\nu(\tilde{\mathbf{s}}(\sigma))) > 0$  for all  $\nu \in [0, 1)$  and  $F(\varphi_1(\tilde{\mathbf{s}}(\sigma))) = 0$ . Since  $F(\varphi_\nu(\mathbf{s}))$  is Lipschitz-continuous, there exists  $K > 0$  such that

$$|F(\varphi_1(\tilde{\mathbf{s}}(\sigma))) - F(\varphi_\nu(\tilde{\mathbf{s}}(\sigma)))| \leq K|1 - \nu|,$$

and hence, since  $F$  is decreasing in  $\nu$ ,  $F(\varphi_\nu(\tilde{\mathbf{s}}(\sigma))) \leq K(1 - \nu)$  for all  $\nu \in [0, 1]$ .

Therefore,

$$\begin{aligned} I(\tilde{\mathbf{s}}(\sigma)) &= \lim_{\nu \rightarrow 1} y_1(\bar{s}_1^+ - \bar{s}_1) \int_0^\nu \left( 1 - \frac{D}{F(\varphi_\tau(\tilde{\mathbf{s}}(\sigma)))} \right) d\tau \\ &\leq \lim_{\nu \rightarrow 1} y_1(\bar{s}_1^+ - \bar{s}_1) \int_0^\nu \left( 1 - \frac{D}{K(1 - \tau)} \right) d\tau = -\infty. \end{aligned}$$

For  $z < \sigma$ ,  $\tilde{\mathbf{s}}(z) \in \Omega_1$  and  $I(\tilde{\mathbf{s}}(z))$  is continuous. Since  $I(\tilde{\mathbf{s}}(0)) = I(\widehat{\mathbf{s}}^+) = \mu(r) > 0$ , by the intermediate-value theorem there exists  $z \in (0, \sigma)$  such that  $I(\tilde{\mathbf{s}}(z)) = 0$ . Let  $\rho = \sup\{z \in (0, \sigma) : I(\tilde{\mathbf{s}}(z)) > 0\}$ . Thus, the set  $\Gamma_\rho^+$  is well defined, and all that is left is to show that  $\Gamma_\rho^+ \subset G^+$ .

Let  $\mathbf{s} \in \Gamma_\rho^+$ . Then there exists  $\varepsilon > 0$  such that  $V_i(\mathbf{s}) > -\rho + \varepsilon = V_i(\tilde{\mathbf{s}}(\rho - \varepsilon))$

for each  $i = 2, \dots, n$ . This implies that  $s_i > \hat{s}_i - (\rho - \varepsilon)$ . By the definition of  $\rho$ , we have  $I(\tilde{\mathbf{s}}(\rho - \varepsilon)) > 0$ . Since  $F(\mathbf{s})$  is nondecreasing in each of the  $s_i$ ,

$$I(\mathbf{s}) \geq I(\tilde{\mathbf{s}}(\rho - \varepsilon)) > 0. \quad \square$$

If  $n = 2$ , then Lemma 4.3.11 implies that there exists  $s_2^b > 0$  such that  $G^- = \{\bar{s}_1\} \times (s_2^b, \infty)$ . This is the result of Lemma 3.4.9 in Chapter 3 (or equivalently, the result of Lemma 4.9 in [5]). If  $n > 2$ , then we are unable to find such an explicit formulation of  $\Gamma_A^-$ .

We use the set  $G^-$  to define

$$\Omega_G = \{\mathbf{s}^0 \in \Omega_1 : \varphi_1(\mathbf{s}^0) \in G^-\}, \quad (4.22)$$

the set of points in  $\Omega_1$  that will flow through  $G^-$  for some value of  $x^0$ . Using (4.13) and Lemma 4.3.11, we define

$$\Omega^\rho = \{\mathbf{s} \in \Omega_1 : V_i(\mathbf{s}) > -\rho, i = 2, \dots, n\},$$

where  $\rho$  is given in Lemma 4.3.11. It is clear that

$$\Omega^\rho \subseteq \Omega_G. \quad (4.23)$$

**Lemma 4.3.12.** *Assume that  $\mathbf{s}^{\text{in}} \in \Omega_1$  and  $\mu(r) > 0$ . Let  $(s_1(t), \dots, s_n(t), x(t))$  be a solution of system (4.1) with  $x^0 > 0$  and  $\mathbf{s}^0 \in \Omega_G$ .*

1. *If  $x^0 \leq -I(\mathbf{s}^0)$ , then there are no impulses.*

2. As  $t \rightarrow \infty$ ,  $(s_1(t), \dots, s_n(t), x(t))$  converges to the unique periodic orbit given by Theorem 4.3.7 if and only if  $x^0 > -I(\mathbf{s}^0)$ .

*Proof.* Suppose  $x^0 \leq -I(\mathbf{s}^0)$  and there is at least one impulse. By (4.9) and the definition of  $I(\mathbf{s}^0)$ ,

$$u_1(\mathbf{s}^0, x^0) = x^0 + I(\mathbf{s}^0) \leq 0.$$

This implies that  $x(t) = 0$  for some finite value of  $t$ , contradicting the uniqueness of initial values problems to ODEs.

If  $x^0 > -I(\mathbf{s}^0)$ , then by (4.9) and the definition of  $I(\mathbf{s}^0)$ , at least one impulse occurs. Let  $t = t_1^-$  be the time of the first impulse. Since  $\mathbf{s}^0 \in \Omega_G$ , we have  $\mathbf{s}(t_1^-) = \varphi_1(\mathbf{s}^0) \in G^-$ . It follows that  $\mathbf{s}^1 = r\mathbf{s}^{\text{in}} + (1-r)\varphi_1(\mathbf{s}^0) \in G^+$  and thus that  $I(\mathbf{s}^1) > 0$ . Therefore, there is a second impulse at  $t = t_2^-$ . Inductively, it follows that impulses occur indefinitely. By Corollary 4.3.2,  $\lim_{k \rightarrow \infty} \|\mathbf{V}(\varphi_\nu(\mathbf{s}^k))\|_\infty = 0$  for all  $\nu \in [0, 1]$ , and therefore  $\mathbf{s}^k \rightarrow \widehat{\mathbf{s}}^+$  as  $t \rightarrow \infty$ . By (4.9) and the relationship  $I(\widehat{\mathbf{s}}^+) = \mu(r)$ ,

$$\lim_{k \rightarrow \infty} (u_1(\mathbf{s}^k, x^k) - u_0(\mathbf{s}^k, x^k)) = \mu(r).$$

On the other hand, the impulse map in (4.1b) gives

$$\lim_{k \rightarrow \infty} (u_0(\mathbf{s}^{k+1}, x^{k+1}) - (1-r)u_1(\mathbf{s}^k, x^k)) = 0.$$

Combining these, and using the fact that  $u_0(\mathbf{s}^k, x^k) = x^k$ , leads to

$$\lim_{k \rightarrow \infty} (x^{k+1} + (1-r)x^k) = (1-r)\mu(r). \quad (4.24)$$

This implies that  $\lim_{k \rightarrow \infty} x^k = \frac{1-r}{r} \mu(r)$  and  $\lim_{k \rightarrow \infty} u_1(\mathbf{s}^k, u^k) = \frac{1}{r} \mu(r)$ .  $\square$

**Corollary 4.3.13.** *If  $\mathbf{s}^{\text{in}} \in \Omega_1$  and  $\mu(r) > 0$ , then all solutions to (4.1) with  $x^0 > 0$  and  $\mathbf{s}^0 = \mathbf{s}^{\text{in}}$  converge to the periodic orbit given in Theorem 4.3.7.*

*Proof.* Since  $\mathbf{s}^0 = \mathbf{s}^{\text{in}}$ ,  $I(\mathbf{s}^0) > \mu(r) > 0$ , and so  $x^0 > 0 > -I(\mathbf{s}^0)$ .  $\square$

For each  $\mathbf{s}^0 \in \Omega_1$  let  $N_0 = N_0(\mathbf{s}^0)$  be the smallest positive integer such that  $\mathbf{s}^{N_0} \in \Gamma_A^+$ . Clearly, if  $\mathbf{s}^0 \in \Omega_G$ , we have  $N_0(\mathbf{s}^0) = 1$ .

In general, we are unable to get an exact characterization of  $\Omega_G$  in terms of  $\mathbf{V}(\mathbf{s}^0)$ . However, we can approximate  $N_0$  using  $\Omega^\rho$ . Let  $N^\rho$  be the smallest positive integer such that  $\mathbf{s}^{N^\rho} \in \Omega^\rho$ . By applying Lemma 4.3.1 repeatedly,

$$V_i(\mathbf{s}^k) = (1-r)^k V_i(\mathbf{s}^0). \quad (4.25)$$

The condition that  $\mathbf{s}^0 \in \Omega_1 \setminus \Omega^\rho$  is equivalent to  $V_i(\mathbf{s}^0) \leq -\rho$  for at least one of  $i = 2, \dots, n$ . By applying this to (4.25) and solving for  $k$ ,

$$N^\rho = \max \left\{ \left\lceil \frac{\ln(V_i(\mathbf{s}^0) / -\rho)}{-\ln(1-r)} \right\rceil : V_i(\mathbf{s}^0) \leq -\rho \right\}, \quad (4.26)$$

where  $\lceil x \rceil$  is least integer greater than  $x$ . By Lemma 4.3.1 and (4.23),  $N_0 \leq N^\rho$ . From (4.26), we see that  $N^\rho$  has the upper bound

$$\bar{N} = \max \left\{ \left\lceil \frac{\ln(\bar{V}_i / -\rho)}{-\ln(1-r)} \right\rceil : i = 2, \dots, n \right\},$$

and so  $N_0 \leq \bar{N}$ ; i.e., every trajectory enters  $\Omega_G$  after finitely many impulses, or the reactor fails before then.

For any solution to (4.1) with  $x^0 > 0$  and  $\mathbf{s}^0 \in \Omega_1$ , if there exists  $t_1^-$  with  $s_1(t_1^-) = \bar{s}_1$ ,

$$x(t_1^-) = u_1(\mathbf{s}^0, x^0) = x^0 + I(\mathbf{s}^0),$$

and, for any  $k = 2, 3, \dots$ , the value of  $x(t_k^-)$  is given by

$$x(t_k^-) = x^k + I(\mathbf{s}^k).$$

Inductively,

$$x(t_k^-) = (1-r)^{k-1}x^0 + \sum_{j=1}^k (1-r)^{k-j} I((g \circ \varphi_1)^{j-1}(\mathbf{s}^0)),$$

and therefore,  $x(t_k^-) > 0$  is equivalent to

$$x^0 > - \sum_{j=1}^k (1-r)^{1-j} I((g \circ \varphi_1)^{j-1}(\mathbf{s}^0)).$$

We define  $X(\mathbf{s}^0)$  to be the minimum value of  $x^0$  required for  $\mathbf{s}(t_*^-) \in G^-$  for some  $t_*^-$ ,

$$X(\mathbf{s}^0) = - \min_{1 \leq k \leq N_0} \left( \sum_{j=1}^k (1-r)^{1-j} I((g \circ \varphi_1)^{j-1}(\mathbf{s}^0)) \right). \quad (4.27)$$

In particular, if  $\mathbf{s}^0 \in \Omega_G$ , then  $X(\mathbf{s}^0) = -I(\mathbf{s}^0)$ , since  $N_0 = 1$ .

**Proposition 4.3.14.** *Assume  $\mathbf{s}^{\text{in}} \in \Omega_1$  and  $\mu(r) > 0$ . Let  $(s_1(t), \dots, s_n(t), x(t))$  be a solution of (4.2) with  $\mathbf{s}^0 \in \Omega_1$  and  $x^0 > 0$ .*

(i) *If  $x^0 \leq X(\mathbf{s}^0)$ , then there are at most  $N_0 - 1$  impulses.*

(ii) *If  $x^0 > X(\mathbf{s}^0)$ , then the solutions converge to the periodic orbit given in Theorem 4.3.7.*

*Proof.* (i) Suppose  $x^0 \leq X(\mathbf{s}^0)$  and there are at least  $N_0$  impulses. Denote the first  $N_0$  impulse times by  $t_1 < t_2 < \dots < t_{N_0}$ . By (4.9) and the definition of  $X(\mathbf{s}^0)$ ,

$$x(t_k^-) = u_1(\mathbf{s}^{k-1}, x^{k-1}) = (1-r)^{k-1}(x^0 - X(\mathbf{s}^0)) \leq 0,$$

for some  $k < N_0$ , which contradicts Corollary 4.2.3.

(ii) If  $x^0 > X(\mathbf{s}^0)$ , then the solution has at least  $N_0$  impulses. Then  $\mathbf{s}^{N_0} = (g \circ \varphi_1)^{N_0}(\mathbf{s}^0) \in \Omega_G$ . Since  $\mathbf{s}^{N_0} \in G^+$ , we have  $I(\mathbf{s}^{N_0}) > 0$ , and the result follows from Lemma 4.3.12.  $\square$

**Example 4.3.15.** Consider (4.1) with  $n = 3$ ,

$$F(\mathbf{s}) = \min \left\{ \frac{0.5s_1}{1+s_1}, \frac{0.7s_2}{0.4+s_2}, \frac{s_3}{1+s_3} \right\},$$

and  $r = 0.3$ ,  $\mathbf{Y} = (2.0, 0.2, 1.0)^T$ ,  $\bar{s}_1 = 0.25$ ,  $D = 0.1$  and  $\mathbf{s}^{\text{in}} = (0.5, 0.1, 0.5)$ .

By definition,  $\bar{V}_2 = -0.375$ , and  $\bar{V}_3 = -0.375$ . Therefore,  $\bar{V}_2 = \bar{V}_3 = \max\{\bar{V}_2, \bar{V}_3\}$ . We are free to project solutions onto either the  $s_1$ - $s_2$  plane, or the  $s_1$ - $s_3$ . Notice  $\mathbf{s}^{\text{in}} \in \Omega_1$  and  $\mu(r) \approx 0.0037 > 0$ . By Theorem 4.3.7 there exists a periodic solution. With the initial conditions  $\mathbf{s}^0 = (0.3, 0.01, 1)^T$ , we have  $V(\mathbf{s}^0) = (0, -0.35, 0.6)^T$ , and so  $\mathbf{s}^0 \in \Omega_1$ . We calculate the sum in (4.27) for  $n = 1, \dots, N_0$  where  $N_0$  is the first integer such that  $(1-r)^{1-n}I(\mathbf{s}^{n-1}) > 0$ . The approximate values are as follows:

$n$	1	2	3	4	5	6
$(1-r)^{1-n}I(\mathbf{s}^{n-1})$	-0.1766	-0.0575	-0.330	-0.206	-0.0104	0.0007

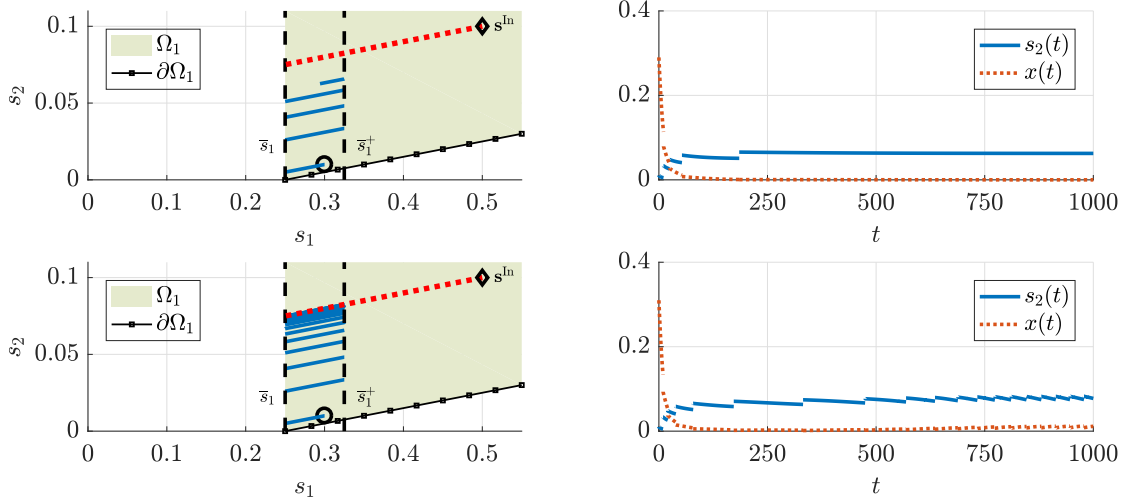


FIGURE 4.4: The dynamics of Example 4.3.15 illustrated by projecting orbits onto  $s_1$ - $s_2$  space, with the line through  $\mathbf{s}^{\text{in}}$  shown in dotted red on the left. Solutions of  $s_2$  and  $x$  as functions of time are shown on the right. On the top,  $x^0 < X(\mathbf{s}^0)$  and so  $x(t) \rightarrow 0$  as  $t \rightarrow \infty$  after at most  $N_0 = 4$  impulses. On the bottom  $x^0 > X(\mathbf{s}^0)$  and so solutions converge to the periodic solution.

We therefore calculate  $X(\mathbf{s}^0) \approx 0.1766 + 0.0575 + 0.330 + 0.206 + 0.0104 = 0.2981$ . In Figure 4.4 (top) the initial biomass concentration is  $x^0 = 0.29 < X(\mathbf{s}^0)$  and so by Proposition 4.3.14,  $x(t) \rightarrow 0$  after at most 4 impulses. In Figure 4.4 (bottom) the initial biomass concentration is  $x^0 = 0.31 > X(\mathbf{s}^0)$ , and so by Proposition 4.3.14, the solution converges to the periodic solution as  $t \rightarrow \infty$ .

The following theorem summarizes the results.

**Theorem 4.3.16.** *Let  $(s_1(t), \dots, s_n(t), x(t))$  be a solution of (4.1) with positive initial conditions.*

- (i) *If  $\mathbf{s}^{\text{in}} \in \Omega_0$ , then  $(s_1(t), \dots, s_n(t), x(t))$  has only finitely many impulses, and  $x(t) \rightarrow 0$  as  $t \rightarrow \infty$ .*
- (ii) *If  $\mathbf{s}^{\text{in}} \in \Omega_1$  and  $\mu(r) \leq 0$ , then  $(s_1(t), \dots, s_n(t), x(t))$  either has only finitely*

many impulses and  $x(t) \rightarrow 0$  as  $t \rightarrow \infty$  or the time between impulses tends to infinity and  $\liminf_{t \rightarrow \infty} x(t) = 0$ .

(iii) If  $\mathbf{s}^{\text{in}} \in \Omega_1$  and  $\mu(r) > 0$ , then there is a unique periodic orbit. Either  $(s_1(t), \dots, s_n(t), x(t))$  has infinitely many impulses and converges to the periodic orbit or  $(s_1(t), \dots, s_n(t), x(t))$  has only finitely many impulses and  $x(t) \rightarrow 0$  as  $t \rightarrow \infty$ . The case with infinitely many impulses occurs if and only if

$$\mathbf{s}^0 \in \Omega_1, \quad \text{and} \quad x^0 > X(\mathbf{s}^0).$$

*Proof.* The results follow from Lemmas 4.3.3 and 4.3.4, Theorem 4.3.7, and Propositions 4.3.9 and 4.3.14. □

## 4.4 Conclusions

We have modelled the self-cycling-fermentation process assuming that there are an arbitrary number of essential resources,  $\mathbf{s} \in \mathbb{R}^n$ , that are growth limiting for a population of microorganisms,  $x$ , using a system of impulsive differential equations. We assume that the criterion for decanting the reactor occurs when the concentration of the first nutrient reaches a threshold,  $\bar{s}_1$ . The process is considered successful if, once initiated, it proceeds indefinitely without intervention.

By solving the associated system of ODEs in terms of the first nutrient,  $s_1$ , we have shown that the solutions, when projected onto the nutrient hyperplane, are lines in the direction of  $(1/y_1, \dots, 1/y_n)^T$ , where  $y_i$  is the yield coefficient of the  $i$ th

nutrient. Using a vector Lyapunov function, we divide the nutrient hyperplane into two regions,  $\Omega_0$  and  $\Omega_1$ . The model predicts that if the initial nutrient concentrations lie in  $\Omega_0$  then solutions will approach the faces of  $\mathbb{R}_+^n$  before  $s_1$  reaches  $\bar{s}_1$ , and the reactor will fail. If the initial nutrient concentrations lie in  $\Omega_1$ , then the concentration of  $s_1$  may reach  $\bar{s}_1$ , but successful operation of the reactor may still be limited by other factors.

In reality, we expect that the the initial nutrient concentrations are equal to the nutrient concentrations in the input; i.e.  $\mathbf{s}(0) = \mathbf{s}^{\text{in}}$ . If, for any solution with initial nutrient concentration  $\mathbf{s}^{\text{in}}$  and positive initial biomass concentration ( $x(0) > 0$ ), the threshold concentration of  $s_1$  is reached with net positive growth of the biomass, then we can pick a fraction of medium to remove,  $r$ , so that the reactor will cycle indefinitely. In this case, the solutions converge to a periodic solution, with period equal to the length of one cycle.

If the model has a periodic solution, the nutrient components of the periodic solution lie along the line through  $\mathbf{s}^{\text{in}}$  in the direction of  $(1/y_1, \dots, 1/y_n)^T$ . The net change in biomass along the periodic orbit, denoted  $\mu(r)$ , must be positive. For other initial nutrient concentrations in  $\Omega_1$ , the solutions may converge to the periodic solution. However, there is a minimum concentration of biomass,  $X$ , that is dependent on the initial nutrient concentrations, required for the successful operation of the reactor. If the initial biomass concentration is higher than  $X$ , then the reactor will cycle indefinitely and solutions will approach the periodic solution. If the initial biomass concentrations are less than  $X$ , then the reactor will fail after a finite number of cycles. If the model does not have a periodic solution, then the reactor will either fail after a finite number of cycles or it will cycle indefinitely,

but the time each cycle takes will grow larger and larger, approaching infinity.

The model presented here can be thought of as an extension of the single resource model developed in Smith and Wolkowicz [10]. In that model, it was shown that, when a periodic orbit exists, the reactor will either cycle indefinitely or the reactor will fail without reaching the threshold concentration of  $s_1$ . We have shown that if there are more essential limiting nutrients but only one is used for the decanting criteria, then the reactor may fail after many cycles, even if the system has a periodic solution. An example of failure after 4 cycles is shown in Figure 4.4. This may offer an explanation for failure of the reactor when the analysis of the single resource model suggests the reactor should operate successfully.

# Bibliography

- [1] F. Bader. Analysis of double-substrate limited growth. *Biotechnol. and Bioeng.*, 20(2):183–202, 1978.
- [2] D. D. Baïnov and P. S. Simeonov. *Impulsive differential equations*, volume 28 of *Series on Advances in Mathematics for Applied Sciences*. World Scientific Publishing Co., Inc., River Edge, NJ, 1995. Asymptotic properties of the solutions, Translated from the Bulgarian manuscript by V. Covachev [V. Khr. Kovachev].
- [3] F. Córdovea-Lepe, R. D. Valle, and G. Robledo. Stability analysis of a self-cycling fermentation model with state-dependent impulses. *Math. Methods Appl. Sci.*, 37:1460–1475, 2014.
- [4] G. Fan and G. S. K. Wolkowicz. Analysis of a model of nutrient driven self-cycling fermentation allowing unimodal response functions. *Discrete Cont. Dyn. S.*, 8(4):801–831, 2007.
- [5] T.-H. Hsu, T. Meadows, L. Wang, and G. S. K. Wolkowicz. Growth on two limiting essential nutrients in a self-cycling fermentor. *Math. BioSci. Eng.*, 16:78–100, 2019.

## BIBLIOGRAPHY

---

- [6] S. M. Hughes and D. G. Cooper. Biodegradation of phenol using the self-cycling fermentation process. *Biotechnol. Bioeng.*, 51:112–119, 1996.
- [7] A. Samoilenko and N. A. Perestyuk. *Impulsive differential equations*. World Scientific, Singapore, 1995.
- [8] B. E. Sarkas and D. G. Cooper. Biodegradation of aromatic compounds in a self-cycling fermenter. *Can. J. Chem. Eng.*, 72(5):874–880, 1994.
- [9] D. Sauvageau, Z. Storms, and D. G. Cooper. Synchronized populations of *Escherichia coli* using simplified self-cycling fermentation. *J. Biotechnol.*, 149:67–73, 2010.
- [10] R. J. Smith and G. S. K. Wolkowicz. Analysis of a model of the nutrient driven self-cycling fermentation process. *Dyn. Contin. Discret. I.*, 11:239–265, 2004.
- [11] Z. J. Storms, T. Brown, D. Sauvageau, and D. G. Cooper. Self-cycling operation increases productivity of recombinant protein in *Escherichia coli*. *Biotechnol. Bioeng.*, 109(9):2262–2270, 2012.
- [12] M. Strous, J. J. Heijnen, J. G. Kuenen, and M. S. M. Jetten. The sequencing batch reactor as a powerful tool for the study of slowly growing anaerobic ammonium-oxidizing microorganisms. *Appl. Microbiol. Biotechnol.*, 50:589–596, 1998.
- [13] K. Sun, Y. Tian, L. Chen, and A. Kasperski. Universal modelling and qualitative analysis of an impulsive bioprocess. *Comput. Chem. Eng.*, 35(3):492 – 501, 2011.

## BIBLIOGRAPHY

---

- [14] D. Tilman. *Resource competition and community structure*. Princeton University Press, New Jersey, 1982.
- [15] J. Von Liebig. *Die organische Chemie in ihrer Anwendung auf Agrikultur und Physiologie*. Friedrich Vieweg, Braunschweig, 1840.
- [16] J. Wang, M. Chae, D. Sauvageau, and D. C. Bressler. Improving ethanol productivity through self-cycling fermentation of yeast: a proof of concept. *Biotechnol. Biofuels*, 10(1):193, 2017.
- [17] B. M. Wincure, D. G. Cooper, and A. Rey. Mathematical model of self-cycling fermentation. *Biotechnol. Bioeng.*, 46(2):180–183, 1995.

# Chapter 5

## Conclusions

In this thesis, we investigated three different models of engineered biological systems. Each of these systems is applied to a form of green technology, used to reduce the amount of produced waste that enters the environment or to make use of the waste produced in a different process. In each of the cases, we have completely characterized the dynamics of the system based on initial conditions and parameter values present in the system. Each model is either the simplification of a more realistic model (Chapter 2) or is a modification of a more basic model that only focused on one or two mechanisms in the system (Chapter 3 and Chapter 4). The goal of this type of modelling is to make general qualitative observations about the systems modelled to try to understand the complete spectrum of dynamics possible. In each case, we have made some observation from the analysis that could be useful to those who operate such systems.

The first system uses the anaerobic digestion process to convert animal waste into fuel in the form of biogas. The model of this process that we analyze is a system of five ordinary differential equations and was introduced by Bornhöft *et*

*al.* [4]. We complete a global analysis of the system, determining the complete range of possible dynamics for any parameter regime. In particular, we show that the dynamics of the full five-dimensional system reduce to the dynamics of a two-dimensional limiting system. We show that the limiting system is equivalent to the model of growth in a basic chemostat when the microorganism death rate is considered and the growth functions are non-monotone. The dimensional reduction of systems in this way is a common method involving the theory of asymptotically autonomous systems [16] (although we use the slightly weaker condition that the system is quasi-autonomous). We consider stochastic simulations of the model using the Gillespie stochastic simulation algorithm, the tau-leaping algorithm, and two stochastic simulations in which the parameters are treated as random variables. All four algorithms give similar results and suggest that if the reactor is going to fail, it will do so shortly after startup. This result implies that operators should avoid restarting the system too often, since the reactor is most vulnerable early in its operation.

The chemostat model that we obtain as the two-dimensional limiting system had not been completely studied. When only one equilibrium point is locally asymptotically stable, it is clear that the locally stable equilibrium point is also globally asymptotically stable. When both an interior equilibrium point and a boundary equilibrium point are locally asymptotically stable, it was not clear whether periodic orbits could exist. By using the level sets of a local Lyapunov function, we were able to approximate the basin of attraction for the interior equilibrium point. By coupling our estimation of the basin of attraction with standard phase-plane analysis, we were able to show that trajectories must either

enter the basin of attraction or converge to one of the other equilibria and therefore that no periodic solutions are possible.

The second system studied was the self-cycling fermentation process used to purify wastewater. The model of this system is represented by a system of three impulsive differential equations, with impulses occurring when both nutrient concentrations fall below set threshold levels. We used a symmetry inherent in the system to visualize solutions in the nutrient plane and decompose the nutrient plane into two regions,  $\Omega_0$  and  $\Omega_1$ . We showed that if nutrient concentrations begin in  $\Omega_0$ , then the population of microorganisms is destined to die out. If the nutrient concentration begins in  $\Omega_1$ , then the reactor may succeed; however, this is not the only criterion that is required for success. We showed if the input nutrient concentrations are in  $\Omega_0$ , then the microorganism is destined to die out after finitely many cycles. However, when the input concentrations are in  $\Omega_1$ , there is the potential for an attracting periodic solution. The periodic solution only exists if a specific growth condition on the microorganism population is met. We find further initial-condition-dependent criteria that must be satisfied for solutions to converge to the periodic solution, which is equivalent to successful operation of the reactor.

Operators of self-cycling fermentors often set up their reactors to be as simple as possible. In many cases, this means that the fraction of medium emptied and subsequently refilled each cycle is approximately  $1/2$ . By considering a system that is operating successfully, we numerically optimize the throughput of the reactor using the emptying/refilling fraction,  $r$ . The throughput of the reactor is the volume of liquid removed from the reactor per unit time. In a toy example, we

show that the optimal refilling fraction does not necessarily have to be  $1/2$ . With the application of wastewater treatment in mind, the self-cycling process can likely be implemented more efficiently by determining the optimal emptying/refilling fraction.

The third model investigates the self-cycling fermentation process when there is an arbitrary number of limiting essential nutrients. We model the nutrient uptake using an arbitrary increasing positive function, and model the self-cycling fermentation process using a system of  $n + 1$  impulsive differential equations with impulses when the first nutrient concentration falls below a prescribed threshold. Using a symmetry of the system, we show that the time between impulses can be effectively measured using one of the nutrient concentrations. By making this change of variables, we can obtain closed-form solutions for the nutrient concentrations and an implicit solution for the biomass concentration between impulses. We use a vector Lyapunov-type function to show that if impulses occur indefinitely, then nutrient concentrations converge to a periodic solution, which is a line when projected onto the  $n$ -dimensional nutrient hyperplane. Like the two nutrient case, we show that the nutrient hyperplane can be split into two regions,  $\Omega_0$  and  $\Omega_1$ . We show that if nutrient concentrations begin in  $\Omega_0$ , then the microorganism population is destined to die off. If nutrient concentrations begin in  $\Omega_1$ , then the survival of the microorganism population depends on the location of the input nutrient concentrations in nutrient space, the net growth of the microorganism population on the solution curve through the input nutrient concentrations and an additional initial-condition-dependent criterion on the initial biomass concentration.

Self-cycling fermentation depends on the ability to be able to make regular on-line measurements of the system. These measurements can be difficult and expensive, so operators often find ways around measuring the exact quantities of interest. For example, in the turbidostat [17], the turbidity (cloudiness of the liquid) is used to estimate the biomass in the liquid, and the dissolved oxygen concentration is a common proxy measurement for limiting nutrient concentrations [19]. If the measured quantity also becomes limiting or there is a shortage of other nutrients in the input medium, then the multiple-nutrient model suggests that the reactor may fail, even if the single-nutrient model would predict success.

# Bibliography

- [1] R. A. Armstrong and R. McGehee. Competitive exclusion. *Am. Nat.*, 115:151–170, 1980.
- [2] M. Ballyk and H. L. Smith. A model of microbial growth in a plug flow reactor with wall attachment. *Math. Biosci.*, 158:95–126, 1999.
- [3] D. Batstone, J. Keller, I. Angelidaki, S. Kalyuzhnyi, S. Pavlosthathis, A. Rozzi, W. Sanders, H. Siegrist, and V. Vavilin. *Anaerobic Digestion Model No.1 (ADM1)*. IWA Publishing, London UK, 2002.
- [4] A. Bornhöft, R. Hanke-Rauschenbach, and K. Sundmacher. Steady-state analysis of the anaerobic digestion model no.1 (ADM1). *Nonlinear Dyn.*, 73:535–549, 2013.
- [5] G. J. Butler and G. S. K. Wolkowicz. A mathematical model of the chemostat with a general class of functions describing nutrient uptake. *SIAM J. Appl. Math.*, 45:138–151, 1985.
- [6] S. R. Hansen and S. P. Hubbell. Single-nutrient microbial competition: qualitative agreement between experimental and theoretically forecast outcomes. *Science*, 207(4438):1491–1493, 1980.

## BIBLIOGRAPHY

---

- [7] S.-B. Hsu. Limiting behavior for competing species. *SIAM J. Appl. Math.*, 34:760–763, 1978.
- [8] S.-B. Hsu. A competition model for a seasonally fluctuating nutrient. *J. Math. Biology*, 9:115–132, 1980.
- [9] S.-B. Hsu, H. S., and W. P. A mathematical theory of single nutrient competition in continuous cultures of micro-organisms. *SIAM J. Appl. Math.*, 32:366–383, 1977.
- [10] S.-B. Hsu and P. Waltman. On a system of reaction-diffusion equations arising from competition in an unstirred chemostat. *SIAM J. Appl. Math.*, 53(4):1026–1044, 1993.
- [11] T.-H. Hsu, T. Meadows, L. Wang, and G. S. K. Wolkowicz. Growth on two limiting essential nutrients in a self-cycling fermentor. *Math. BioSci. Eng.*, 16:78–100, 2019.
- [12] MAPLE. *Maplesoft, a division of Waterloo Maple Inc.* Waterloo, Ontario, 2017.
- [13] T. Meadows, M. Weederemann, and G. S. K. Wolkowicz. Global analysis of a simplified model of anaerobic digestion and a new result for the chemostat. *SIAM J. Appl. Math.*, 79(2):668–669, 2019.
- [14] A. Novick and L. Szilard. Experiments with the chemostat on spontaneous mutations of bacteria. *Proc. Natl. Acad. Sci. U S A*, 36(12):708–719, 1950.

## BIBLIOGRAPHY

---

- [15] H. L. Smith and P. Waltman. *The theory of the chemostat*, volume 13 of *Cambridge Studies in Mathematical Biology*. Cambridge University Press, Cambridge, 1995. Dynamics of microbial competition.
- [16] H. Thieme. Asymptotically autonomous differential equations in the plane II. Stricter Poincaré-Bendixson type results. *Diff. Int. Eq.*, 7:1625–1640, 1994.
- [17] T. G. Watson. The present status and future prospects of the turbidostat. *J. Appl. Chem. Biotechnol.*, 22:229–243, 1972.
- [18] M. Weedermann, G. S. K. Wolkowicz, and J. Sasara. Optimal biogas production in a model for anaerobic digestion. *Nonlinear Dyn.*, 81:1097–1112, 2015.
- [19] B. M. Wincure, D. G. Cooper, and A. Rey. Mathematical model of self-cycling fermentation. *Biotechnol. Bioeng.*, 46(2):180–183, 1995.
- [20] G. S. K. Wolkowicz and Z. Lu. Global dynamics of a mathematical model of competition in the chemostat: general response function and differential death rates. *SIAM J. Appl. Math.*, 52:222–233, 1992.